

AD-A213 249

AFWAL-TR-88-2149

PROBABILISTIC FINITE ELEMENT ANALYSIS OF DYNAMIC
STRUCTURAL RESPONSE

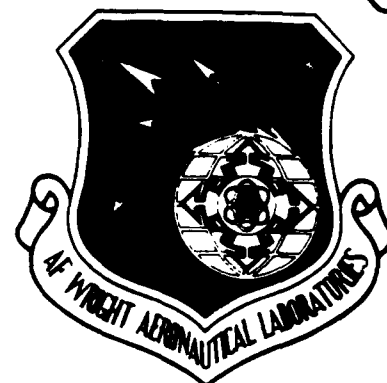
R. A. Brockman
F. Y. Lung
W. R. Braisted

University of Dayton
Research Institute
300 College Park
Dayton, OH 45469

March 1989

Final Report for Period October 1985 - October 1987

Approved for public release; distribution is unlimited



DTIC
ELECTE
OCT 10 1989
S B D

AEROPROPULSION AND POWER LABORATORY
AIR FORCE WRIGHT AERONAUTICAL LABORATORIES
AIR FORCE SYSTEMS COMMAND
WRIGHT-PATTERSON AIR FORCE BASE, OHIO 45433-6563

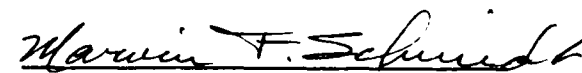
NOTICE

When Government drawings, specifications, or other data are used for any purpose other than in connection with a definitely Government-related procurement, the United States Government incurs no responsibility or any obligation whatsoever. The fact that the government may have formulated or in any way supplied the said drawings, specifications, or other data, is not to be regarded by implication, or otherwise in any manner construed, as licensing the holder, or any other person or corporation; or as conveying any rights or permission to manufacture, use, or sell any patented invention that may in any way be related thereto.


This report is releasable to the National Technical Information Service (NTIS). At NTIS, it will be available to the general public, including foreign nations.

This technical report has been reviewed and is approved for publication.


JOHN D. REED, Aerospace Engineer
Propulsion Integration
Engine Integration & Assessment Branch


MARVIN F. SCHMIDT, Chief
Engine Integration & Assessment Branch

FOR THE COMMANDER


ROBERT E. HENDERSON
Deputy for Technology
Turbine Engine Division
Aero Propulsion & Power Laboratory

If your address has changed, if you wish to be removed from our mailing list, or if the addressee is no longer employed by your organization please notify WRDC/POTA, WPAFB, OH 45433-6563 to help us maintain a current mailing list.

Copies of this report should not be returned unless return is required by security considerations, contractual obligations, or notice on a specific document.

REPORT DOCUMENTATION PAGE

1a. REPORT SECURITY CLASSIFICATION Unclassified			1b. RESTRICTIVE MARKINGS			
2a. SECURITY CLASSIFICATION AUTHORITY			3. DISTRIBUTION/AVAILABILITY OF REPORT Approved for public release; distribution is unlimited.			
2b. DECLASSIFICATION/DOWNGRADING SCHEDULE						
4. PERFORMING ORGANIZATION REPORT NUMBER(S) UDR-TR-87-130			5. MONITORING ORGANIZATION REPORT NUMBER(S) AFWAL-TR-88-2149			
6a. NAME OF PERFORMING ORGANIZATION University of Dayton Research Institute		6b. OFFICE SYMBOL (If applicable)	7a. NAME OF MONITORING ORGANIZATION Air Force Wright Aeronautical Labs. Aeropropulsion and Power Lab. (AFWAL/POTC)			
6c. ADDRESS (City, State and ZIP Code) 300 College Park Dayton, Ohio 45469			7b. ADDRESS (City, State and ZIP Code) Wright-Patterson Air Force Base, OH 45433-6563			
8a. NAME OF FUNDING/SPONSORING ORGANIZATION		8b. OFFICE SYMBOL (If applicable)	9. PROCUREMENT INSTRUMENT IDENTIFICATION NUMBER F 33615-85-C-2585			
8c. ADDRESS (City, State and ZIP Code)			10. SOURCE OF FUNDING NOS.			
			PROGRAM ELEMENT NO.	PROJECT NO.	TASK NO.	WORK UNIT NO.
			62203 F	3066	12	21
11. TITLE (Include Security Classification) Probabilistic Finite Element Analysis of Dynamic Structural Response						
12. PERSONAL AUTHOR(S) Brockman, R. A., Lung, F. Y., Braisted, W. R.						
13a. TYPE OF REPORT Final		13b. TIME COVERED FROM OCT85 TO OCT87		14. DATE OF REPORT (Yr., Mo., Day) March 1989		15. PAGE COUNT 217
16. SUPPLEMENTARY NOTATION						
17. COSATI CODES			18. SUBJECT TERMS (Continue on reverse if necessary and identify by block number)			
FIELD	GROUP	SUB. GR.				
20	11		Finite Elements			
21	05		Plates and Shells			
			Probabilistic Analysis			
			Sensitivity Analysis			
			Structural Dynamics			
			Vibration			
19. ABSTRACT (Continue on reverse if necessary and identify by block number)						
<p>This report describes techniques for the probabilistic dynamic analysis of plate and shell structures. Statistical variables, which may include material properties, thicknesses, or arbitrary geometric parameters, are treated as discrete random parameters with normal distribution. Structural response sensitivities and variance estimates for statistical variables are used to estimate the variances of response variables such as displacement, stress, or natural frequency. Basic solutions and sensitivity analyses are performed using finite element techniques. The methods described require very little information beyond that needed for a deterministic analysis, but can be used to develop useful probabilistic data for large models at very low cost.</p> <p>Several key developments discussed in the report contribute to the effectiveness of the probabilistic analysis method, but have potential</p> <p style="text-align: right;">(continued)</p>						
20. DISTRIBUTION/AVAILABILITY OF ABSTRACT UNCLASSIFIED/UNLIMITED <input checked="" type="checkbox"/> SAME AS RPT <input type="checkbox"/> OTIC USERS <input type="checkbox"/>			21. ABSTRACT SECURITY CLASSIFICATION Unclassified			
22a. NAME OF RESPONSIBLE INDIVIDUAL John Reed			22b. TELEPHONE NUMBER (Include Area Code) (513) 255-2081		22c. OFFICE SYMBOL AFWAL/POTC	

UNCLASSIFIED

SECURITY CLASSIFICATION OF THIS PAGE

application in other areas of structural mechanics. The problem of stabilizing low-order elements with reduced order quadrature for use in dynamic problems is addressed; a potential source of instability is identified and a mass formulation which produces a stable and accurate element is presented. Layered elements are considered using a shear flexibility correction which helps to account for large differences in layer moduli; this device is demonstrated for layered composites and sandwich wall construction. Very general sensitivity relationships are developed for isoparametric elements, for sensitivity parameters which may affect both the nodal element of an element and the relationship between local and global coordinate axes. These sensitivity formulas require much less computation than others in common use, and have potential application in shape optimization.

UNCLASSIFIED

SECURITY CLASSIFICATION OF THIS PAGE

FOREWORD

The work described herein was performed between October 1985 and October 1987 at the University of Dayton Research Institute (UDRI), Dayton, Ohio. This task, "Stochastic Analysis of Bladed Disk Systems", is part of the program conducted under contract F33615-85-C-2585, "Structural Testing and Analytical Research (STAR) of Turbine Components," for the Air Force Wright Aeronautical Laboratories Aero Propulsion and Power Laboratory, AFWAL/POTC, Wright-Patterson Air Force Base, Ohio.

Technical direction and support for this project were provided by Messrs. William A. Stange and John D. Reed (AFWAL/POTC). The effort was conducted within the Structures Group (Blaine S. West, Group Leader) of the Aerospace Mechanics Division (Dale H. Whitford, Project Supervisor). The UDRI Principal Investigator was Mr. Michael L. Drake.

The authors also wish to acknowledge the contributions of several individuals who made essential contributions to this work. Dr. Anthony K. Amos of AFOSR made numerous suggestions on the overall direction of the effort. Mr. Robert J. Dominic of UDRI provided day-to-day support and encouragement, as well as technical suggestions and experimental data. Mr. Thomas W. Held (UDRI) lent expertise in computer operations and communications whenever it was needed. Dr. Ronald F. Taylor, formerly Group Leader, Analytical Mechanics, provided administrative and technical guidance through much of the project.

Accession For	
NTIS GRA&I	<input checked="checked" type="checkbox"/>
DTIC TAB	<input type="checkbox"/>
Unannounced	<input type="checkbox"/>
Justification	
By	
Distribution/	
Availability Codes	
Dist	Avail and/or Special
A-1	



TABLE OF CONTENTS

<u>Chapter</u>		<u>Page</u>
1	INTRODUCTION	1
2	ANALYSIS PROCEDURES	5
	2.1 LINEAR STATIC SOLUTION	5
	2.2 NATURAL FREQUENCY SOLUTION	7
	2.3 STEADY-STATE HARMONIC SOLUTION	9
3	SENSITIVITY ANALYSIS	11
	3.1 SENSITIVITY FORMULAS FOR ISOPARAMETRIC ELEMENTS	11
	3.1.1 Shape Functions and the Jacobian	12
	3.1.2 Stiffness and Stress Sensitivities	15
	3.1.3 Applied Loads Sensitivities	16
	3.2 ORIENTATION SENSITIVITY	18
	3.2.1 Example of Orientation Sensitivity	19
	3.2.2 Basis Coordinate Transformation	22
	3.2.3 Derivatives of Coordinate Transformation	24
	3.2.4 Computational Considerations	25
	3.2.5 Example: Line Element in Space	26
	3.2.6 Application to Plate and Shell Elements	27
	3.3 SENSITIVITY ANALYSIS PROCEDURES	29
	3.3.1 Element-Level Calculations	29
	3.3.1.1 Intrinsic Parameters	30
	3.3.1.2 Geometric Parameters	31
	3.3.1.3 Mass Matrix Sensitivities	32
	3.3.2 System-Level Solution	33
	3.3.2.1 Static Response Sensitivity	33
	3.3.2.2 Frequency and Mode Shape Sensitivity	34
	3.3.2.3 Steady-State Harmonic Sensitivity	36

TABLE OF CONTENTS (Continued)

<u>Chapter</u>		<u>Page</u>
4	PROBABILISTIC ANALYSIS	37
	4.1 INTRODUCTION	37
	4.2 STATISTICAL PARAMETERS	39
	4.3 VARIANCE RELATIONSHIPS	42
	4.4 INTERPRETATION OF RESULTS	43
5	FINITE ELEMENT APPROXIMATION	51
	5.1 BACKGROUND	52
	5.2 BILINEAR MINDLIN PLATE ELEMENT	54
	5.3 STIFFNESS MATRIX STABILIZATION	58
	5.4 EFFECT OF STABILIZATION IN DYNAMICS	60
	5.5 MASS MATRIX FORMULATION	61
	5.5.1 Fully Integrated Consistent Mass	62
	5.5.2 Lobatto Integrated Consistent Mass	62
	5.5.3 Consistent Mass via a Projection	63
	Method	
	5.5.4 Consistent Mass by Reduced Integration	65
	5.5.5 Comparison of Mass Matrix Formulations	65
6	MATERIAL MODELING	72
	6.1 BACKGROUND	72
	6.2 LAMINATE STIFFNESS CHARACTERISTICS	73
	6.3 SHEAR FLEXIBILITY CORRECTIONS	74
	6.4 UNCOUPLED CORRECTIONS FOR ORTHOTROPIC	79
	LAMINATES	
	6.5 SHEAR STRESS RECOVERY	80
7	NUMERICAL EXAMPLES	81
	7.1 DYNAMICS EXAMPLES	81
	7.1.1 Comparison of Mass Formulations for	82
	Axial Vibration	
	7.1.2 Vibration of a Corner-Supported Plate	85
	7.1.3 Vibration of Free-Free Square Plate	89
	7.2 COMPOSITES AND LAYERED STRUCTURES	89
	7.2.1 Unsymmetric Laminated Plate	91
	7.2.2 Three-Layered Plate under Pressure	91
	7.2.3 Circular Sandwich Plate	95
	7.2.4 Rectangular Sandwich Plate	100
	7.2.5 Vibration of a Layered Panel	100

TABLE OF CONTENTS (Concluded)

<u>Chapter</u>	<u>Page</u>
7.3 SENSITIVITY ANALYSIS EXAMPLES	104
7.3.1 Static Analysis of a Tension Strip .	104
7.3.2 Statics of a Cantilever Beam	104
7.3.3 Orientation Sensitivity of a Beam .	107
7.3.4 Frequency Sensitivity of a Flat Strip	112
7.3.5 Frequency Sensitivity of a Beam . .	115
7.3.6 Twisted Plate Frequency Sensitivity	117
7.4 PROBABILISTIC ANALYSIS EXAMPLES	121
7.4.1 Forced Vibration of a Cantilever Beam	121
7.4.2 Natural Frequencies of a Twisted Blade	132
REFERENCES	139
Appendix A. PROTEC Input Data Descriptions	A-1
Appendix B. POSFIL Results File Description	B-1
Appendix C. LAYSTR Layer Stress File Description	C-1
Appendix D. PATRAN Interfaces (PATPRO/PROPAT)	D-1
Appendix E. DISSPLA Interface (PRODIS)	E-1

LIST OF FIGURES

<u>Figure</u>		<u>Page</u>
1	Bladed Disk	2
2	Truss Member with One Geometric Variable	20
3	Local Coordinate System Definition	23
4	Local Coordinates for Quadrilateral Element	28
5	Circular Arc with Variable Radius	41
6	Graphical Interpretation of the Distribution Function $\phi(z)$	47
7	Percentile Values of Natural Frequency for a Plate with Thickness Variation	49
8	Bilinear Mindlin Plate Element	55
9	Hourglass Displacement Pattern	57
10	Combined Hourglass-rotation Mode	67
11	Hourglass-rotation Mode in a Regular Mesh	69
12	Slender Strip Geometry and Properties	83
13	Corner-supported Square Plate	87
14	Semi-infinite Plate with Sinusoidal Pressure	92
15	Transverse Shear Stresses in Unsymmetric Plate	93
16	Square [0/90/0] Plate under Pressure Load	94
17	Circular Sandwich Plate	97
18	Moment Resultants in Circular Sandwich Plate	98
19	Shear Forces in Circular Sandwich Plate	99
20	Clamped Sandwich Panel under Uniform Pressure	101
21	Rectangular [0/90/0] Laminate	102
22	Cantilever Beam with Tip Load	106
23	Cantilever with Specified Angular Orientation	110
24	Twisted Cantilever Plate	118
25	Frequency Response of Cantilever Beam	122
26	Amplitude Sensitivities for Cantilever Beam	124
27	Displacement Amplitude Variance versus Frequency	126
28	Tip Displacement versus Frequency and Confidence Level	127
29	Displacement-Frequency-Confidence Level Surface	128
30	Moment Amplitude Variance versus Frequency	129
31	Root Moment versus Frequency and Confidence Level	130
32	Moment-Frequency-Confidence Level Surface	131
33	Finite Element Model of 45-Degree Twist Blade	133
34	Twist Profiles versus Twist Parameter "C"	134
35	Blade Frequencies as Functions of Twist Parameter	137
36	Frequency Variances for Twisted Blade	138

LIST OF TABLES

<u>Table</u>		<u>Page</u>
1	Number of Standard Deviations versus Percentile Level	48
2	Shear Factors for Graphite/Epoxy Laminates	78
3	Comparison of Results for Planar Vibration of Thin Strip	84
4	Vibration Modes of Thin Strip (Four-Element Solution)	86
5	Natural Frequencies for Corner-Supported Plate	88
6	Natural Frequencies for Free-Free Plate	90
7	Normalized Stresses for Square [0/90/0] Plate	96
8	Natural Frequencies of [0/90/0] Plate	103
9	Sensitivity Data for Simple Tension Problem	105
10	Displacement Sensitivity Data for Cantilever Beam	108
11	Force Sensitivity Data for Cantilever Beam	109
12	Results for Angular Orientation Problem ($\theta=0$)	111
13	Results for Angular Orientation Problem ($\theta=26.565^\circ$)	113
14	Frequency Sensitivities for Axial Vibration Problem	114
15	Frequency Sensitivities for Cantilever Beam	116
16	Frequency Comparison for 30° Twisted Plate	119
17	Frequency Sensitivities for 32° Twisted Plate	120
18	Natural Frequencies for 45° Twisted Plate	136

CHAPTER 1

INTRODUCTION

Turbomachinery components exhibit more diverse and complex structural behavior than most classes of engineering structures. Stress analysis of rotating propulsion system components has been a driving force in the development of many of the most sophisticated numerical methods in common use: substructuring and cyclic symmetry techniques, large-scale eigensolution algorithms, creep and thermoplasticity models, and modal and reduced basis methods. Even with the powerful analytical tools and software which exist today, the stress and vibration analysis of turbomachine components is usually a challenging task. The most important contributors to this analytical complexity are:

- 1. intricacy of the structure geometry and properties;
- 2. nonlinearity and its influence on other responses; and
- 3. uncertainty in properties, loading, and other variables.

Applied research in finite element methods and numerical solution algorithms at the present time is concerned, in large measure, with addressing these problem areas.

This report addresses the issue of uncertainty in defining a structural analysis model and interpreting the results. A bladed disk (Figure 1) is a useful example of the sources of uncertainty which may exist for a single model. Blade-to-blade variations may occur for overall dimensions or thickness profiles because of the manufacturing processes involved. Material properties, even within a batch of material, change from point to point. At the blade roots, the connection between blade and disk is slightly different for each blade. Furthermore, each of these effects is likely to change as a result of usage and wear. Finally, the external forces acting on the system include body (centripetal) forces, surface pressures, and perhaps contact forces (when a shroud or platform damper is present). With the exception of the

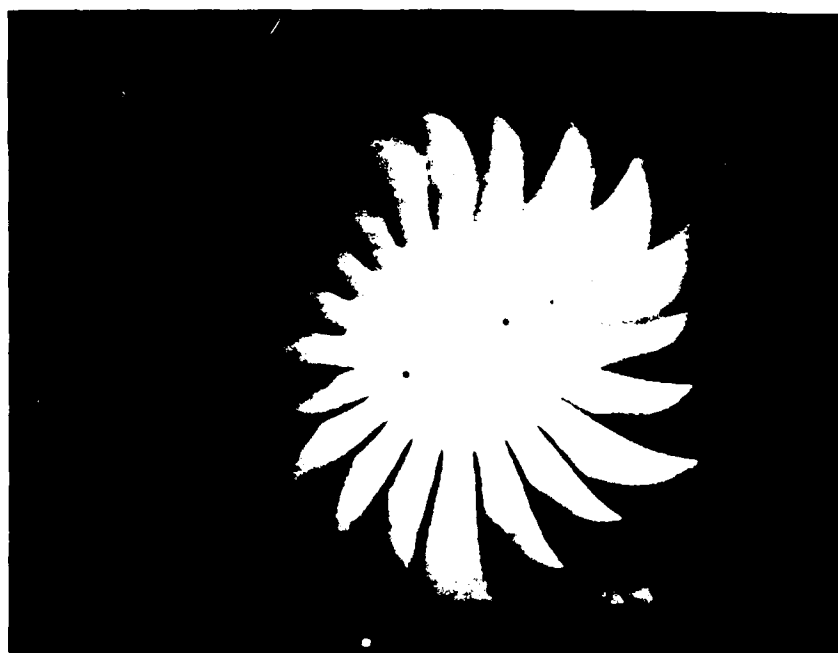
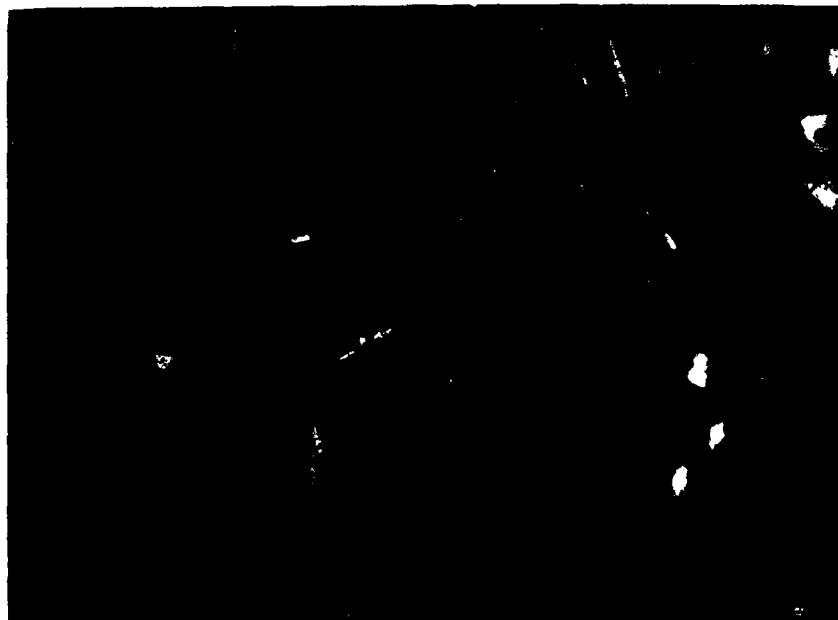


Figure 1. Bladed Disk.

centripetal forces, these loads are usually difficult to define. Pressures, for instance, vary because of flow paths established by earlier stages, and the presence of struts and other obstructions.

All of the effects mentioned above are statistical in nature. It is common practice to estimate them, conservatively if possible, for the purpose of analysis, and then to perform extensive testing of the finished system. However, certain of these statistical effects are fundamental to the structural behavior of interest. For example, the mistuning¹⁻⁵ which results from blade-to-blade property variations in a bladed disk system may help to stabilize the flutter behavior of the system due to mode localization effects⁶, but may have a deleterious effect on forced vibration amplitudes⁷.

This report presents the development of probabilistic methods for the analysis of turbomachinery components. A considerable body of work exists in probabilistic structural dynamics,⁸ and the present study builds upon these concepts. We adopt a middle ground in the complexity of our statistical technique, in return for ease in specifying the analytical problem and the ability to solve large problems at reasonable cost. While the statistical approach is relatively simple, it is consistent with the level of information which is typically available concerning variations in geometry and properties. The probabilistic solution relies heavily on sensitivity analysis techniques, and for this reason is applicable to models which are large and complex. We address static, steady-state forced vibration, and natural frequency problems, all in a similar fashion.

Chapters 2 through 4 describe the analysis methods and solution algorithms used, from a systems point of view. A finite element discretization is assumed, but the development is otherwise general. We begin with the basic solution paths in Chapter 2. Chapter 3 develops the sensitivity analysis techniques used

to drive the probabilistic calculations. The methods described include new developments in geometric shape sensitivity analysis which also have potential application in shape optimization. The probabilistic analysis is then outlined in Chapter 4.

Chapters 5 and 6 deal with finite element technology. In the interest of streamlining both the basic solution and the sensitivity calculations, we employ a Mindlin plate element based upon uniformly reduced numerical integration. While substantial efforts have been devoted to developing improved elements of this type,⁹ researchers have neglected some important issues which are crucial in dynamic problems; this is the main topic in Chapter 5. Chapter 6 describes the methods used for considering layered components using conventional plate/shell elements. Although the analysis of composite blades is not the central issue in this work, it is likely to become a routine requirement in the future.

Chapter 7 discusses a number of numerical examples which illustrate various aspects of the present study. We demonstrate the correctness and importance of the element-level techniques of Chapters 5 and 6. Several sensitivity analyses show the capability of the methods described here, and point out the modeling techniques which are preferred for geometric sensitivities. The probabilistic solution is applied to analytical examples as well as comparisons with experimental data.

The Appendices contain the documentation of all computer software associated with the work described. Computer programs have been implemented for the finite element solution methods developed herein, and for data communications with modeling and graphics software such as PATRAN¹⁰ and DISSPLA.¹¹

CHAPTER 2

ANALYSIS PROCEDURES

This Chapter reviews the basic methods of solution used in the deterministic portion of the finite element analysis. Primary emphasis is placed upon the system-level equations resulting from a finite element discretization, which have the general form:

$$KU + M\ddot{U} = F \quad (1)$$

Here K and M are the stiffness and mass matrices, which normally are large, sparse, and symmetric; $U(t)$ are the generalized displacements at the nodes of the finite element model, and $F(t)$ are the corresponding generalized forces. The details of the finite element approximation are described separately in Chapters 5 and 6. For more information on the basics of numerical algorithms as applied to finite element systems, the reader is encouraged to consult the standard texts on finite element analysis.¹²⁻¹⁵

2.1 LINEAR STATIC SOLUTION

For quasi-static loading and response, the applied forces $F(t)$ are constant, and the accelerations \ddot{U} vanish. The system of ordinary differential equations (Equation 1) describing the model then becomes the algebraic system:

$$KU = F \quad (2)$$

which must be solved for the (constant) nodal displacements U .

An effective solution of the static system (2) must exploit the symmetry and sparsity of matrix K , since unique nonzero terms occupy only 10-20 percent of the matrix in most problems. The solution technique also must permit economical re-solution of the system for new right-hand vectors; this facility is useful for

considering multiple loading conditions and for performing sensitivity analysis.

In the present work we adopt the triple factorization, or Gauss-Doolittle, technique.^{12,16} The first step, which involves only the coefficient matrix, is the symmetric factorization:

$$K = LDL^T \quad (3)$$

in which L is a unit lower triangular matrix:

$$L_{ij} = \begin{cases} 1, & i = j \\ 0, & i < j \end{cases} \quad (4)$$

and D is diagonal. It is straightforward to show that the local bandwidth of L never exceeds that of K. Therefore, the strict lower triangle of L can replace that of K, and D can be stored on the diagonal of K to minimize storage requirements. Computations on elements outside the envelope of nonzero coefficients are easy to eliminate, leading to an efficient solution procedure.

Once the factorization is complete, the equivalent system

$$LDL^T U = F \quad (5)$$

can be solved in three steps:

$$\begin{aligned} LZ &= F && \text{(forward substitution)} \\ Dy &= z && \text{(scaling)} \\ L^T U &= y && \text{(backward substitution)} \end{aligned} \quad (6)$$

for each right-hand side of interest.

The equation-solving routines used in this work are based upon the solution package published by Felippa.¹⁷ The original

code is efficient and well-documented, and has been tested extensively.

2.2 NATURAL FREQUENCY SOLUTION

In the natural frequency problem, the applied forces are set to zero and all displacements are assumed to vary sinusoidally in time:

$$U = X \sin(\omega t) \quad (7)$$

The resulting discrete equations of motion become:

$$KX = \lambda MX \quad (8)$$

in which $\lambda = \omega^2$. This symmetric generalized eigenvalue problem is solved using the subspace iteration algorithm.¹⁸

Subspace iteration is a vector iteration method in which a relatively small number of trial vectors, which are modified in a systematic manner to span the least-dominant p -dimensional subspace of K and M (where ' p ' is the number of trial vectors used in the calculation). The number of trial vectors is selected automatically; for a system of order N , for which n eigenvalues are to be computed, we take:

$$p = \min [N, 2n, n+8] \quad (9)$$

The essential steps in the algorithm are as follows:

1. Let $k=1$, and define starting vectors Y_0 .
2. Solve $KX_{k+1} = Y_k$ for X_{k+1} .
3. Form subspace stiffness $k_{k+1} = X_{k+1}^T K X_{k+1} = X_{k+1}^T Y_k$.

4. Compute $\bar{Y}_{k+1} = MX_{k+1}$.
5. Form subspace mass matrix $m_{k+1} = X_{k+1}^T MX_{k+1} = X_{k+1}^T \bar{Y}_{k+1}$.
6. Solve the subspace eigenvalue problem (of order p):

$$K_{k+1} q_{k+1} = m_{k+1} q_{k+1} \Lambda_{k+1}$$

for the diagonal matrix of eigenvalues Λ and the eigenvectors q .

7. Arrange the eigenvalues Λ in ascending order; normalize the eigenvectors q .
8. Form new trial vectors $Y_{k+1} = \bar{Y}_{k+1} q_{k+1}$.
9. Check for convergence; for each eigenvalue, convergence is declared whenever $\frac{|\lambda_{k+1} - \lambda_k|}{\lambda_{k+1}} \leq \epsilon$, where ϵ is a tolerance on the order of 10^{-6} .
10. If not converged, let $k \leftarrow k+1$ and return to Step (2).

The strong points of the algorithm are its efficiency for large systems, and its ability to maintain a respectable convergence rate for systems having repeated roots.

For unconstrained systems, the stiffness K is singular, and the solution indicated in Step (2) of the algorithm is undefined. In such cases, we employ an eigenvalue shift which renders the coefficient matrix positive definite. In place of the original system, we solve:

$$(K+sM)X = (\lambda+s)MX \quad (10)$$

for the shifted eigenvalues $\lambda+s$ and the eigenvectors X . The shift s is a positive number which must be sufficiently large to make the coefficient matrix $(K+sM)$ numerically non-singular. The eigenvectors X are unchanged from those of the original system, and the natural frequencies may be recovered using $\omega = \sqrt{\lambda}$, after subtracting the shift s from the computed eigenvalues.

The individual mode shapes X are normalized so that the magnitude of the largest displacement component is equal to one. Stress data obtained from the eigenvalue solution are computed from the normalized mode shapes, and indicate only the relative magnitudes for each mode.

2.3 STEADY-STATE HARMONIC SOLUTION

In steady-state harmonic analysis, the nodal forces vary sinusoidally in time, so that:

$$F = F_0 \sin(\omega t) \quad (11)$$

where ω is a known forcing frequency. For an undamped elastic system the steady-state solution $U(t)$ is sinusoidal, and in phase with the forcing frequency,

$$U = U_0 \sin(\omega t) \quad (12)$$

The dynamic equations of motion reduce to:

$$(K - \omega^2 M) U_0 = F_0 \quad (13)$$

For a given frequency, then, the problem resembles a linear static system and may be solved directly for U_0 . The usual stress recovery procedures, based upon the amplitudes U_0 , result in stress amplitude data, since $\sigma = \sigma_0 \sin(\omega t)$.

In practice, we are normally interested in the response of the system throughout a specified range of forcing frequencies. The solution accepts a series of forcing frequencies, recomputing the harmonic stiffness $K - \omega^2 M$ at each frequency. The resulting displacement, strain, and stress amplitudes at selected nodes or elements may be plotted versus forcing frequency to characterize the frequency response of the system.

CHAPTER 3

SENSITIVITY ANALYSIS

This chapter describes the calculation of sensitivity data by direct methods for isoparametric plate or shell elements. Sensitivity parameters of interest include intrinsic properties such as material modulus and plate thickness, as well as geometry variables which influence the size and shape of a structure. The sensitivity calculation therefore must consider the parametric mapping within an element, as well as the influence of geometric variables on the orientation of an element in space. The methods presented specialize directly to continuum elements, in which the coordinate transformation is omitted, or to simple structural members situated arbitrarily in space.

We begin with the development of the general relationships needed for performing geometric (or shape) sensitivity analysis with isoparametric finite elements. The additional contribution to geometric sensitivity caused by a changing local-to-global axis transformation is considered in Section 3.2. Finally, the application of these methods, as well as standard techniques for computing property sensitivities, to plate and shell finite elements is discussed in Section 3.3.

3.1 SENSITIVITY FORMULAS FOR ISOPARAMETRIC ELEMENTS

This section presents the development of several analytical relationships needed for shape sensitivity calculations. Methods for computing sensitivities with respect to intrinsic properties of an element, such as thickness, density, or modulus, are relatively straightforward; techniques of this type are used widely in structural optimization.¹⁹⁻²² When control parameters affect the nodal positions within a model, however, the effect of changing a given parameter is much more complex. Both the shape and orientation of an isoparametric element depend upon the nodal

positions, and the sensitivity analysis must account for each effect properly. A number of researchers have addressed the topic of geometric sensitivity analysis,²³⁻²⁷ but the formulation of efficient computational techniques remains an important area of research.

The techniques discussed here for geometric sensitivity analysis are oriented toward two- and three-dimensional continua modeled with isoparametric finite elements. The notable feature of these formulas is their simplicity, which leads to quick and systematic computational algorithms for most standard elements. While our use of these methods is in probabilistic analysis, the same approach is suitable for use in structural optimization.

3.1.1 Shape Functions and the Jacobian Determinant

In isoparametric finite elements, element stiffness and mass matrices and consistent load vectors are computed by numerical integration. For example, the element stiffness has the general form

$$K = \int_{\Omega_e} B^T D B |J| d\Omega_e \quad (14)$$

in which B contains the strain-displacement relationship, D the elastic constants, and $|J|$ is the Jacobian determinant. The area or volume element $d\Omega_e$ refers to the unit (or biunit) square or cube in parametric coordinates. The element geometry enters this calculation through the strain-displacement matrix B , which consists of Cartesian derivatives of the element shape functions, and the determinant $|J|$. In a two-dimensional continuum element, for instance, the portion of the strain-displacement relation pertaining to node I of an element is:

$$B_I = \begin{bmatrix} \partial N_I / \partial x_1 & 0 \\ 0 & \partial N_I / \partial x_2 \\ \partial N_I / \partial x_2 & \partial N_I / \partial x_1 \end{bmatrix} \quad (15)$$

in which N_I is the shape function for node I. The Jacobian determinant is:

$$|J_{i\alpha}| = \left| \frac{\partial x_i}{\partial \xi_\alpha} \right| = \left| x_{iK} \frac{\partial N_K}{\partial \xi_\alpha} \right| \quad (16)$$

where x_{iK} is the coordinate x_i at nodal point K of an element. The coordinates ξ_α in Equation (16) refer to parametric directions within an element.

First consider the derivatives of the elements of B with respect to the nodal positions; these have the form $\partial(N_{J,n})/\partial x_{kI}$. We begin with the identity $JJ^{-1} = I$, which can be expressed in indicial form as follows:

$$\frac{\partial \xi_\alpha}{\partial x_m} \frac{\partial x_m}{\partial \xi_\beta} = \xi_{\alpha,m} x_{m,\beta} = \xi_{\alpha,m} N_{K,\beta} x_{mK} = \delta_{\alpha\beta} \quad (17)$$

Here lower-case Latin indices refer to the Cartesian coordinate directions, upper-case indices to the nodes of an element, and Greek indices to the parametric coordinate directions of an element. The summation convention is used here for all three types of indices; a comma indicates partial differentiation with respect to the coordinate following. Note also the interpolation used for the spatial coordinate x_m within an element, in terms of the shape functions $N_K(\xi)$ and the nodal coordinate values x_{mK} .

Since Equation (17) must hold for any values of the nodal coordinates,

$$\frac{\partial}{\partial x_{kI}} (\xi_{\alpha,m} N_{K,\beta} x_{mK}) = \frac{\partial}{\partial x_{kI}} (\delta_{\alpha\beta}) = 0 \quad (18)$$

Because the nodal positions are independent of one another, we have $\partial x_{kI}/\partial x_{mK} = \delta_{km} \delta_{IK}$, and Equation (18) becomes:

$$x_{m,\beta} \frac{\partial}{\partial x_{kI}} (\xi_{\alpha,m}) = -\xi_{\alpha,k} N_{I,\beta} \quad (19)$$

or, since $x_{m,\beta} \xi_{\beta,n} = \delta_{mn}$,

$$\frac{\partial}{\partial x_{kI}} (\xi_{\alpha,n}) = -\xi_{\alpha,k} \xi_{\beta,n} N_{I,\beta} = -\xi_{\alpha,k} N_{I,n} \quad (20)$$

For the derivatives of $N_{J,n}$ with respect to the nodal coordinates, then, we obtain:

$$\frac{\partial}{\partial x_{kI}} (N_{J,n}) = N_{J,\alpha} \frac{\partial}{\partial x_{kI}} (\xi_{\alpha,n}) = -N_{J,\alpha} \xi_{\alpha,k} N_{I,n} \quad (21)$$

or

$$\frac{\partial}{\partial x_{kI}} (N_{J,n}) = -N_{J,k} N_{I,n} \quad (22)$$

In general, if the nodal coordinates depend upon a set of control parameters P_m , it follows that

$$\frac{\partial}{\partial P_m} (N_{J,n}) = -N_{J,k} N_{I,n} \frac{\partial x_{Ik}}{\partial P_m} \quad (23)$$

The necessary computations to determine $\partial B / \partial P_m$, then, involve only the original shape function derivatives and known data describing the dependence of the nodal coordinates upon the parameters P_m .

For the derivatives of $|J|$, we note that

$$|J| = \epsilon_{ijk} x_{i,\xi_1} x_{j,\xi_2} x_{k,\xi_3} \quad (24)$$

or in terms of the nodal coordinates:

$$|J| = \epsilon_{ijk} x_{iM} x_{jN} x_{kP} N_{M,\xi_1} N_{N,\xi_2} N_{P,\xi_3} \quad (25)$$

in which ϵ_{ijk} is the permutation tensor. Note that each nodal coordinate x_{kI} appears linearly in Equation (25); it follows that

$\partial|J|/\partial x_{kI}$ may be obtained by replacing $x_{k,\alpha}$ by $N_{I,\alpha}$ and evaluating the resulting determinant. The expressions so obtained correspond to the determinants encountered in solving the system

$$\xi_{\alpha,k} N_{I,k} = N_{I,\alpha} \quad (26)$$

for $N_{I,k}$ by Cramer's rule; we observe directly that

$$\frac{\partial|J|}{\partial x_{kI}} = |J| N_{I,k} \quad (27)$$

Therefore, the derivatives of the Jacobian determinant can be computed directly using only the shape function derivatives and the Jacobian determinant for the original element. When the node coordinates in turn depend upon geometric parameters P_m , we have

$$\frac{\partial|J|}{\partial P_m} = |J| N_{I,k} \frac{\partial x_{kI}}{\partial P_m} \quad (28)$$

The relationships (22), (23), (27), and (28) above describe completely the dependence of the element matrices upon the nodal positions, and provide the basis for many important sensitivity calculations. The next two subsections illustrate their use in some common cases of geometric sensitivity analysis.

3.1.2 Stiffness and Stress Sensitivities

The simplest and perhaps most common sensitivity calculation involves the determination of static response derivatives with respect to control parameters. In what follows, we will denote the response derivative with respect to a typical parameter P by a prime; that is, $()' = \partial()/\partial P$.

For the displacement sensitivities, we begin with the static equilibrium equations $Ku = F$ for the complete model, and note that

$$K'u + Ku' = F' \quad (29)$$

The sensitivities u' therefore may be found using the already-factored stiffness, since

$$Ku' = F' - K'u \quad (30)$$

The internal force sensitivity $K'u$ in Equation (30) is best evaluated directly in vector form, element by element, and then assembled in the same way as the element loading vectors. Since the element stresses are

$$\sigma = DBu \quad (31)$$

the product $K'u$ is simply

$$K'u = \int_{\Omega_e} [(B')^T \sigma |J| + B^T DB'u |J| + B^T \sigma |J|'] d\Omega_e \quad (32)$$

The computation of $K'u$ is possible only after the basic solution is complete, but requires much less arithmetic than the element matrices themselves. At each sampling point, it is necessary to form B and B' , compute the stresses $\sigma = DBu$ and the derivatives $DB'u$; two matrix-vector products then complete the contribution to the integral, since the last two terms may be combined.

Once the solution for u' from Equation (30) is complete, the stress sensitivities may be obtained from

$$\sigma' = DB'u + DBu' \quad (33)$$

for each element.

3.1.3 Applied Loads Sensitivities

The load sensitivity F' in Equation (30) may be zero, as in the case of point forces, or may depend upon the model geometry, as for pressure loads and body forces. Consider a nonuniform

body force, whose nodal values within an element are f_{kI} ; that is, the components f_k of the force vector per unit volume at any point are $N_I f_{kI}$. The consistent force vector is then

$$F_{kJ} = \int_{\Omega_e} f_{kI} N_I N_J |J| d\Omega_e \quad (34)$$

Only $|J|$ is affected by the nodal coordinates, and therefore

$$F'_{kJ} = \int_{\Omega_e} f_{kI} N_I N_J |J|' d\Omega_e \quad (35)$$

in which the derivative $|J|'$ may be computed from Equation (28). Notice that, because the load sensitivity does not depend upon the displacement solution, F_{kJ} and F'_{kJ} may be computed simultaneously with the original consistent loads vector.

Surface load sensitivities are more complex, since geometry changes may affect not only the element of surface area but the orientation of the surface. The original force vector involves the surface integral

$$F_{kI} = \int_{\omega_e} p N_I n_k |J_\omega| d\omega_e \quad (36)$$

Here $n_k |J_\omega| d\omega_e = n_k dA_e$ is the element of surface area in physical coordinates, and ω_e refers to the loaded surface in parametric space. As for the body forces above, the pressure can be interpolated from nodal pressure values, $p(\xi) = N_K(\xi) p_K$. If R denotes the position vector of a point on the surface in question, then

$$n dA_e = \frac{\partial R}{\partial \xi_1} \times \frac{\partial R}{\partial \xi_2} d\xi_1 d\xi_2 \quad (37)$$

where ξ_α denote the parametric coordinates within the surface. In terms of the nodal coordinates, then,

$$F_{kI} = \int_{\omega_e} p \epsilon_{ijk} x_{iM} x_{jN} N_{M,\xi_1} N_{N,\xi_2} N_I d\omega_e \quad (38)$$

The corresponding derivatives with respect to nodal positions are given by

$$\frac{\partial F_{kI}}{\partial x_{nJ}} = \int_{\omega_e} p \epsilon_{ink} (x_{i,\xi_1} N_{J,\xi_2} - N_{J,\xi_1} x_{i,\xi_2}) N_I d\omega_e \quad (39)$$

Recall that the derivatives $R_{,\xi_1}$ and $R_{,\xi_2}$ are the surface tangents needed for the original surface pressure calculation; in terms of these two vectors, formula (39) becomes:

$$\frac{\partial F_{kI}}{\partial x_{nJ}} = \int_{\omega_e} p N_I [N_{J,\xi_1} (i_n \times R_{,\xi_2}) - N_{J,\xi_2} (i_n \times R_{,\xi_1})] d\omega_e \quad (40)$$

or, in terms of a design parameter P ,

$$F'_{kI} = \int_{\omega_e} p N_I [N_{J,\xi_1} (i_n \times R_{,\xi_2}) - N_{J,\xi_2} (i_n \times R_{,\xi_1})] \frac{\partial x_{nJ}}{\partial P} d\omega_e \quad (41)$$

Again, the necessary computations depend upon quantities which must be evaluated to form the original load vector, and can be performed at the same time as the consistent loads calculation.

3.2 ORIENTATION SENSITIVITY

The dimensionality of truss, beam, membrane and shell finite elements is often less than that of the global coordinate system, and element calculations must be performed in local coordinates. Statistical parameters or design variables which affect the nodal coordinates in such elements control both the element dimensions and orientation, and element design sensitivity calculations must account for both effects. The influence of geometric variables may be separated into two distinct contributions, which must be applied at separate stages of the sensitivity calculation.

In components built up from bars, beams, and panels, or in shell structures, one additional complication arises. Element stiffness and mass properties must be formulated in a local coordinate system, and then transformed to a common coordinate system for assembly and solution. Geometric parameters which affect the global coordinates X at a node may influence both the element coordinates x and the axis transformation relating the two. For instance, given the derivatives $\frac{\partial X}{\partial p}$ for a single parameter p , and the global-to-local transformation $x = AX$,

$$\frac{\partial x}{\partial p} = A \cdot \frac{\partial X}{\partial p} + \frac{\partial A}{\partial p} \cdot X \quad (42)$$

The effect of parameter p upon A cannot be neglected; nor can the relationship (42) always be applied directly in a single step. The example in the next section illustrates both of these points.

In subsequent sections, we propose a simple form for a general coordinate transformation, for which derivatives may be computed explicitly. The appropriate calculations are outlined, and the method is applied to a quadrilateral element in three dimensions.

3.2.1 Example of Orientation Sensitivity

The planar truss problem shown in Figure 2 demonstrates the need for including the effect of geometric parameters on the coordinate transformation for an element, and helps to clarify the proper methods for introducing this effect into the sensitivity calculation. For the axial force member in the Figure, we wish to determine the derivative $K' = \frac{\partial K}{\partial \theta}$. The exact result, for K referred to degrees of freedom $[U_A, V_A, U_B, V_B]$, is:

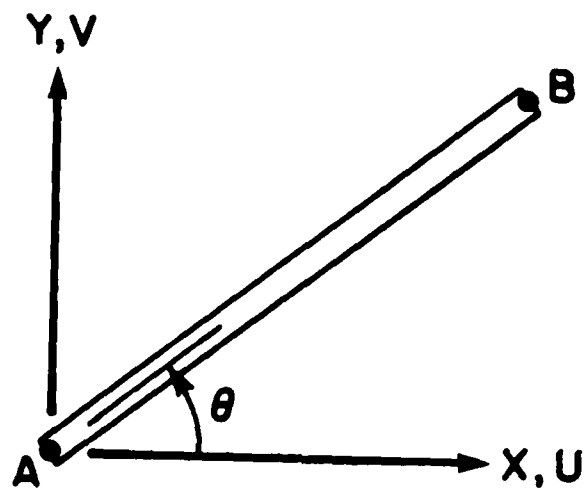


Figure 2. Truss Member with One Geometric Variable.

$$K' = \frac{EA}{L} \begin{bmatrix} -2\alpha\beta & \beta^2 - \alpha^2 & 2\alpha\beta & \alpha^2 - \beta^2 \\ \beta^2 - \alpha^2 & 2\alpha\beta & \alpha^2 - \beta^2 & -2\alpha\beta \\ 2\alpha\beta & \alpha^2 - \beta^2 & -2\alpha\beta & \beta^2 - \alpha^2 \\ \alpha^2 - \beta^2 & -2\alpha\beta & \beta^2 - \alpha^2 & 2\alpha\beta \end{bmatrix} \quad (43)$$

in which $\alpha = \sin\theta$, $\beta = \cos\theta$. The local coordinate transformation is

$$\begin{bmatrix} x \\ y \end{bmatrix} = \begin{bmatrix} \cos\theta & \sin\theta \\ -\sin\theta & \cos\theta \end{bmatrix} \begin{bmatrix} X \\ Y \end{bmatrix} \quad (44)$$

and the coordinates at end 'B' are $X_B = L\cos\theta$, $Y_B = L\sin\theta$.

Since θ does not affect the element length, neglecting $\frac{\partial A}{\partial \theta}$ leads to $x' = 0$, and hence $K' = 0$. However, it is easy to verify that applying equation (42) directly yields $x' = y' = 0$, and thus $K' = 0$. For correct results, it is necessary to introduce the two contributions in equation (42) at appropriate stages of the element calculation. During the element stiffness computation in local coordinates, only the overall shape and dimensions affect the computed results; here it is appropriate to introduce the "shape effect", $\frac{\partial x}{\partial \theta} = A \frac{\partial X}{\partial \theta}$, holding A constant. When the element matrices are transformed to global axes, the "orientation effect" $\frac{\partial x}{\partial \theta} = \frac{\partial A}{\partial \theta} x$ is significant. If the local stiffness K_ℓ and global stiffness K_g are related by

$$K_g = T^T K_\ell T \quad (45)$$

the appropriate geometric sensitivity is, in general,

$$K'_g = (T')^T K_\ell T + T^T K'_\ell T + T^T K_\ell T' \quad (46)$$

in which:

$$K'_\ell = \frac{\partial K_\ell}{\partial x_K} x'_K \quad (47)$$

Here x_K is the position of the K^{th} node of the element in local coordinates. The range of summation on K is equal to the number of nodes connected to the element.

The observation above is true for one- or two-dimensional elements situated in three-dimensional space as well. In practice, it is possible to avoid much of the computation implied in Equation (46), as outlined later in the discussion.

3.2.2 Basic Coordinate Transformation

Below, we propose a form of the local-to-global coordinate transformation which: (a) can be related to most common methods of establishing an element local axis system; (b) is simple enough that analytical expressions for its derivatives are easily obtained; and (c) requires relatively little computation to form both the original transformation and its derivatives. In what follows, we assume that the global nodal coordinates depend upon certain geometric parameters, and denote a typical one of these by "p". Furthermore, the effect of parameter p on the absolute location of the element centroid is neglected; that is, we let:

$$\frac{\partial x_K}{\partial p} = \frac{\partial x_K}{\partial p} - \frac{1}{N} \sum_{M=1}^N \frac{\partial x_M}{\partial p} \quad (48)$$

in which N is the number of nodes per element. With this assumption, the origin in both the local and global systems may be taken to coincide at all times without loss of generality. The effect of parameter changes on absolute position must be accounted for only in axisymmetric elements, for which the coordinate transformation is often unnecessary, and for load sensitivities which depend on absolute position, such as centrifugal forces.

Consider a local axis system defined by the centroid and two additional points (Figure 3). The positions of Points 1 and 2

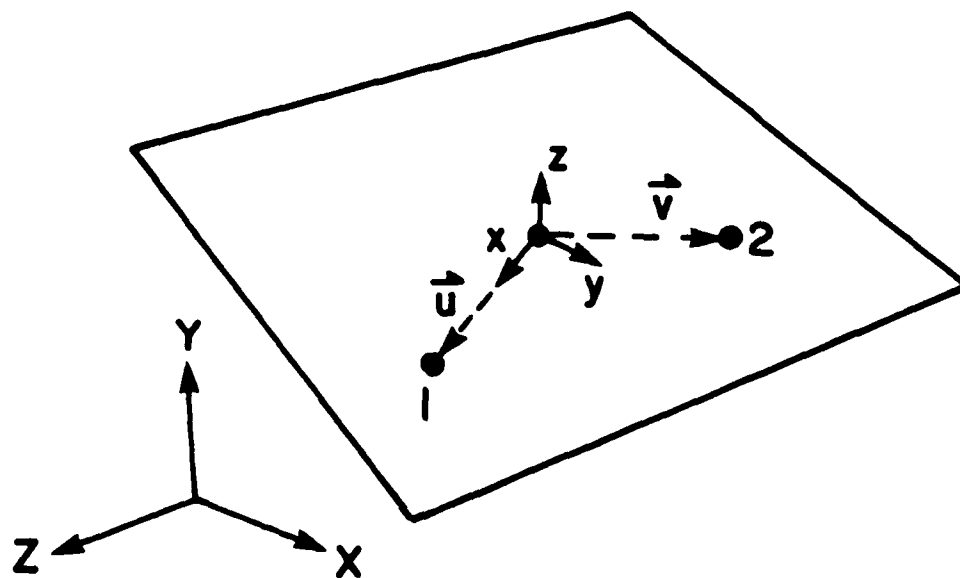


Figure 3. Local Coordinate System Definition.

relative to the element center are (X_1, Y_1, Z_1) and (X_2, Y_2, Z_2) , respectively. The local x axis is determined by the centroid and Point 1; Point 2 provides a third point in the local (x,y) plane. In terms of vectors u and v , shown in the Figure, the unit vectors defining the local axes are:

$$e_1 = \frac{u}{|u|}; \quad e_3 = \frac{u \times v}{|u \times v|}; \quad e_2 = e_3 \times e_1 \quad (49)$$

Define the constants

$$\begin{aligned} C_{yz} &= Y_1 Z_2 - Y_2 Z_1 \\ C_{zx} &= Z_1 X_2 - Z_2 X_1 \\ C_{xy} &= X_1 Y_2 - X_2 Y_1 \end{aligned} \quad (50)$$

$$\begin{aligned} D_x &= Z_1 C_{zx} - Y_1 C_{xy} \\ D_y &= X_1 C_{xy} - Z_1 C_{yz} \\ D_z &= Y_1 C_{yz} - X_1 C_{zx} \end{aligned} \quad (51)$$

and the length measures

$$\begin{aligned} \alpha_1 &= \sqrt{X_1^2 + Y_1^2 + Z_1^2} \\ \alpha_3 &= \sqrt{C_{yz}^2 + C_{zx}^2 + C_{xy}^2} \\ \alpha_2 &= \alpha_1 \alpha_3 \end{aligned} \quad (52)$$

Then the transformation matrix A , whose rows are the elements of the unit vectors e_i , is simply:

$$A = \begin{bmatrix} X_1/\alpha_1 & Y_1/\alpha_1 & Z_1/\alpha_1 \\ D_x/\alpha_2 & D_y/\alpha_2 & D_z/\alpha_2 \\ C_{yz}/\alpha_3 & C_{zx}/\alpha_3 & C_{xy}/\alpha_3 \end{bmatrix} \quad (53)$$

3.2.3 Derivatives of Coordinate Transformation

Given the derivatives $X'_1, Y'_1, Z'_1, X'_2, Y'_2, Z'_2$, it is a simple matter to compute the derivatives of the transformation matrix A . The derivatives of the constants above are (for example):

$$C'_{yz} = Y'_1 Z_2 + Y_1 Z'_2 - Y'_2 Z_1 - Y_2 Z'_1 \quad (54)$$

$$D'_x = Z'_1 C_{zx} + Z_1 C'_{zx} - Y'_1 C_{xy} - Y_1 C'_{xy} \quad (55)$$

and

$$\alpha'_1 = (X_1 X'_1 + Y_1 Y'_1 + Z_1 Z'_1) / \alpha_1 \quad (56)$$

$$\alpha'_3 = (C_{yz} C'_{yz} + C_{zx} C'_{zx} + C_{xy} C'_{xy}) / \alpha_3 \quad (57)$$

$$\alpha'_2 = \alpha'_1 \alpha_3 + \alpha_1 \alpha'_3 \quad (58)$$

The derivative of A is then:

$$A' = \begin{bmatrix} \frac{X'_1 \alpha_1 - X_1 \alpha'_1}{\alpha_1^2} & \frac{Y'_1 \alpha_1 - Y_1 \alpha'_1}{\alpha_1^2} & \frac{Z'_1 \alpha_1 - Z_1 \alpha'_1}{\alpha_1^2} \\ \frac{D'_x \alpha_2 - D_x \alpha'_2}{\alpha_2^2} & \frac{D'_y \alpha_2 - D_y \alpha'_2}{\alpha_2^2} & \frac{D'_z \alpha_2 - D_z \alpha'_2}{\alpha_2^2} \\ \frac{C'_{yz} \alpha_3 - C_{yz} \alpha'_3}{\alpha_3^2} & \frac{C'_{zx} \alpha_3 - C_{zx} \alpha'_3}{\alpha_3^2} & \frac{C'_{xy} \alpha_3 - C_{xy} \alpha'_3}{\alpha_3^2} \end{bmatrix} \quad (59)$$

It is easy to verify that the original transformation A , computed as indicated in the previous section, requires 10 additions or subtractions, 28 multiplies or divides, and two square roots. If the derivatives of A are computed at the same time, an additional 32 additions or subtractions, 61 multiplies or divides, and no additional square roots are required per geometric parameter.

3.2.4 Computational Considerations

In practice, computation of the matrix form of K' is usually unnecessary. For example, sensitivities for static analysis may be determined from:

$$Ku' = F' - K'u \quad (60)$$

and only the product $K'u$, formed element-by-element and assembled as a vector, is required.

Consistent with the transformation in Equation (45), we assume that the element displacements referred to local coordinates are $u_\ell = Tu_g$. Thus, the product to be formed is, from equation (46):

$$K'_g u_g = (T')^T (K_\ell u_\ell) + T^T (K'_\ell u_\ell + K_\ell T' u_g) \quad (61)$$

The vector $K_\ell u_\ell$ in the first term represents the internal element forces in local coordinates, which may be computed directly from:

$$F_\ell = K_\ell u_\ell = \int_{\Omega_e} B^T \sigma |J| d\Omega_e \quad (62)$$

The vector $K_\ell T' u_g$ appearing in the last term can be obtained in a similar fashion, after computing the stresses corresponding to a fictitious set of local nodal displacements $\bar{u}_\ell = T' u_g$. As noted in Section 3.1.2, an efficient means of calculating the remaining vector $K'_\ell u_\ell$ is to use the relationship

$$K'_\ell u_\ell = \int_{\Omega_e} [(B')^T \sigma |J| + B^T \sigma' |J| + B^T \sigma |J|'] d\Omega_e \quad (63)$$

Therefore, the calculation of sensitivities related to the local coordinate transformation requires only two additional internal force evaluations, and transformation of the resulting vectors to global coordinates.

3.2.5 Example: Line Element in Space

For the truss member considered earlier, and the geometric parameter θ , $K'_2 = 0$, and the sensitivity is due solely to the effect of θ on the coordinate transformation. Let the origin of coordinates correspond to Point A, and Point B to the first point defining the coordinate transformation (Point 1 above). Point 2 may correspond to any point in the plane not situated on the line AB. For simplicity, we will select $X_2 = 0$, Y_2 arbitrary. Since $X_1 = L\cos\theta$, $Y_1 = L\sin\theta$, $X'_1 = -L\sin\theta$, $Y'_1 = L\cos\theta$, it is easy to show, from Equation (59), that:

$$A' = \begin{bmatrix} -\sin\theta & \cos\theta & 0 \\ -\cos\theta & -\sin\theta & 0 \\ 0 & 0 & 0 \end{bmatrix} \quad (64)$$

Using Equation (46) with $K'_2 = 0$ yields the exact result shown in Equation (43).

3.2.6 Application to Plate and Shell Elements

Numerical examples for a two-dimensional element situated in three dimensions are somewhat difficult to present in a meaningful form. For the present, we simply outline the application of the procedure above for this important case. Numerical examples involving orientation sensitivity are presented in Chapter 7.

Figure 4 shows a quadrilateral element in three-space, with a common choice of local axes. The local x direction is oriented between the midpoints of edges 4-1 and 2-3; a vector between midpoints of the remaining edges completes the definition of the local (x,y) plane. We denote the coordinates of the corners by (X_{Ni}, Y_{Ni}, Z_{Ni}) . The coordinates X_1 and X_2 (for example) are then:

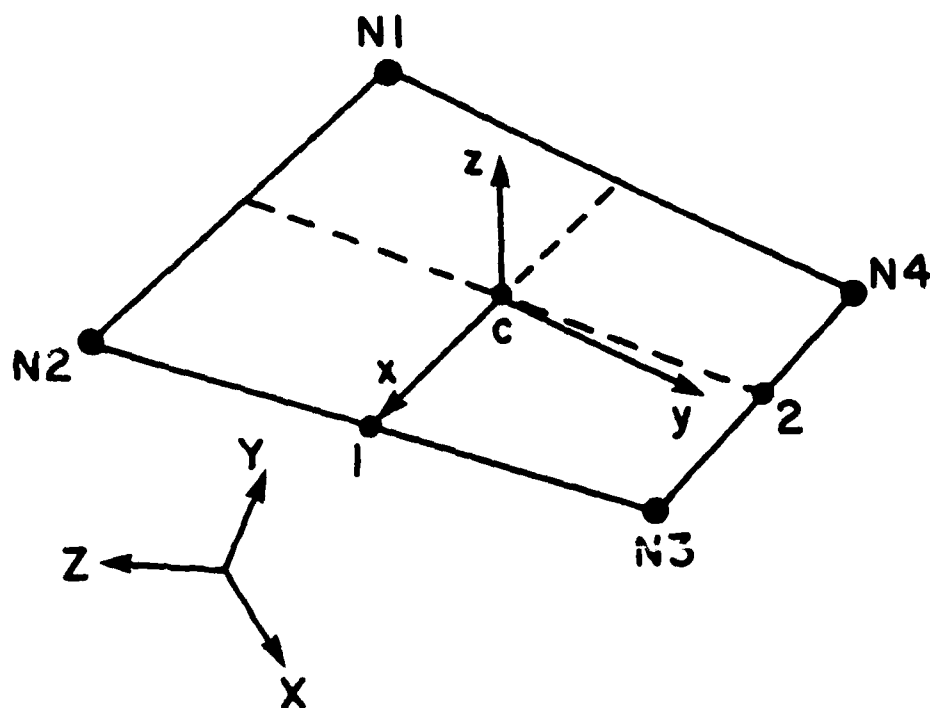


Figure 4. Local Coordinates for Quadrilateral Element.

$$\begin{aligned} X_1 &= \frac{1}{4} (-X_{N1} + X_{N2} + X_{N3} - X_{N4}) \\ X_2 &= \frac{1}{4} (-X_{N1} - X_{N2} + X_{N3} + X_{N4}) \end{aligned} \quad (65)$$

Coordinates Y_1, Z_1, Y_2, Z_2 are defined in a similar way. For the derivatives of these coordinates, we may use:

$$\begin{aligned} X'_1 &= \frac{1}{4} (-X'_{N1} + X'_{N2} + X'_{N3} - X'_{N4}) \\ X'_2 &= \frac{1}{4} (-X'_{N1} - X'_{N2} + X'_{N3} + X'_{N4}) \end{aligned} \quad (66)$$

and condition (48) is satisfied automatically. At this point, Equations (49) through (63) apply directly.

3.3 SENSITIVITY ANALYSIS PROCEDURES

The preceding Sections present the mathematical relationships necessary for geometric sensitivity calculations in isoparametric finite elements. In what follows, we outline the computational procedures used in sensitivity solutions for a complete finite element model. The sensitivity parameters of interest include intrinsic variables such as material properties and thicknesses, as well as geometric control variables which govern the size and shape of the model by controlling the nodal positions. The procedures discussed here for plates and shells may be specialized to other isoparametric elements (where the coordinate transformation is omitted), and to simpler structural elements. The methods described are efficient and accurate, and relatively simple to implement for most standard element types.

3.3.1 Element-Level Calculations

Consider a linear static problem for which a finite element discretization leads to the algebraic system $KU = F$. If the stiffness characteristics of the system or the applied forces are

dependent upon a parameter p , then the dependence of the nodal displacements U upon p may be obtained by solving:

$$KU' = F' - K'U \quad (67)$$

in which $()' = \partial() / \partial p$. Notice that the coefficient matrix in (67) is identical to that of the original problem, so that the factors of K may be reused in the sensitivity solution. We will focus upon the calculation of the product $K'U$, which is best performed element-by-element, and then assembled for the complete system.

While it is possible to compute K' directly for an element and then obtain the product $K'U$, this approach is unnecessarily time-consuming. We prefer to form $K'U$ directly in vector form, which reduces both the number of arithmetic operations and the computer memory required.

Let the stiffness matrix for an element be given by:

$$K = \int_{\Omega_e} A^T B^T D B A |J| d\Omega_e \quad (68)$$

in which A is a transformation from local to global coordinates, $u=AU$, B is a strain-displacement matrix, and D is the elasticity matrix. The region Ω_e is the domain of the element in parametric coordinates. The transformation matrix A may vary from point to point for curvilinear elements, but is constant over an element in most simpler elements.

3.3.1.1 Intrinsic Parameters

The product $K'U$ is simplest to obtain when parameter p corresponds to an intrinsic property, such as the modulus or thickness, since only the elasticity matrix is affected. Noting that $AU=u$, the local displacement vector, we can compute:

$$\bar{\sigma} = D' B u \quad (69)$$

and

$$\mathbf{K}'\mathbf{U} = \int_{\Omega_e} \mathbf{A}^T \mathbf{B}^T \bar{\sigma} |J| d\Omega_e \quad (70)$$

The computation indicated in Equation (69) is identical in form to the usual process of stress recovery, so that the calculation of $\mathbf{K}'\mathbf{U}$ for an element resembles an evaluation of the internal nodal forces. In fact, the element internal force routines may be used directly, with the exception of calculating \mathbf{D}' .

3.3.1.2 Geometric Parameters

When the parameter of interest affects the nodal positions, nonzero derivatives may occur for the element of area $|J|$, the strain matrix \mathbf{B} , and for the coordinate transformation matrix \mathbf{A} . We assume that the derivatives of the nodal coordinates are known, and represent these by $X'_{iK} = \partial X_{iK} / \partial p$, in which i ranges from one to three, and K from one to the number of nodes per element.

The calculation of \mathbf{B}' and $|J|'$ depends primarily upon the sensitivities of the shape function derivatives, $\partial(N_{K,i})/\partial p$ (Section 3.1.1). The transformation sensitivity \mathbf{A}' depends only upon the global nodal coordinates X_{iK} and their derivatives X'_{iK} , as discussed in Section 3.2. From the relationships developed in Sections 3.1 and 3.2, we can compute the product $\mathbf{K}'\mathbf{U}$ from:

$$\begin{aligned} \mathbf{K}'\mathbf{U} = \int_{\Omega_e} \{ & [(\mathbf{A}')^T \mathbf{B}^T + \mathbf{A}^T (\mathbf{B}')^T] \sigma |J| \\ & + \mathbf{A}^T \mathbf{B}^T [(\bar{\sigma} + \bar{\sigma}) |J| + \sigma |J|'] \} d\Omega_e \end{aligned} \quad (71)$$

in which:

$$\sigma = \mathbf{D}\mathbf{B}\mathbf{u} \quad (72)$$

$$\bar{\sigma} = \mathbf{D}\mathbf{B}\bar{\mathbf{u}} \quad (73)$$

$$\bar{\bar{\sigma}} = \mathbf{D}\mathbf{B}'\mathbf{u} \quad (74)$$

$$\mathbf{u} = \mathbf{A}\mathbf{U} \quad (75)$$

$$\bar{\mathbf{u}} = \mathbf{A}'\mathbf{U} \quad (76)$$

The operations indicated in Equations (71-76) are analogous to the usual displacement transformation, stress calculation, and internal force evaluation steps performed in a linear analysis.

3.3.1.3 Mass Matrix Sensitivities

Mass sensitivity calculations, as required in sensitivity analysis of natural frequencies, are simpler in form. Suppose that a solution has been performed for several of the dominant modes of a system:

$$KU - \omega^2 MU = 0 \quad (77)$$

Differentiating (77) with respect to the parameter of interest leads to the frequency sensitivity expression:²⁸

$$\omega'_i = \frac{U_i^T (K' - \omega_i^2 M') U_i}{2\omega_i U_i^T M U_i} \quad (i \text{ not summed}) \quad (78)$$

for the i^{th} mode of vibration. Equation (78) remains valid when repeated roots are present, and for any method of normalizing the eigenvectors U_i . The denominator is a scalar multiple of the generalized mass for mode i , which we choose to evaluate at the system level. The product $U_i^T K' U_i$ may be computed element by element, using the procedure outlined previously. We discuss the evaluation of the vector $M' U_i$ below.

Letting ξ, Ξ denote a particular component of the element displacement vector in local and global axes, respectively, we write the contribution to the mass matrix for component Ξ as:

$$M_{\Xi\Xi} = \int_{\Omega_e} \beta A^T N N^T A |J| d\Omega_e \quad (79)$$

in which β is a function of the element density and thickness. The best procedure for the sensitivity calculation in this case is element dependent. However, the fact that $\mathbf{N}^T \mathbf{A} \bar{\mathbf{E}} = \xi(\mathbf{x})$, the pointwise value of ξ , can always be exploited. Similarly, the product $\mathbf{N}^T \mathbf{A}' \bar{\mathbf{E}}$ resembles a point displacement value, but without the same physical interpretation. Again, the basic sensitivity calculations needed are limited to \mathbf{A}' and $|\mathbf{J}|$.

3.3.2 System-Level Solution

This section outlines typical procedures for performing sensitivity solutions, assuming that element-level routines are available for evaluating the vectors $\mathbf{K}'\mathbf{U}$ and $\mathbf{M}'\mathbf{U}$, and the scalar products $\mathbf{U}^T \mathbf{K}'\mathbf{U}$ and $\mathbf{U}^T \mathbf{M}'\mathbf{U}$ as required. In our implementation of these methods, we perform element calculations for a number of load cases or modes and for a number of sensitivity parameters, all in parallel. Sensitivity parameters may include the material modulus or density, element thickness, and any geometric control parameter defined in terms of derivatives of the global Cartesian coordinates at selected nodes with respect to the parameter.

3.3.2.1 Static Response Sensitivity

In static analysis, we first factor the original stiffness and solve for the nodal displacements:

$$\mathbf{K} = \mathbf{LDL}^T \quad (80)$$

$$\mathbf{LDL}^T \mathbf{U} = \mathbf{F} \quad (81)$$

For the first pass of sensitivity calculation, form the right hand side and solve for displacement sensitivities:

$$\mathbf{R} = \mathbf{F}' - \sum_{e=1}^{N_{el}} (\mathbf{K}'\mathbf{U})_e \quad (82)$$

$$LDL^T U' = R \quad (83)$$

The second pass of element sensitivity calculations yields the element stress sensitivities:

$$\sigma' = (DBA)'U + DBAU' \quad (84)$$

Which of the matrices D, B, A possesses nonzero derivatives is a function of parameter type.

Notice that if a particular sensitivity parameter does not affect a given element directly, the calculation of $K'U$ may be skipped, and the stress sensitivity reduces to $\sigma' = DBAU'$. In practice it is convenient to maintain a list of switches for each element, indicating the status (active or inactive) of all parameters. The selection of parameters such as modulus, density, and thickness may be tied to material or property set numbers, making it easy to determine whether or not a specific element is affected. If geometric parameters are defined in terms of nodal coordinate derivatives, the parameter is inactive for a given element only if all derivatives for each node connected to the element are zero.

3.3.2.2 Frequency and Mode Shape Sensitivity

For eigenvalue problems, we first solve the eigensystem and compute a generalized mass for each mode:

$$KU_i - \omega_i^2 MU_i = 0 \quad (85)$$

(i not summed)

$$m_i = U_i^T MU_i \quad (86)$$

For each parameter and mode, the frequency sensitivity Equation (78) may be summed element by element:

$$\omega_i' = \frac{1}{2\omega_i m_i} \sum_{e=1}^{N_{el}} [U_i^T K' U - \omega_i^2 U_i^T M' U_i] \quad (i \text{ not summed}) \quad (87)$$

In computing sensitivities of the eigenvectors, we adopt a modal representation, as suggested in Reference 28. For the i^{th} mode, let the eigenvector derivative be:

$$\mathbf{U}'_i = \Psi \beta_i \quad (88)$$

in which

$$\Psi = [\mathbf{U}_1, \mathbf{U}_2, \dots, \mathbf{U}_n] \quad (89)$$

is the modal matrix, and β_i is a vector of modal participation factors. Introducing (88) into the derivative of the original eigenvalue equation, and premultiplying by Ψ^T gives, for the i^{th} mode:

$$(\mathbf{k} - \omega_i^2 \mathbf{m}) \beta_i = -\Psi^T (\mathbf{K}' - \omega_i^2 \mathbf{M}') \mathbf{U}_i + 2\omega_i \omega'_i \Psi^T \mathbf{M} \mathbf{U}_i \quad (i \text{ not summed}) \quad (90)$$

Here $\mathbf{k} = \Psi^T \mathbf{K} \Psi$ and $\mathbf{m} = \Psi^T \mathbf{M} \Psi$ are the diagonal generalized stiffness and mass matrices. Notice that only the i^{th} component of the product $\Psi^T \mathbf{M} \mathbf{U}_i$, which is a column of \mathbf{m} , is nonzero. The element of β_i corresponding to mode 'n' is therefore:

$$(\beta_i)_n = \frac{-\mathbf{U}_n^T (\mathbf{K}' - \omega_i^2 \mathbf{M}') \mathbf{U}_i}{(k_{nn} - \omega_i^2 m_{nn})} \quad (i \neq n; \omega_i \neq \omega_n; i, n \text{ not summed}) \quad (91)$$

Let J be the degree of freedom which attains the largest value for mode i ; that is:

$$(\mathbf{U}_i)_J = \sup_n (\mathbf{U}_i)_n \quad (92)$$

As suggested by Rogers,²⁸ we force the normalizing basis for mode i to remain constant by requiring $(\mathbf{U}'_i)_J = 0$. This condition is sufficient to determine the remaining element of β_i :

$$(\beta_i)_i = - \frac{1}{(U_i)_J} \sum_{\substack{n=1 \\ n \neq i}}^N (\beta_i)_n (U_n)_J \quad (93)$$

in which N is the number of modes retained for the sensitivity solution. The necessary products besides the system generalized stiffness and mass consist of $U_n^T K' U_i$ and $U_n^T M' U_i$, which may be evaluated on an element basis.

3.3.2.3 Steady-State Harmonic Sensitivity

The steady-state forced response solution resembles a linear static solution, with the coefficient matrix K replaced by $K - \omega^2 M$ for a given forcing frequency. For a single value of the forcing frequency ω , we perform both the basic solution and all possible sensitivity solutions together, since the coefficient matrix remains constant. The numerical procedure is precisely the same as for static analysis, with obvious changes to the coefficient matrix and its derivatives.

The interpretation of values from the harmonic response sensitivity solution is different from static or free vibration problems. The displacement and stress solutions now represent amplitudes of these quantities, which vary sinusoidally with time at the forcing frequency (Section 2.3). The computed sensitivity values therefore represent derivatives of these amplitudes with respect to the parameters of interest.

CHAPTER 4

PROBABILISTIC ANALYSIS

This chapter outlines a general approach for estimating the variance of structural response variables, given the mean values and variances of system properties which are probabilistic in nature. The statistical analysis adopted here is rudimentary, to be sure; however, the treatment is consistent with the level of information which is readily available to the engineer, and lends itself to the analysis of relatively large and complex systems. The sections below discuss the philosophy of the approach, the statistical parameters of interest, and the mathematical relationships needed for computing variances of response quantities such as displacement, stress, and natural frequency.

4.1 INTRODUCTION

The notion of a probabilistic analysis encompasses numerous possible analytical techniques. Given that certain properties or dimensions of a system are subject to uncertainty, the proper choice of analysis method depends strongly upon the difficulty or cost of a single simulation, and upon one's knowledge about the statistical parameters of interest. We note some of the possible approaches below.

Stochastic analysis involves stating the differential system of interest in terms of stochastic quantities, and solving directly for the response in statistical terms. This approach is an active research area in applied mathematics²⁹. One-dimensional problems still represent a formidable challenge with this class of methods,³⁰ and the consideration of very complex systems is not feasible at this time.

Random field simulation is a relatively new approach developed by Liu and co-workers.³¹ In addition to discretizing the deterministic system of interest, new unknowns are introduced in

a finite element (or other numerical) model which describe higher statistical moments of the response. This augmented problem is solved in a single step for both the mean values (deterministic response) and the additional statistical variables. This method is capable of considering detailed autocorrelations for the statistical variables, but is best suited to moderately sized systems.

Monte Carlo simulation is appropriate if the statistical nature of the (few) independent variables is well-known, and the cost of a single analysis is small. Known information about the statistical parameters is used to generate a series of samples with representative values. A deterministic analysis is performed for each sample. The result is a sample of the response from which statistical data can be derived by standard methods.³²

In the present analysis we view probabilistic properties of a system as discrete random variables. The elastic modulus of a turbine blade, for instance, might vary from point to point in a different fashion for every blade manufactured; we choose to characterize this modulus by a mean value, and a single value of the variance. The information needed to perform a meaningful probabilistic analysis with this approach is usually available or can be estimated with a fair degree of accuracy. For example, if a modulus value is quoted as being " $E \pm \Delta E$ ", we normally interpret the quantity ΔE as representing three standard deviations; the range $E \pm \Delta E$ therefore includes approximately 99.7 percent of all samples.

The discrete random variable approach requires a similar level of information about all statistical variables. Therefore, routine quality control data or manufacturer's tolerances are the only additional information needed beyond that used to construct a deterministic finite element model. Together with the relatively low cost associated with solving relatively large models,

this simplicity makes the present method attractive for routine analysis work.

It should be noted that the results of an analysis based on the discrete random variable approach are not related in a simple way to results from the alternative methods mentioned previously. However, the basic trends predicted by either method will agree; that is, if the dispersion in a particular variable is large, and if the structural response varies significantly with the variable in question, then we expect a large variance in the response. In some cases, it is possible to show that the variances predicted using the present method are conservative (overestimated). For example, the variance in natural frequencies predicted when a physical property is assumed to vary with position is generally less than that computed when the property is constant throughout the model, but subject to the same variation in magnitude.

4.2 STATISTICAL PARAMETERS

In the present work, we consider four specific types of probabilistic variables:

- ☐ elastic modulus
- ☐ material density
- ☐ thicknesses
- ☐ arbitrary geometric variables

The modulus and density are tied to a specific material number in the finite element model. Each statistical variable is defined by specifying a property set number, the variable type (modulus or density), and the variance expressed in consistent units. In a similar fashion, a thickness variable may be defined for any existing property set in the model by specifying the number of the property set and a numerical value of the thickness variance.

Property variables (modulus, density, thickness) represent the simplest cases in terms of finite element implementation, since each one influences the stiffness and mass characteristics

in a simple way. In most cases the stiffness or mass matrix depends linearly upon the variable in question; for thickness variables, bending stiffnesses vary cubically; however, the necessary computations are still relatively simple.

"Arbitrary geometric variables" are implicitly defined quantities which influence the overall structural geometry. In the context of a finite element model, these geometric variables influence the nodal coordinates for all or part of the model. The geometric variables influence the stiffness and mass characteristics of individual elements, but in a more complex way than for property-based variables.

A simple example of a geometric statistical variable is useful to illustrate the nature of such a variable and the technique used to define it. Figure 5 shows a segment of a circular arc, whose radius R is chosen as a statistical variable. For a node located on the arc with angular coordinate θ , the Cartesian coordinates of the node corresponding to the nominal (mean) value of the radius, R_μ , are:

$$X_\mu = X_C + R_\mu \cos\theta \quad ; \quad Y_\mu = Y_C + R_\mu \sin\theta \quad (94)$$

In specifying the nominal coordinates of the node, the value of R is not defined explicitly. We define the statistical variable in terms of the numerical value of the variance, $\text{Var}[R]$, and the effect of the variable on the existing coordinates:

$$\frac{\partial X}{\partial R} = \cos\theta \quad ; \quad \frac{\partial Y}{\partial R} = \sin\theta \quad (95)$$

For a response variable $\tau(X,Y)$ which depends upon the coordinates X and Y , which in turn vary with R , it is possible to compute the derivative $\frac{\partial \tau}{\partial R}$ without knowing the nominal value of R explicitly:

$$\frac{\partial \tau}{\partial R} = \frac{\partial \tau}{\partial X} \frac{\partial X}{\partial R} + \frac{\partial \tau}{\partial Y} \frac{\partial Y}{\partial R} \quad (96)$$

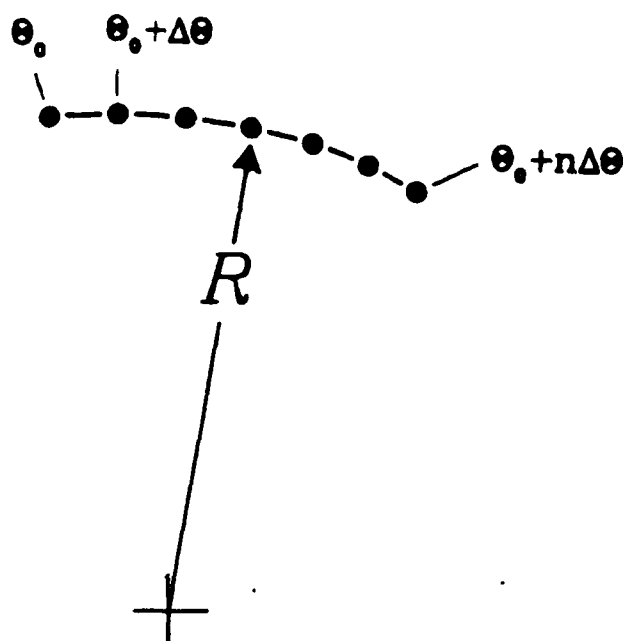


Figure 5. Circular Arc with Variable Radius.

This derivative and the variance of R are sufficient to complete the calculation of $\text{Var}[\tau]$, as described in the following Section.

4.3 VARIANCE RELATIONSHIPS

We wish to formulate a relationship between the mean values and variances of a series of random variables (moduli, densities, thicknesses, and geometric parameters) and those of one or more structural response quantities. Denote the random variables by p_i , and a typical response function by $\tau(p_1, p_2, \dots, p_n)$. If the function τ is linear in p_i , then:

$$\tau = \sum_{i=1}^n a_i p_i \quad (97)$$

then the expected value $E(\tau)$ is simply³³

$$E[\tau] = \sum_{i=1}^n a_i E[p_i] \quad (98)$$

and the variances are related by:

$$\text{Var}[\tau] = \sum_{i=1}^n a_i^2 \text{Var}[p_i] + 2 \sum_{i=1}^{n-1} \sum_{j=i+1}^n a_i a_j \text{Cov}[p_i, p_j] \quad (99)$$

in which the notation $\text{Cov}[a, b]$ denotes the covariance. When the function τ is more general, linearization of τ about the mean values $\mu_i = E[p_i]$ leads to:

$$\text{Var}[\tau] = \sum_{i=1}^n \left(\frac{\partial \tau}{\partial p_i} \right)^2 \text{Var}[p_i] + 2 \sum_{i=1}^{n-1} \sum_{j=i+1}^n \frac{\partial \tau}{\partial p_i} \frac{\partial \tau}{\partial p_j} \text{Cov}[p_i, p_j] \quad (100)$$

Note that the derivatives $\frac{\partial \tau}{\partial p_i}$ are to be evaluated at the point $p_i = \mu_i; i=1, 2, \dots, n$. This fact is exploited in constructing an efficient solution procedure.

For the present, we will consider the statistical parameters of interest to be completely independent, so that $\text{Cov}[p_i, p_j] = 0$ in all cases. The variance of any response quantity $r(p)$ therefore is given by:

$$\text{Var}[r] = \sum_{i=1}^n \left[\frac{\partial r}{\partial p_i} \right]^2 \text{Var}[p_i] \quad (101)$$

Computation of the response variances requires only the variance of each statistical parameter, and the parameter sensitivities $\frac{\partial r}{\partial p_i}$. Chapter 3 describes these calculations in detail.

4.4 INTERPRETATION OF RESULTS

The results of a probabilistic analysis include a basic solution (expected or mean values), and sensitivity and variance data for all displacement and stress variables. Each of these components of the solution data is useful in its own way. The basic solution identifies the type of response which occurs, and is used to identify critical areas in the structure.

Sensitivity data is often informative for design purposes, because it indicates which variables most influence the response in critical regions. It is important to recognize that the relative magnitude of sensitivities to different parameters is not necessarily significant. For instance, the sensitivity of a displacement or natural frequency to thickness may be several orders of magnitude larger than the sensitivity to modulus, only because of the difference in magnitude typical of these two quantities. In many cases, the product $\frac{\partial ()}{\partial p_i} \sigma[p_i]$, where $\sigma[]$ denotes the standard deviation, is a good basis for comparing the relative importance of dissimilar parameters.

Statistical data generated from the solution are, we think, easiest to assimilate when presented in terms of a single scalar

quantity: displacement at a location of interest, stress at a critical point, or system natural frequency. Variance data may be of interest directly, particularly when multiple parameters are involved. Histograms (bar-graphs) are often a useful format for presenting and assimilating this data, because they reveal the relative influence of each random variable on the uncertainty in the response.

Another concept useful in interpreting the probabilistic analysis results is that of a percentile value. A mean value, as computed in the basic finite element solution, is by definition a 50th percentile value; that is, we expect the actual value to be less than the mean in 50 percent of all samples. A Qth percentile value τ_Q is such that the true value of the variable is less than or equal to τ_Q in Q percent of all cases. Let τ_μ represent the mean value of the variable τ , and τ_σ the standard deviation (the square root of the variance). If τ has a normal (or Gaussian) probability distribution, the interval $(\tau_\mu - \tau_\sigma, \tau_\mu + \tau_\sigma)$ represents about 68 percent of all possible values of τ . The interval $(\tau_\mu, \tau_\mu + \tau_\sigma)$ therefore includes approximately 34 percent of all possible values of τ ; this means that the value of τ will be less than $\tau_\mu + \tau_\sigma$ 84 percent of the time. That is, the value $\tau_\mu + \tau_\sigma$ is the 84th percentile value of τ . The percentile value also can be viewed as a figure of reliability or confidence level. The changes between percentile values provide a direct indication of the relative uncertainty in a particular response quantity.

A simple example is useful to illustrate the interpretation of a probabilistic solution in terms of percentile values. A thin plate supported on all four edges has modulus E, Poisson's ratio ν , density ρ , thickness h, and side length a. The lowest natural frequency of the plate is then:³⁴

$$\omega = \frac{\pi^2 h}{6(1-\nu^2) a^2} \sqrt{E/\rho} \quad (102)$$

The sensitivity of this frequency to the plate thickness h , evaluated at the nominal thickness value h_0 , is:

$$\frac{\partial \omega}{\partial h} = \omega/h_0 \quad (103)$$

Accordingly, if thickness is the only statistical variable, we can state (from Equation 101):

$$\text{Var}[\omega] = \left[\frac{\omega}{h_0}\right]^2 \text{Var}[h] \quad (104)$$

or

$$\sigma_\omega = \frac{\omega}{h_0} \sigma_h \quad (105)$$

in which σ_ω , σ_h are the standard deviations of frequency and thickness, respectively. Equations (104) and (105) apply in the neighborhood of h_0 , because of the linearization implied in (101) and (104).

As a particular case, suppose that the plate is made from 2024T3 aluminum flat sheet, mill finish. Manufacturer's data³⁵ for actual stock thicknesses indicate that acceptable thickness variations are on the order of ± 10 percent for very thin stock (less than 0.030), and ± 5 percent for thicker sheet. Interpreting these values as $\pm 3\sigma_h$, we take $\sigma_h = h_0/30$ for thin sheet, and $\sigma_h = h_0/60$ for thick sheet. From Equation (105), the standard deviations of the natural frequency are simply $\sigma_\omega = \omega/30$ and $\sigma_\omega = \omega/60$ for the thin and thick cases, respectively.

If we assume a particular statistical distribution for the statistical variables, we can interpret the result in terms of percentile values. In this work we assume a normal distribution for all variables. For a normal distribution with mean μ and standard deviation σ , the probability of a value less than or equal to 'x' is given by the distribution function:

$$F(x) = \frac{1}{\sigma\sqrt{2\pi}} \int_{-\infty}^x e^{-\frac{1}{2}\left(\frac{v-\mu}{\sigma}\right)^2} dv \quad (106)$$

This value is normally written in terms of the normalized value $z=(x-\mu)/\sigma$; in effect, the "number of standard deviations" by which x is separated from μ . With this definition,

$$F(x) = \Phi(z) = \frac{1}{\sqrt{2\pi}} \int_{-\infty}^z e^{-u^2/2} du \quad (107)$$

This normalized form of the probability distribution function is tabulated in most statistics texts and collections of mathematical tables. The meaning of $\Phi(z)$ is illustrated in geometric terms in Figure 6.

For a 0.99 confidence level (99th percentile value), we let $\Phi(z)=0.99$, and from the statistical tables read the value $z=2.33$. Recalling the definition $z=(x-\mu)/\sigma$, we find the 99th percentile value:

$$x_{99} = \mu + 2.33\sigma \quad (108)$$

Values of the normalized variable z are tabulated for selected percentile levels in Table 1.

For the plate problem, we might wish to determine a value of natural frequency which is not exceeded by most plates. To bound Q percent of all cases (the Q^{th} percentile value), this frequency is $\Delta\omega=\omega_0+z\sigma_\omega$, where z is the value of $(x-\mu)/\sigma$ corresponding to Q . In other words,

$$\frac{\Delta\omega}{\omega_0} = 1 + z(Q) \frac{\sigma_\omega}{\omega_0} \quad (109)$$

Figure 7 shows this relationship for $\sigma_\omega/\omega_0 = 1/30$ and $1/60$; the curves are labeled "normal" and "high" quality, respectively.

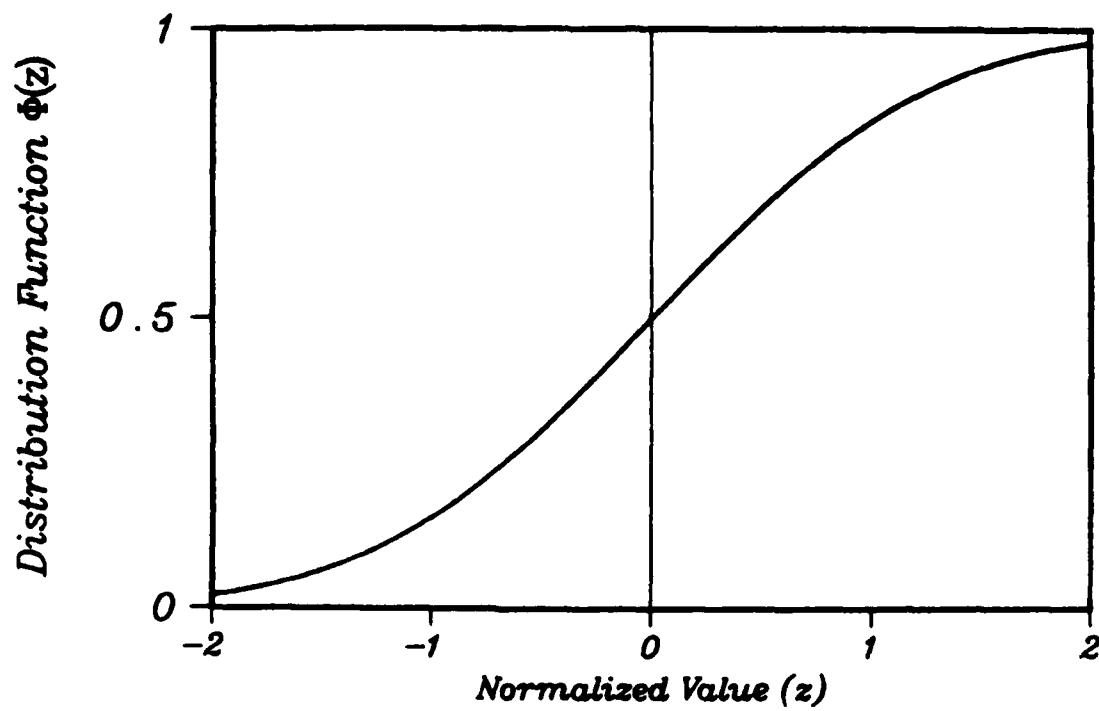


Figure 6. Graphical Interpretation of the Distribution Function $\Phi(z)$.

Table 1. Number of Standard Deviations versus Percentile Level

Percentile, Q	$\Phi(z)$	z^{\dagger}
90.	0.90	1.282
95.	0.95	1.645
99.	0.99	2.326
99.5	0.995	2.576
99.9	0.999	3.090
99.99	0.9999	3.719

$^{\dagger}x = \mu + z\sigma$, with z corresponding to percentile Q , is greater than or equal to the sample value for $Q\%$ of all samples.

Frequency Variation with Thickness

Aluminum 2024-T3 Plate

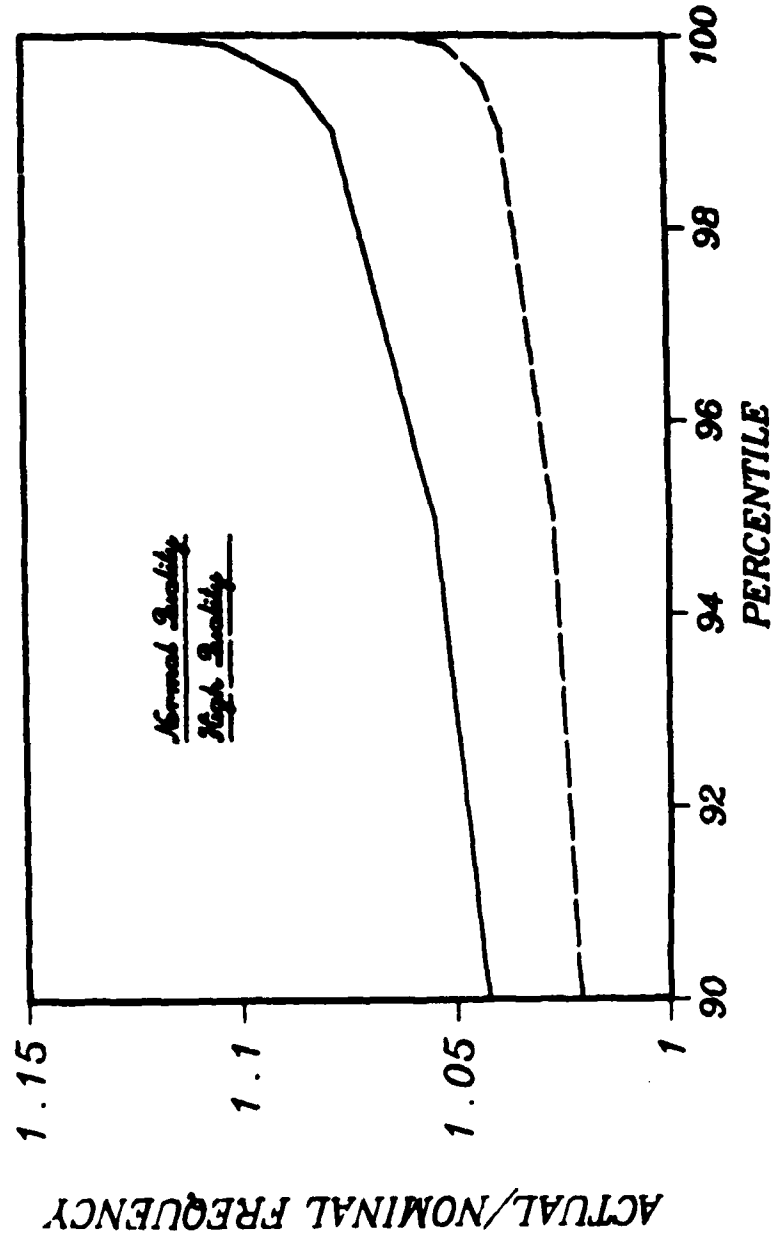


Figure 7. Percentile Values of Natural Frequency for a Plate with Thickness Variation.

Note that the 99.9th percentile frequencies are about 12 percent and 6 percent greater than the nominal natural frequency, due only to the uncertainty in sheet thickness.

CHAPTER 5

FINITE ELEMENT APPROXIMATION

This Chapter discusses the finite element approximations to be used in the present study. The choice of elements is dictated by the need to perform accurate solutions for both thin and thick shells, and by the complexity of the sensitivity calculations. A number of very accurate plate and shell elements exist for which the sensitivity computations outlined in Chapter 3 become hopelessly complex. On the other hand, most very simple elements, which would lend themselves to compact and efficient sensitivity computations, do not possess sufficient accuracy for routine use.

The finite element selected for use in this work is a four-node, bilinear displacement element based upon the Mindlin theory of plates.³⁶ Such elements exhibit good accuracy for both thick and thin plates when reduced (one-point) numerical integration is used to evaluate the element matrices. However, the resulting element is rank-deficient, and must be "stabilized" to achieve reliable behavior. Methods for achieving full rank of the stiffness and for stabilizing element behavior in static analysis and in explicit dynamic calculations exist and are quite effective. To date, however, very little attention has been devoted to the proper formulation of such an element for vibration analysis or in implicit transient solutions.

After describing the origin and formulation of the basic Mindlin element, this Chapter addresses the issue of controlling spurious modes of response in dynamic analysis. Several alternatives for the element mass formulation are examined in detail. We show that non-physical dynamic modes exist and present a potential problem with most mass matrix formulations, and that spurious modes other than the familiar hourglassing motion are possible. A combination of projection methods and reduced integration is suggested which eliminates these deficiencies and produces accurate numerical results. The remaining techniques

investigated give rise to anomalous behavior which make them unsuitable for general use.

5.1 BACKGROUND

The quadrilateral Mindlin plate element with bilinear displacement and rotation fields, based on single-point quadrature, was introduced by Hughes, Cohen, and Haroun³⁷ and designated U1. The attractiveness of such an element stems from its simplicity, computational efficiency, and high accuracy (since the single quadrature point is an optimal sampling point¹³). However, the basic U1 element is rank-deficient, since bilinear contributions to the displacement field are not captured by the single-point integration. Therefore, the assembled stiffness for a mesh of U1 elements may exhibit singularities when properly constrained, or lead to the prediction of spurious oscillatory displacements with which little or no strain energy is associated.

Subsequent development of the bilinear Mindlin plate element focused largely upon the stabilization of these spurious modes of behavior. In the context of explicit dynamic computations, the concept of hourglass stabilization, as discussed by Kosloff and Frazier³⁸ and further developed by Belytschko and co-workers^{39,40} is an effective means of controlling this behavior. However, the explicit solution provides an opportunity for individual elements to "react" to unstable oscillatory motions, while a static or implicit dynamic solution does not.

MacNeal⁴¹ and Hughes and Tezduyar⁴² have proposed schemes for stabilizing the bilinear element by redefining the interpolation of the transverse shear strain field. However, these techniques require a four-point quadrature, and the simplicity of the basic element is lost. Taylor⁴³ and Belytschko, Liu, and co-workers⁴⁴⁻⁴⁷ have pursued the idea of hourglass mode stabilization for static analysis, and present several correction methods

which work well while preserving the advantages of the one-point-integrated element. Park, Stanley, and Flaggs⁴⁸ have presented related methods of stabilization, obtained as a by-product of studies on element behavior with increasing mesh refinement.

Thus far, dynamic calculations based upon the hourglass stabilization techniques appear to have used the usual consistent mass for the quadrilateral element, and very little information is available concerning the effect of the stabilization scheme on dynamic behavior. Since the generalized stiffnesses used in the stabilization scheme must be small to avoid locking, one suspects (correctly) that there are pitfalls to be encountered in dynamic calculations. Belytschko and Tsay⁴⁵ have performed eigenvalue solutions for plates which reveal anomalous behavior in some relatively low-frequency modes, and which may be traced directly to the effect of the stabilization operator.

In what follows, we study the problem of formulating the appropriate mass characteristics for the bilinear Mindlin plate element with hourglass stabilization. The purpose of this exercise is to associate the proper kinetic energy with those motions for which the element correctly represents strain energy, and to eliminate the kinetic energy linked to the spurious modes. The useful frequency range should be free of vibration modes controlled by the stabilization operator, although displacements associated with these modes must be permitted to occur naturally as a part of lower-frequency mode shapes. Modes dominated by the stabilization operator should be relegated to the higher part of the frequency spectrum, which is already dominated by the finite element discretization rather than by the problem physics.

We first present a synopsis of the bilinear element development, and introduce some useful notation. A typical stiffness stabilization method is described. We then examine four methods of mass matrix formulation, and identify their most important characteristics. An "optimum" mass formulation is suggested

which associates the proper kinetic energy with basic motions of the element while eliminating spurious dynamic modes caused by the stiffness stabilization scheme.

5.2 BILINEAR MINDLIN PLATE ELEMENT

The kinematic assumptions of Mindlin plate theory³⁶ relate the displacements (U,V,W) at a generic point in a flat plate to displacements (u,v,w) and rotations (θ_x, θ_y) of the midsurface by:

$$\begin{aligned} U(x,y,z) &= u(x,y) + z\theta_y(x,y) \\ V(x,y,z) &= v(x,y) - z\theta_x(x,y) \\ W(x,y,z) &= w(x,y) \end{aligned} \quad (110)$$

in which z is the direction normal to the midsurface. The state of deformation is described by eight generalized strains,

$$\epsilon^t = [\epsilon_x, \epsilon_y, \gamma_{xy}, \kappa_x, \kappa_y, \kappa_{xy}, \gamma_{xz}, \gamma_{yz}] \quad (111)$$

and the stress state by the corresponding generalized forces,

$$\sigma^t = [N_x, N_y, N_{xy}, M_x, M_y, M_{xy}, Q_{xz}, Q_{yz}] \quad (112)$$

In the stress-strain relationships for the in-surface strains and curvatures, plane stress assumptions are used. The transverse shear quantities are related by $Q_{\alpha z} = kGt\gamma_{\alpha z}$, in which k is a shear correction factor⁴⁹; here we consider only isotropic plates and employ the value $k=\frac{5}{6}$ throughout.

For the bilinear finite element (Figure 8), we use the shape functions:

$$N = \frac{1}{4} (s + \xi\xi + \eta\eta + h\xi\eta) \quad (113)$$

in which:

$$s^t = [1, 1, 1, 1] \quad (114)$$

$$\xi^t = [-1, 1, 1, -1] \quad (115)$$

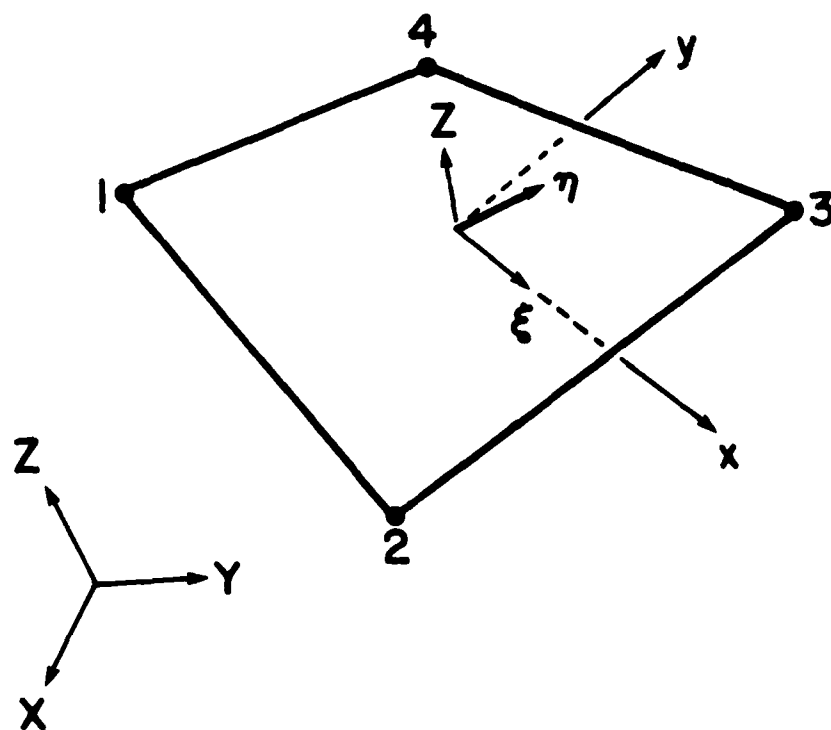


Figure 8. Bilinear Mindlin Plate Element.

$$\eta^t = [-1, -1, 1, 1] \quad (116)$$

$$h^t = [1, -1, 1, -1] \quad (117)$$

Following Liu and Belytschko⁴⁷, we also define the following useful quantities:

$$b_1^t = \frac{1}{2A} [y_{24}, y_{31}, y_{42}, y_{13}] \quad (118)$$

$$b_2^t = \frac{1}{2A} [x_{42}, x_{13}, x_{24}, x_{31}] \quad (119)$$

in which $x_{ij} = x_i - x_j$ and $y_{ij} = y_i - y_j$. Note that the element area is $A = \frac{1}{2}(x_{31}y_{42} + x_{24}y_{31})$. With some algebra, it is possible to verify that:

$$b_1 = \left. \frac{\partial N}{\partial x} \right|_{\xi=\eta=0} \quad b_2 = \left. \frac{\partial N}{\partial y} \right|_{\xi=\eta=0} \quad (120)$$

Finally, we will make use of the element corner coordinates in the form of the four-dimensional column vectors:

$$x^t = [x_1, x_2, x_3, x_4] \quad (121)$$

$$y^t = [y_1, y_2, y_3, y_4] \quad (122)$$

It is useful to note the following relationships which exist among the vector quantities defined above:⁴⁵

$$s^t h = s^t b_1 = s^t b_2 = h^t b_1 = h^t b_2 = b_1^t y = b_2^t x = 0 \quad (123)$$

$$b_1^t x = b_2^t y = 1 \quad (124)$$

Equations (123) and (124) are particularly useful in identifying the linearly independent modes of behavior for the element. For example, $u=s$, where u are nodal displacements, defines a uniform (rigid-body) motion, while $u=h$ defines one possible hourglass deformation pattern in a rectangular element (Figure 9).

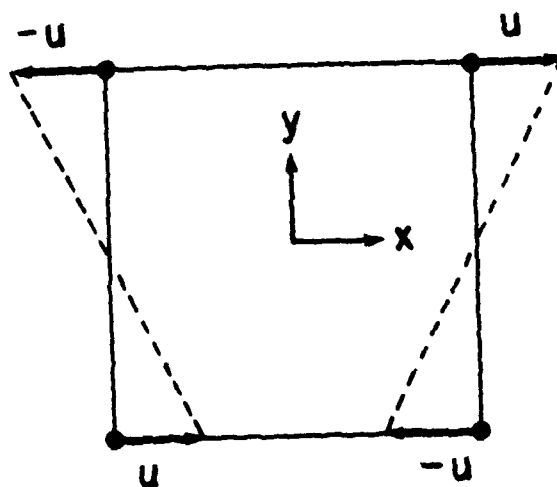


Figure 9. Hourglass Displacement Pattern.

With the definitions above, the strain-displacement operator evaluated at the element center can be written as:

$$B = \begin{bmatrix} b_1^t & 0 & 0 & 0 & 0 \\ 0 & b_2^t & 0 & 0 & 0 \\ b_2^t & b_1^t & 0 & 0 & 0 \\ 0 & 0 & 0 & 0 & b_1^t \\ 0 & 0 & 0 & -b_2^t & 0 \\ 0 & 0 & 0 & -b_1^t & b_2^t \\ 0 & 0 & b_1^t & 0 & \frac{1}{4}s^t \\ 0 & 0 & b_2^t & -\frac{1}{4}s^t & 0 \end{bmatrix} \quad (125)$$

Writing the element displacement vector as:

$$d^t = [u, v, w, \theta_x, \theta_y] \quad (126)$$

then $\epsilon = Bd$ are the element generalized strains sampled at the centroid of the element. With the stress-strain relation $\sigma = D\epsilon$, the element stiffness obtained through one-point quadrature is:

$$K = \int_A B^t D B \, dA = B^t D B A \quad (127)$$

5.3 STIFFNESS MATRIX STABILIZATION

We will employ a stabilization technique for the stiffness matrix based upon the generation of hourglass suppression forces, as suggested in References 44-47. The plate element of the previous section contains twenty degrees of freedom; we first segregate the possible modes of behavior for the element into the eight uniform-strain modes captured by the single-point quadrature rule, the six proper rigid body motions, and the six remaining modes which must be stabilized. The rigid body motions are:

$u = s$		(x translation)
$v = s$		(y translation)
$w = s$		(z translation)
$w = y$	$\theta_x = s$	(x rotation)
$w = -x$	$\theta_y = s$	(y rotation)
$u = -y$	$v = x$	(z rotation)

The six spurious modes consist of five hourglass deformation patterns $u=h$, $v=h$, $w=h$, $\theta_x=h$, $\theta_y=h$, and the twisting mode:

$$w = \frac{1}{4}(s^t y)x + \frac{1}{4}(s^t x)y; \quad \theta_x = x; \quad \theta_y = y \quad (128)$$

The stabilization scheme must inhibit the hourglassing modes to produce a stable element. The spurious twisting mode exists for a single element, but cannot occur in a mesh of two or more elements, as shown by Hughes.⁵⁰

Belytschko and Tsay⁴⁵ define generalized hourglass strains associated with each component of displacement and rotation by $\gamma^t u_i$ and $\gamma^t \theta_\alpha$, in which:

$$\gamma = h - (h^t x)b_1 - (h^t y)b_2 \quad (129)$$

The last two terms of Equation (129) are important for irregular elements, if the hourglass strains are to vanish in the presence of rigid body motion and uniform strain. We will use a definition which is only slightly different, letting:

$$\tilde{\gamma} = 2 \frac{x_{31}y_{31} + x_{24}y_{42}}{A^2} \gamma = \left. \frac{\partial^2 N}{\partial x \partial y} \right|_{\xi=\eta=0} \quad (130)$$

In the stabilization method used for the present study, we define a generalized hourglass strain associated with each of the displacement components (e.g., $\epsilon_u^{(h)} = \tilde{\gamma}^t u$), and associate with this strain a generalized stiffness determined through numerical

experiments. The generalized hourglass stiffnesses for the individual displacement components are:

$$E_u^{(h)} = E_v^{(h)} = \frac{0.10 Et}{(1 + \frac{1}{A})} \quad (131)$$

$$E_w^{(h)} = E_{\theta_x}^{(h)} = E_{\theta_y}^{(h)} = \frac{0.10 Et^3}{(1 + \frac{1}{A})} \quad (132)$$

The factor of $(1 + \frac{1}{A})$ in the hourglass stiffnesses is motivated by locking problems observed in elements with extremely small dimensions. For small element areas, the correction terms contain an additional factor proportional to the area, which reduces the artificial strain energy; when the element area is significant, the $1/A$ contribution becomes small. While the above scheme is not optimal for some problems, we have obtained good behavior for aspect ratios $0.0001 \leq (L/t) \leq 0.1$ over a range of six orders of magnitude in the planform dimension L .

5.4 EFFECT OF STABILIZATION IN DYNAMICS

The stabilization scheme outlined above is effective for static problems, in which the anti-hourglass stiffnesses may be adjusted freely to produce good element behavior. In dynamics, however, low-energy deformation patterns consisting mainly of hourglassing motions represent likely modes of low-frequency oscillation; the resulting non-physical solutions may contaminate that portion of the vibration spectrum which frequently is of greatest interest. It is useful to view this problem in terms of generalized stiffness and mass quantities, as follows.

Given a vibration mode shape $d = \psi$, the generalized stiffness and mass associated with the mode are the projections:

$$k = \psi^t K \psi \quad m = \psi^t M \psi \quad (133)$$

The corresponding frequency of vibration is $\omega = \sqrt{k/m}$. Since the hourglassing modes identified in the preceding section are orthogonal to both the rigid body motions and the constant strain states, the generalized stiffness associated with hourglass modes depends solely upon the hourglass stiffnesses $E_i^{(h)}$, which are made small deliberately to avoid locking problems. It is easy to show that at the same time, the kinetic energy associated with the unstable modes is similar in magnitude to that of the rigid body and uniform strain motions. Consequently, artificial vibration modes whose frequency is governed exclusively by the generalized hourglass stiffnesses appear low in the element spectrum, intermixed with the lower-frequency vibration modes which are commonly of interest.

This difficulty can be corrected by reducing or eliminating the kinetic energy associated with unstable modes of the element, while leaving the energy associated with rigid body motions and uniform strain states unchanged. In other words, we wish to minimize the projection of the mass matrix on the unstable modes of the element, so that spurious modes of vibration occur only beyond the useful frequency range of the model. At the same time, motions which are legitimate but which contain hourglassing components (such as torsional or inplane bending modes) may occur with only the minimal constraint imposed by the antihourglassing mechanism.

5.5 MASS MATRIX FORMULATION

In this Section, we examine several possible constructions of the bilinear element mass matrix. The point of this exercise is to identify a mass formulation which is reliable when used in conjunction with the hourglass stabilization technique described previously. We show that among the obvious choices for the element mass formulation, there is only one method which eliminates the possibility of unstable solutions for dynamic problems.

5.5.1 Fully Integrated, Consistent Mass

For the mass properties of the bilinear element, we define:

$$(R_1, R_2, R_3) = \int_{-t/2}^{t/2} \rho(1, z, z^2) dz \quad (134)$$

and

$$H = \int_A NN^t dA \quad (135)$$

The kinetic energy

$$T = \frac{1}{2} \int_A [R_1(\dot{u}^2 + \dot{v}^2 + \dot{w}^2) + 2R_2(\dot{u}\theta_y - \dot{v}\theta_x) + R_3(\theta_x^2 + \theta_y^2)] dA \quad (136)$$

then leads to the consistent mass matrix:

$$M = \begin{bmatrix} R_1 H & 0 & 0 & 0 & R_2 H \\ 0 & R_1 H & 0 & -R_2 H & 0 \\ 0 & 0 & R_1 H & 0 & 0 \\ 0 & -R_2 H & 0 & R_3 H & 0 \\ R_2 H & 0 & 0 & 0 & R_3 H \end{bmatrix} \quad (137)$$

With the assumption of a constant Jacobian determinant, matrix H may be evaluated directly in closed form, giving:

$$H = \frac{A}{36} \begin{bmatrix} 4 & 2 & 1 & 2 \\ 2 & 4 & 2 & 1 \\ 1 & 2 & 4 & 2 \\ 2 & 1 & 2 & 4 \end{bmatrix} \quad (138)$$

5.5.2 Lobatto Integrated, Consistent Mass

A lumped mass matrix for the bilinear element can be formed using Lobatto integration¹⁶, with the quadrature points placed at the four nodes of the element. The resulting matrix is diagonal provided $R_2=0$, which is the case for isotropic plates or midplane symmetric laminates. The translational and rotational inertias associated with each node are $\frac{1}{4}R_1A$ and $\frac{1}{4}R_3A$, respectively.

5.5.3 Consistent Mass via a Projection Method

One obvious problem exists with the consistent mass matrix evaluated with 2x2 quadrature, in that the kinetic energy of the hourglass modes is relatively large compared with the hourglass stiffnesses used for stabilization. Anticipating this, we adopt a simple projection method, designed to eliminate the kinetic energy associated with the hourglassing modes, and formulate the mass matrix as follows.

Consider the kinetic energy associated with the inplane displacement u :

$$T_u = \int_A \frac{1}{2} R_1 \dot{u}^2 dA \quad (139)$$

We wish to eliminate the kinetic energy associated with that part of the velocity field ignored by the single-point integration of the element stiffness. To this end, we expand the velocity field $\dot{u}(x,y)$ about $x=y=0$ (which we assume coincides with the element center):

$$\dot{u}(x,y) = \dot{u}(0,0) + x \dot{u}_{,x}(0,0) + y \dot{u}_{,y}(0,0) + \dots \quad (140)$$

or

$$\dot{u}(x,y) = \frac{1}{4} \mathbf{s}^t \dot{\mathbf{u}} + x(\mathbf{b}_1^t \dot{\mathbf{u}}) + y(\mathbf{b}_2^t \dot{\mathbf{u}}) + \xi \eta (\gamma^t \dot{\mathbf{u}}) \quad (141)$$

We now form a modified kinetic energy based on the purely linear part of the velocity field,

$$\dot{u}_\ell(x,y) = \frac{1}{4} \mathbf{s}^t \dot{\mathbf{u}} + x(\mathbf{b}_1^t \dot{\mathbf{u}}) + y(\mathbf{b}_2^t \dot{\mathbf{u}}) \quad (142)$$

giving:

$$T_\ell = \frac{1}{2} \dot{\mathbf{u}}^t \left[\int_A R_1 \left(\frac{1}{4} \mathbf{s} + x \mathbf{b}_1 + y \mathbf{b}_2 \right) \left(\frac{1}{4} \mathbf{s} + x \mathbf{b}_1 + y \mathbf{b}_2 \right)^t dA \right] \dot{\mathbf{u}} \quad (143)$$

As with the stiffness computation, we assume a constant Jacobian determinant over the element. Note that, using (113),

$$\int_A \mathbf{N} dA = \int_{-1}^1 \int_{-1}^1 \frac{1}{4} (\mathbf{s} + \xi\xi + \eta\eta + h\xi\eta) |\mathbf{J}| d\xi d\eta = |\mathbf{J}| \mathbf{s} \quad (144)$$

If the center of the element is $x=y=0$, then:

$$\int_A x dA = \int_A \mathbf{N}^t \mathbf{x} dA = |\mathbf{J}| (\mathbf{s}^t \mathbf{x}) = 0 \quad (145)$$

and terms linear in x or y do not survive the integration. Using (135), we define:

$$\int_A x^2 dA = \mathbf{x}^t \mathbf{H} \mathbf{x} = c_{xx} \quad (146)$$

$$\int_A y^2 dA = \mathbf{y}^t \mathbf{H} \mathbf{y} = c_{yy} \quad (147)$$

$$\int_A xy dA = \mathbf{x}^t \mathbf{H} \mathbf{y} = c_{xy} \quad (148)$$

and the modified kinetic energy becomes:

$$T_\ell = \frac{1}{2} \mathbf{R}_1 \dot{\mathbf{u}}^t \tilde{\mathbf{H}} \dot{\mathbf{u}} \quad (149)$$

in which:

$$\tilde{\mathbf{H}} = \frac{A}{16} \mathbf{s} \mathbf{s}^t + c_{xx} \mathbf{b}_1 \mathbf{b}_1^t + c_{yy} \mathbf{b}_2 \mathbf{b}_2^t + c_{xy} (\mathbf{b}_1 \mathbf{b}_2^t + \mathbf{b}_2 \mathbf{b}_1^t) \quad (150)$$

The evaluation of $\tilde{\mathbf{H}}$ requires no numerical integration, and the necessary vector products are identical with existing terms in the element stiffness matrix.

Performing a similar linearization of all displacement and rotation components, we find that the projected element mass matrix is identical in form to equation (137), with \mathbf{H} replaced by $\tilde{\mathbf{H}}$. Using Equations (123) and (124), it is evident that the kinetic energy (and therefore the generalized mass) associated

with all five pure hourglassing modes is identically zero; therefore, modes consisting primarily of hourglassing motions should not appear as spurious low-energy vibration modes.

5.5.4 Consistent Mass by Reduced Integration

With a single point quadrature, the integral in Equation (133) is sampled only at the centroid of the element, where $N=\frac{1}{4}s$. The resulting mass matrix is then identical to that of Equation (137), with H replaced by:

$$H_{(1)} = \frac{A}{16} ss^t = \frac{A}{16} \begin{bmatrix} 1 & 1 & 1 & 1 \\ 1 & 1 & 1 & 1 \\ 1 & 1 & 1 & 1 \\ 1 & 1 & 1 & 1 \end{bmatrix} \quad (151)$$

Note that the mass matrix so obtained should be equally effective to the projection method in eliminating the kinetic energy of the hourglass modes, which are bilinear in x and y .

5.5.5 Comparison of Mass Matrix Formulations

Certain properties of the four mass matrix formulations described above are readily apparent, and numerical experiments (see the next section) reveal additional characteristics which are less obvious. We discuss the most important of these below. In all cases we assume a stiffness matrix formed using single point integration, and stabilized using hourglass control.

With a fully-integrated, consistent mass (Equation 137), the occurrence of spurious, low-frequency hourglass modal patterns is expected. The kinetic energies associated with hourglassing are similar in magnitude to that of other, legitimate vibration modes, while the stiffnesses are typically an order of magnitude less. The generalized stiffness-to-mass ratios for hourglassing patterns are therefore quite low, and spurious modes will appear low in the vibration spectrum.

Similar problems with the lumped mass formulation are to be expected, since a diagonal mass matrix leads to kinetic energy for all possible motions. Likewise, any positive definite consistent mass formulation is destined to predict non-physical dynamic motions.

The mass matrix obtained by projection onto a linearized velocity field is positive semi-definite, since zero kinetic energy is associated with all pure hourglassing patterns. This method is satisfactory for plate bending alone, since the singular modes of the mass matrix coincide precisely with those of the stiffness. Such is not the case for inplane behavior, since spurious low-energy modes which do not correspond to pure hourglass patterns may still occur.

The troublesome vibration mode of Figure 10 involves hourglassing, combined with a uniform rotation about the element centroid. In a rectangular element of dimension $(2a, 2b)$, for example, the inplane motion can be described by:

$$\dot{\mathbf{u}} = \frac{1}{2}(\dot{\boldsymbol{\eta}} + \mathbf{h}) = \begin{bmatrix} 0 \\ -1 \\ 1 \\ 0 \end{bmatrix} ; \quad \dot{\mathbf{v}} = -\frac{a}{2b}(\dot{\boldsymbol{\xi}} + \mathbf{h}) = -\frac{a}{b} \begin{bmatrix} 0 \\ 0 \\ 1 \\ -1 \end{bmatrix} \quad (152)$$

For the rectangular element in question, equations (118)-(119) give:

$$\mathbf{b}_1 = \frac{1}{4a}\boldsymbol{\xi} ; \quad \mathbf{b}_2 = \frac{1}{4b}\boldsymbol{\eta} \quad (153)$$

Since vectors $\boldsymbol{\xi}$ and $\boldsymbol{\eta}$ are orthogonal, the resulting centroidal strains vanish, though the motion is not a rigid-body rotation. The projected mass neglects the hourglass velocity components, and predicts a kinetic energy based on the nodal velocities:

$$\dot{\mathbf{u}}_\ell = \frac{1}{2}\dot{\boldsymbol{\eta}} ; \quad \dot{\mathbf{v}}_\ell = -\frac{a}{2b}\dot{\boldsymbol{\xi}} \quad (34)$$

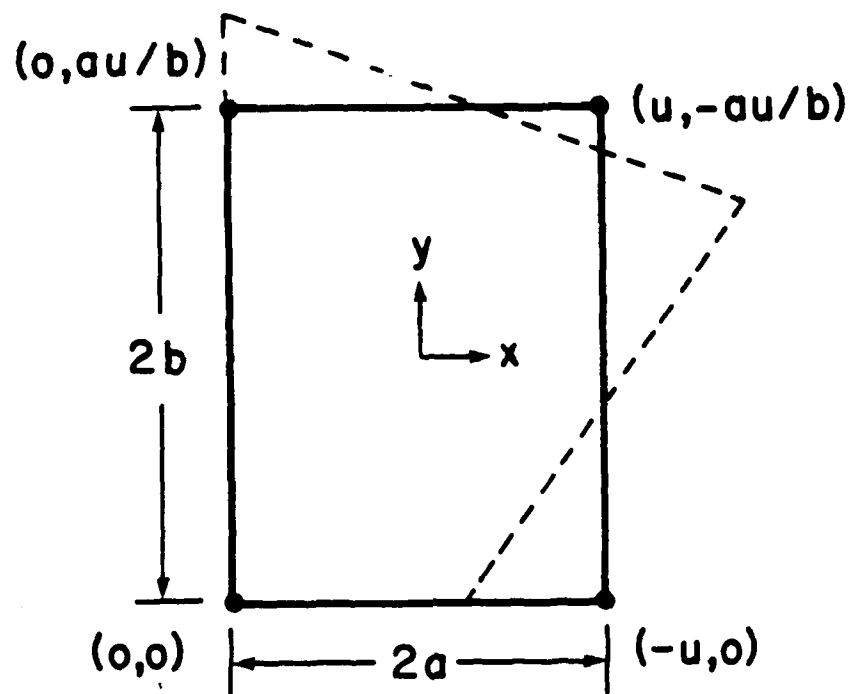


Figure 10. Combined Hourglass-rotation Mode.

corresponding to a uniform rigid body rotation about the element center. It is worth noting that the same non-physical velocity field is possible at low frequency with the exact consistent mass matrix, though the kinetic energy is higher due to the presence of hourglassing.

Figure 11 shows the deformation pattern developed within a uniform mesh of rectangular elements for a mode of this type. Dark lines indicate element edges which experience only pure extension, compression, or rigid-body translation.

Pure hourglass motions and the staircase patterns of Figure 4 are both made possible by the bilinear element displacement field. The hourglass field is a bilinear displacement field which vanishes at the element center, causing zero strain, while the staircase mode consists of a constant rotation field about individual element centers, combined with hourglassing motion.

Correction of the spurious inplane mode problem requires that only true rigid-body rotations lead to a nonzero kinetic energy. The use of a single-point quadrature achieves this property, since kinetic energy results only for mean rotations about a point other than the element centroid. The only unfortunate consequence of this choice is that the kinetic energy of an element whose centroid coincides with an axis of inplane rigid body rotation will be missed.

Deformation patterns analogous to the inplane staircase mode do not appear to exist for out-of-plane vibration. The projected mass matrix therefore may be used with confidence for flat plate bending.

It remains for us to compare the single-point integrated mass matrix with the projected mass (both of which are immune to

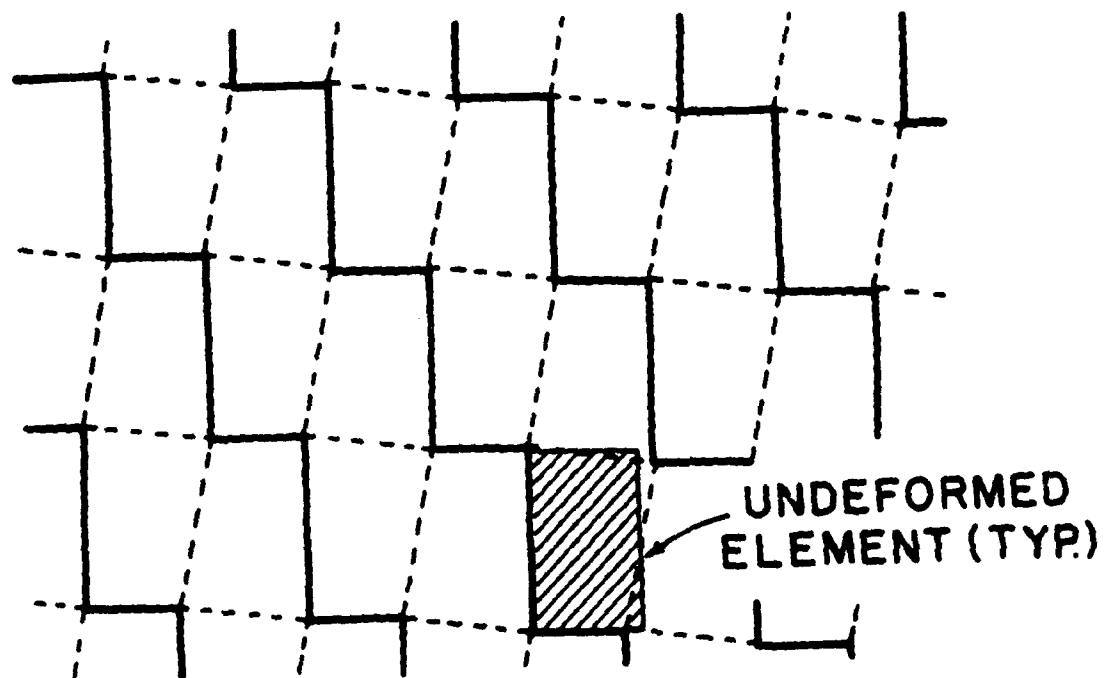


Figure 11. Hourglass-rotation Mode in a Regular Mesh.

hourglass modes) in the bending problems for which both are potentially applicable. Consider the out-of-plane rigid-body modes described earlier, and the uniform strain states:

$$\begin{array}{ll}
 \theta_y = cx & (x \text{ curvature}) \\
 \theta_x = cy & (y \text{ curvature}) \\
 \theta_x = c_1 x & \theta_y = c_2 y \quad (\text{twist}) \\
 w = c_1 x & \theta_y = c_2 s \quad (x\text{-}z \text{ shear}) \\
 w = c_1 y & \theta_x = c_2 s \quad (y\text{-}z \text{ shear})
 \end{array}$$

One useful comparison is based on the kinetic energy associated with each of these motions using the consistent, projected, and reduced-integrated mass matrices. We find that the projected mass matrix yields the proper energy for all eight elementary states, and zero for the hourglass modes. The mass obtained by single-point quadrature leads to a proper energy only for the translational rigid body motion, and in fact gives zero energy for the uniform curvature modes. For the remaining rigid-body and constant strain states, the reduced mass formulation underestimates the kinetic energy and may predict frequencies which are less accurate than the projection method.

Based upon the observations summarized in this section, the recommended mass formulation for the bilinear Mindlin plate element therefore involves a **single-point quadrature** for the inplane motions, and the **projection method** for the transverse displacements and rotations:

$$\mathbf{M}_{\text{opt}} = \begin{bmatrix} R_1 \bar{H}_{(1)} & 0 & 0 & 0 & R_2 \bar{H} \\ 0 & R_1 \bar{H}_{(1)} & 0 & -R_2 \bar{H} & 0 \\ 0 & 0 & R_1 \bar{H} & 0 & 0 \\ 0 & -R_2 \bar{H} & 0 & R_3 \bar{H} & 0 \\ R_2 \bar{H} & 0 & 0 & 0 & R_3 \bar{H} \end{bmatrix} \quad (155)$$

The additional effort required to form the projected mass is minimal, since the necessary submatrices occur also in the stiffness calculation. Furthermore, the mass computation is

usually performed only once per analysis, even in nonlinear problems, and represents a negligible fraction of the complete solution in all but the smallest problems.

The semi-definite property of the single-point-integrated mass and the projected mass matrix appears to present a potential source of difficulty in some methods of eigenvalue extraction, such as subspace iteration. However, the subspace projection of the mass will remain positive definite unless one or more trial vectors correspond precisely to a global deformation mode which is free of kinetic energy. This situation is unlikely provided the number of trial vectors is small compared with the order of the system, which is normally the case.

CHAPTER 6

MATERIAL MODELING

The scope of the present investigation is limited to elastic behavior only. However, the use of advanced composite materials in turbomachinery components is increasing, and effective methods for analyzing these materials are needed. In this Chapter we introduce a technique for modeling multilayered components without increasing the size of the overall finite element model. The approach leads to simple elements which yield reasonably accurate stress data, and is applicable to most shear-flexible structural elements.

6.1 BACKGROUND

Problems of multilayered plates and shells are important in the design of composite structures,⁵¹ impact-resistant vehicle components,⁵² and vibration-control treatments;⁵³ such problems are also of great interest in the design of the next generation of propulsion system components. A wide variety of theoretical and numerical treatments of such problems have been developed, but most of these possess characteristics which limit their widespread use in production analysis software. As a result, many of the more powerful methods available for analyzing multilayered structures are inaccessible to analysts and designers, who must resort to standard elements and methods which are more complex and expensive.

Two types of approaches predominate in the work performed to date in multilayered plate and shell analysis. The first of these involves the use of independent rotations or related unknowns within individual layers to capture the distribution of transverse shear and normal stresses in detail.^{54,55} This class of method works quite well at the expense of introducing new nodal variables whose number depends upon the number of layers, and which are beyond the data-handling scope of many production

analysis codes. The second common approach is through hybrid finite elements with assumed layer stress fields,⁵⁶⁻⁵⁸ with the corresponding layer rotations appearing as degrees of freedom. Recently, Spilker⁵⁹ reported a multilayered hybrid element which uses only six degrees of freedom per node, but which is limited to thin laminates.

The methods presented here deal effectively with multilayered components, require a minimal amount of added computation, and may be used in conjunction with most common plate and shell finite elements. The approach is based upon the definition of shear flexibility corrections to be applied to the basic plate or shell element, and recovery of transverse shear stresses via the equations of equilibrium.

First we describe the basic aspects of the shear flexibility correction as it applies to layered isotropic materials. We then discuss the modifications which are needed for some orthotropic laminates, for which a clear interpretation of the method depends upon uncoupling the transverse shear force resultants. Finally, procedures for point stress recovery are summarized.

6.2 LAMINATE STIFFNESS CHARACTERISTICS

The model used herein is based upon Mindlin's theory of plates.³⁶ Section 5.2 outlines the kinematic assumptions and other pertinent aspects of this theory. We will work in terms of the generalized strains and stresses defined in Equations (111) and (112):

$$\epsilon^T = [\epsilon_x, \epsilon_y, \gamma_{xy}, \kappa_x, \kappa_y, \kappa_{xy}, \gamma_{xz}, \gamma_{yz}] \quad (156)$$

$$\sigma^T = [N_x, N_y, N_{xy}, M_x, M_y, M_{xy}, Q_{xz}, Q_{yz}] \quad (157)$$

The relationship between these generalized deformation and force quantities, as used in Equation (127), is often expressed in the form:

$$D = \begin{bmatrix} A_{11} & A_{12} & A_{16} & B_{11} & B_{12} & B_{16} & 0 & 0 \\ A_{12} & A_{22} & A_{26} & B_{12} & B_{22} & B_{26} & 0 & 0 \\ A_{16} & A_{26} & A_{66} & B_{16} & B_{26} & B_{66} & 0 & 0 \\ B_{11} & B_{12} & B_{16} & D_{11} & D_{12} & D_{16} & 0 & 0 \\ B_{12} & B_{22} & B_{26} & D_{12} & D_{22} & D_{26} & 0 & 0 \\ B_{16} & B_{26} & B_{66} & D_{16} & D_{26} & D_{66} & 0 & 0 \\ 0 & 0 & 0 & 0 & 0 & 0 & A_{44} & A_{45} \\ 0 & 0 & 0 & 0 & 0 & 0 & A_{45} & A_{55} \end{bmatrix} \quad (158)$$

The elastic stiffness resultants A_{ij} , B_{ij} , and D_{ij} are defined as in laminated plate theory⁵¹; that is:

$$(A_{ij}, B_{ij}, D_{ij}) = \int_{-t/2}^{t/2} \bar{Q}_{ij}(1, z, z^2) dz \quad (159)$$

in which \bar{Q}_{ij} are the elements of the elasticity tensor at the point in question, referred to a common system of coordinates.

6.3 SHEAR FLEXIBILITY CORRECTIONS

In most common plate and shell elements, the assumption of linear thickness variations in the tangential displacements (see equation 110) results in an extremely crude representation of the transverse shear strains. In particular, these shear strains are constant through the plate thickness, and neither the pointwise equilibrium equations nor the traction boundary conditions at the surfaces are satisfied in general. For monolithic, isotropic elements, a uniform reduction factor often is applied to the shear strain energy to obtain more realistic behavior. Equating the transverse shear strain energy consistent with the assumed displacements to that of the parabolic shear strain field which satisfies the equilibrium condition yields a correction factor of 5/6, which is commonly used for isotropic plates and shells.

In the present work, we use a generalization of this idea first proposed by Whitney⁴⁹ for arbitrary wall constructions. Such a correction is necessarily approximate, but is usually sufficient to bring the shear strain energy in line with other modes of deformation, in a way which reflects the relative flexibility of these modes for a given material layup.

Consider first a layered construction for which the shear strains and resultant forces are related by:

$$\begin{bmatrix} Q_{xz} \\ Q_{yz} \end{bmatrix} = \begin{bmatrix} k_1 A_{44} & 0 \\ 0 & k_2 A_{55} \end{bmatrix} \begin{bmatrix} \gamma_{xz} \\ \gamma_{yz} \end{bmatrix} \quad (160)$$

Based solely on the elastic stress-strain relationship of the material, factors k_1 and k_2 should both equal one. However, due to the excessive constraint imposed by the kinematic assumptions of the plate or shell theory, the strains γ_{iz} produced by given shear forces Q_{iz} are too large over much of the plate thickness. Accordingly, the total strain energy predicted is too large, and the approximation appears too stiff. This error does not respond to mesh refinement, since the displacement approximation through the thickness remains linear. Our intent is to select values for k_1 and k_2 which lead to stored energies of a more reasonable magnitude, and thus yield better element behavior.

Since the shear resultants are uncoupled for the case of an isotropic material, the basic aspects of the method can be illustrated with reference to a single plane. Below, we discuss the determination of k_1 , the shear correction factor for the (x,z) plane.

The shear corrections suggested by Whitney⁴⁹ depend upon the assumption of cylindrical bending, for which an analytical relationship may be established between the local bending stress and the transverse shear force resultant:⁶⁰

$$\sigma_{x,x}^{(m)} = \frac{-Q_{11}^{(m)}}{D} (B_{11} - A_{11}z) Q_{xz} \quad (161)$$

The superscript (m) refers to a particular layer within the laminate cross-section, and parameter D is defined by:

$$D = D_{11}A_{11} - B_{11}^2 \quad (162)$$

When combined with Equation (161), the equilibrium equation

$$\sigma_{x,x}^{(m)} + \sigma_{xz,z}^{(m)} = 0 \quad (163)$$

can be integrated through the plate thickness to obtain the shear stress within a layer:

$$\sigma_{xz}^{(m)} = \frac{1}{2D} [a^{(m)} + Q_{11}^{(m)}z(2B_{11} - A_{11}z)] Q_{xz} \quad (164)$$

The constants of integration $a^{(m)}$ are determined by the condition that σ_{xz} be continuous at the layer interfaces, and from the free surface boundary condition at either the upper or lower surface. From the condition that $\sigma_{xz}=0$ at $z=-t/2$, we obtain:

$$a^{(1)} = \frac{1}{4} Q_{11}^{(1)} t (A_{11}t + 4B_{11}) \quad (165)$$

in which $m=1$ refers to the bottom layer of the laminate. Letting $z_\ell^{(m)}$ be the lower surface of layer m , the interface continuity conditions for $m=2,3,\dots$ give:

$$a^{(m)} = a^{(m-1)} + [Q_{11}^{(m)} - Q_{11}^{(m-1)}] [A_{11}z_\ell^{(m)} - 2B_{11}] z_\ell^{(m)} \quad (166)$$

With the above definitions, the strain energy density in any layer may be written in the form:⁴⁹

$$v^{(m)} = \frac{1}{2} g^{(m)}(z) Q_{xz} \quad (167)$$

in which

$$g^{(m)}(z) = \frac{1}{G_{xz}^{(m)}} \left[\frac{a^{(m)}}{2D} + \frac{Q_{11}^{(m)} z}{2D} (2B_{11} - A_{11} z) \right]^2 \quad (168)$$

Integrating Equation (167) through the laminate thickness, and equating the result to the total strain energy per unit area obtained from Equation (160),

$$V = \frac{Q_{xz}^2}{2k_1 A_{55}} \quad (169)$$

leads to the shear correction factor:

$$k_1 = \left[A_{44} + \int_{-t/2}^{t/2} g^{(m)}(z) dz \right]^{-1} \quad (170)$$

The remaining factor k_2 may be found in a similar fashion, using the appropriate elastic constants for the (y, z) plane.

As a representative example, consider a typical graphite-epoxy material with the properties

$$\begin{aligned} E_1 &= 25 \times 10^6 & E_2 &= E_3 = 1 \times 10^6 \\ G_{23} &= 0.2 \times 10^6 & G_{12} &= G_{13} = 0.5 \times 10^6 \\ \nu_{12} &= \nu_{13} = 0.25 \end{aligned}$$

For this material, typical shear correction factors computed by the method outlined above are listed in Table 2. The classical shear factor $k=5/6$ represents an upper bound under the assumptions of this Section. When small layers of extremely flexible material are introduced in an otherwise uniform plate, the shear

Table 2. Shear Factors for Gr/Ep Laminates

Laminate	k_x	k_y
$[0_n]$	0.83333	0.83333
$[0/90]$	0.82123	0.82123
$[45/-45]$	0.68027	0.68027
$[0/90]_s$	0.59518	0.72053
$[-45/45]_s$	0.68027	0.68027
$[-60/0/60]$	0.82579	0.60800

factors tend to drop quite rapidly; this is the case with the polymeric materials used in plastic laminate interlayers, and the viscoelastic materials typically employed in constrained-layer vibration damping treatments.

6.4 UNCOUPLED CORRECTIONS FOR ORTHOTROPIC LAMINATES

The interpretation of the shear corrections developed above is clear provided the transverse shear resultants in the (x,z) and (y,z) planes are uncoupled. When the transverse shear moduli in these two planes differ, and when layers with orientations other than 0° and 90° are present, the stress-strain relation has the form:

$$\begin{bmatrix} Q_{xz} \\ Q_{yz} \end{bmatrix} = \begin{bmatrix} A_{44} & A_{45} \\ A_{45} & A_{55} \end{bmatrix} \begin{bmatrix} \gamma_{xz} \\ \gamma_{yz} \end{bmatrix} \quad (171)$$

which we will represent by $Q = S\gamma$. For such cases, the interpretation of the correction factor derived from cylindrical bending assumptions is open to question.

The existence of a positive definite strain energy function implies that the shear stiffness matrix S is real, symmetric, and positive definite. Therefore, there exists a planar transformation of coordinates defining an alternate system of reference axes (x',y'), for which the corresponding stiffness S' is diagonal and the shear resultants are uncoupled. Since the z axis remains unchanged, the transformation by an angle β has the form:

$$S' = \Omega S \Omega^T \quad (172)$$

with

$$\Omega(\beta) = \begin{bmatrix} \cos\beta & -\sin\beta \\ \sin\beta & \cos\beta \end{bmatrix} \quad (173)$$

The required angle of rotation is easily determined in terms of the original shear stiffness coefficients:

$$\tan(2\beta) = \frac{2A_{45}}{A_{55}-A_{44}} \quad (174)$$

6.5 SHEAR STRESS RECOVERY

For pointwise stress recovery consistent with the transverse shear flexibility correction outlined here, Equation (164) may be used directly at any station z within the laminate thickness, with the shear force resultants obtained from Equation (160). The integration constants $a^{(m)}$ may be stored and recalled for use in the stress recovery, at a cost of only one floating point word per layer. With the assumption of linear displacement variation through the plate thickness, the predicted transverse shear stress field is quadratic within each layer.

For the bilinear plate element used in the present work, we choose to evaluate the transverse shear stresses at the element center, which corresponds to the optimal sampling point.¹³ With higher-order displacement elements, it may be possible to obtain accurate transverse shear stresses at a regular grid of points within an element, such as the 2×2 Gauss points. These data may be used in turn for the evaluation of transverse normal stresses on a smaller grid, by integration of the remaining equilibrium equation.

CHAPTER 7

NUMERICAL EXAMPLES

This Chapter presents a number of solved problems which demonstrate the analytical methods discussed earlier. Many of these are small, relatively simple problems for which closed form solutions or previous numerical results exist. Comparisons with known results are made both to verify specific capabilities and to determine the accuracy characteristics of the present analysis techniques.

The numerical solutions are presented in four sections, which pertain to four primary areas of investigation in the work performed. Section 7.1 deals with basic dynamic problems, and illustrates the performance of the stabilization procedure and the optimal mass formulation for the bilinear plate element (see Chapter 5). In Section 7.2, we present several problems involving composite materials or layered wall construction; all of these are solved using a single layer of plate elements, based on the shear correction technique described in Chapter 6. Section 7.3 contains a number of sensitivity analyses (Chapter 3), and Section 7.4 presents analyses using the probabilistic techniques of Chapter 4.

7.1 DYNAMICS EXAMPLES

The problems of this Section demonstrate the bilinear plate element formulation of Chapter 5. In particular, we contrast the recommended mass formulation with other commonly-used alternative forms. The first example is an axial vibration problem which is simple in concept, but which illustrates very well the ability of the present mass formulation to move spurious dynamic modes to the top of the frequency spectrum. The remaining two problems are cases for which troublesome results have been reported in the past; the present method gives a reliable solution with improved accuracy.

7.1.1 Comparison of Mass Formulations for Axial Vibration

This example demonstrates the occurrence of artificial modes controlled by the anti-hourglass stiffness parameters. Consider the planar vibrations of a long, thin strip as shown in Figure 12. One quadrant, with dimensions (1,10,0.05), is modeled by a single element; symmetry is imposed along the axes $x=0$ and $y=0$. The mechanical properties are $E=10^7$, $\nu=0.25$, and $\rho=0.000259$.

Solutions have been calculated with all four of the mass formulations discussed previously, and results are listed in Table 3. Predicted frequencies corresponding to the inplane staircase mode are shown in parentheses. Accurate estimates of the exact natural frequencies are not expected, due to the coarse mesh employed; our intent in this example is to examine the occurrence of spurious low-frequency modes for each of the mass formulations.

The solution with lumped mass exhibits the lowest spurious frequencies, as well as extreme lower bounds on the first two physical modes, since half of the element mass is concentrated at the free end. The consistent and projected masses give similar frequency estimates, with a first spurious mode quite close to the real fundamental frequency; both spurious modes in these two solutions are inplane staircase modes, and the slightly lower frequencies predicted with full consistent masses are due to the nonzero hourglassing kinetic energy.

The single-point integrated mass yields a reliable solution, though the natural frequencies are somewhat higher than with the consistent mass and the projection method. The mass for this case has been augmented by a small fraction (0.1%) of the lumped mass to achieve positive definiteness, since all the modes are solved. The two highest frequencies are controlled by the lumped mass contribution.

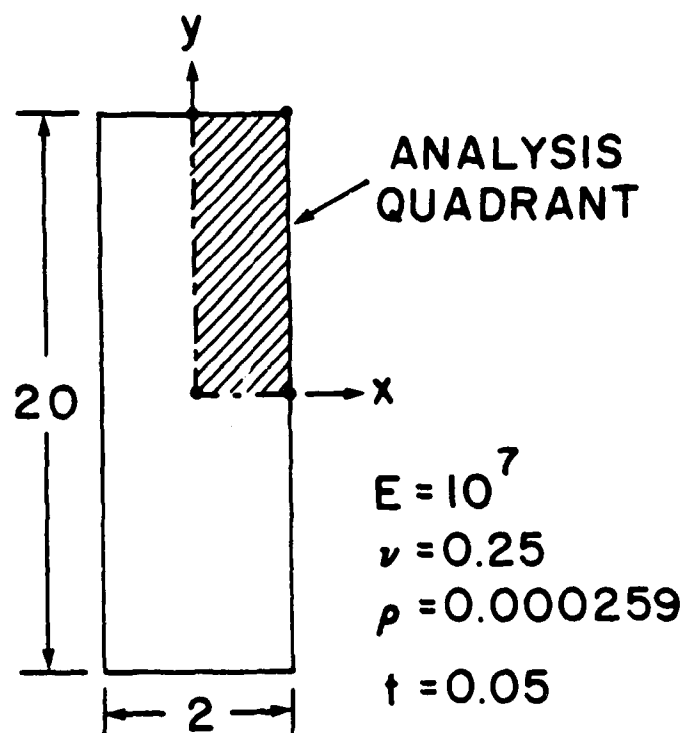


Figure 12. Slender Strip Geometry and Properties.

Table 3. Comparison of Results for Planar Vibration of Thin Strip

Mass	ω_1	ω_2	ω_3	ω_4
Lumped	(16,757.)	27,779. ^a	(177,416.)	287,083. ^b
Consistent	34,023. ^a	(35,547.)	351,611. ^b	(376,364.)
Projected	34,023. ^a	(41,046.)	351,611. ^b	(434,582.)
Reduced	39,277. ^a	405,904. ^b	(1,059,812.)	(11,220,998.)

^a Stretching mode, long direction.

^b Stretching mode, short direction.

Table 3 shows an additional solution using the recommended mass technique (1x1 quadrature) and four elements. The first stretching mode is quick to converge, suggesting that the poor one-element solution is not indicative of an unforeseen pathology in the element.

The energy content of the mode shapes for this example is unambiguous, and the non-physical vibration modes could have been rejected automatically on this basis. However, the occurrence of such spurious solutions in larger problems may limit the number of legitimate modes obtained, and exacts added storage demands which may be unacceptably large.

7.1.2 Vibration of a Corner-Supported Plate

The vibrations of a corner-supported plate (Figure 13) have been considered by Belytschko and Tsay⁴⁵ using the stabilized Mindlin plate element. Reference 45 contains results for the first three frequencies, as functions of the w and θ hourglass stiffnesses; artificial or inaccurate frequencies were obtained only when one or both of these stiffnesses were suppressed.

In our analysis, we assume double symmetry and consider out-of-plane motions only. The length of each edge of the entire plate is 24; the material properties are $E=360,000$, $\nu=0.38$, and $\rho=0.001$. A uniform mesh of 36 elements is used, so that natural frequencies should be directly comparable with those of Reference 45.

Table 5 lists normalized frequency values for the first five symmetric vibration modes of the plate. All values are in reasonable agreement with the exact results, and with the numerical values predicted by Belytschko and Tsay; the minor differences which do exist in the numerical solutions can be attributed to the differing parameters used in the stiffness stabilization. Recall that the recommended technique for bending motions uses

Table 4. Vibration Modes of Thin Strip (Four-Element Solution)

<u>Mode</u>	<u>Predicted Frequency</u>	<u>Exact Frequency</u>	<u>Description of Mode</u>
1	31,259.	30,865.	y stretching, first mode
2	104,840.	92,596.	y stretching, second mode
3	232,755.	154,326.	y stretching, third mode
4	405,266.	308,653.	x stretching, first mode

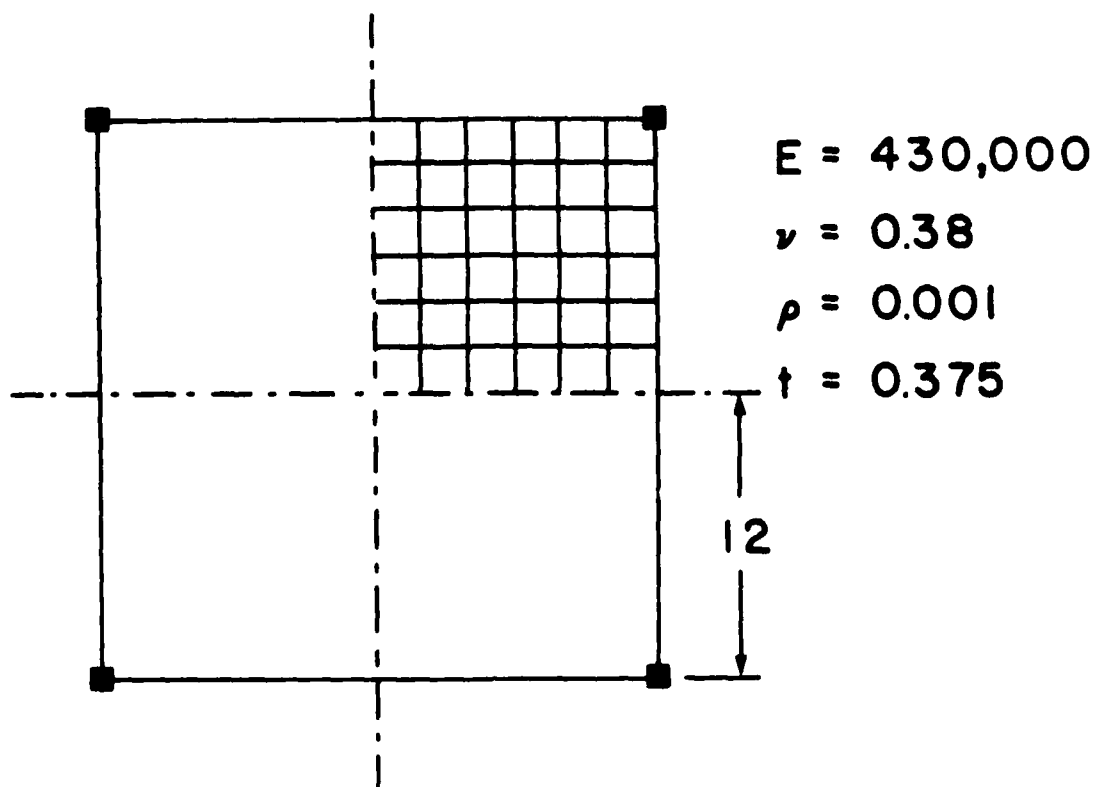


Figure 13. Corner-supported Square Plate.

Table 5. Natural Frequencies for Corner-Supported Plate.

$$\bar{\omega} = \omega a^2 (D/\rho t)^{-1/2}$$

Mode	Consistent Mass	Projection Method	Reduced Quadrature	Belytschko & Tsay [45]	Analytic
1	7.118	7.118	7.124	7.099-7.185	7.120
2	18.79	18.79	19.08	19.18 -19.19	19.60
3	44.01	44.01	44.79	42.70 -43.98	44.40
4	95.18	95.33	98.11	-	-
5	124.13	124.14	132.44	-	-

the projection method. For this case, the mass matrix obtained by single point quadrature leads to slightly higher frequencies, due to neglect of the kinetic energy associated with constant-curvature states.

7.1.3 Vibration of a Free-Free Square Plate

This example, also taken from Reference 45, exhibits a free vibration mode which is sensitive to the w-hourglass stiffness. The geometry and properties are identical to those in the previous example, but the entire plate is modeled. A 36-element mesh is used, to facilitate comparisons with the solutions reported by Belytschko and Tsay.⁴⁵

Table 6 summarizes the normalized frequencies obtained for the first six bending modes of the plate (the first three modes, which correspond to rigid-body motions, are not listed). The projection method is clearly superior, particularly for the third frequency which, according to Reference 45, is quite sensitive to the hourglass stiffness parameter. This frequency corresponds to the (3,1) mode of the plate; the accuracy is particularly good in view of the fact that three half-waves are represented by only six bilinear elements.

7.2 COMPOSITES AND LAYERED STRUCTURES

The examples of this Section involve both advanced composite materials and layered (sandwich) components. They illustrate the use of the shear corrections of Chapter 6 for static and dynamic problems. The overall stiffness effect is very realistic, and good results can be expected for resultant (in the sense of plate theory) quantities. Two examples present point stress results; these are of reasonable quality, but seem somewhat more vulnerable to the errors entailed in the assumption of cylindrical bending than the stiffness properties.

Table 6. Natural Frequencies for Free-Free Plate.

$$\bar{\omega} = \omega a^2 (D/\rho t)^{-1/2}$$

<u>Mode</u>	<u>Projection Method</u>	<u>Reduced Quadrature</u>	<u>Belytschko & Tsay [45]</u>	<u>Analytic</u>
1 (22)	13.07	13.42	13.14	13.47
2 (13)	19.14	20.46	18.12	19.60
3 (31)	25.81	27.46	19.05	24.27
4 (32)	34.11	36.85	-	35.02
5 (23)	34.11	36.85	-	35.02
6 (41)	62.87	70.59	-	61.53

7.2.1 Unsymmetric Laminated Plate

The semi-infinite thick plate shown in Figure 14 is subjected to a sinusoidal pressure load $q(x) = q_0 \sin(\pi x/a)$, and is simply supported on its lateral edges. The 0° direction is the fiber direction in the top layer, and corresponds to the infinite (y) direction. The material properties are $E_L/E_T=25$, $G_{LT}/E_T=0.5$, $G_{TT}/E_T=0.2$, and $\nu_{LT}=\nu_{TT}=0.25$. The plate has a width $2a=24$ and thickness $t=6$. An exact elasticity solution of this problem has been presented by Pagano;⁶¹ finite element results based upon the use of independent layer rotations are reported by Palazotto and Witt.⁵⁴

The plate is modeled using ten elements over half the width, with symmetry conditions applied at the centerline. Transverse shear stresses in the element nearest the support are shown in Figure 15. The results are in reasonable agreement with the exact solution, with the peak shear stress being overestimated by about eight percent. The finite element solution of Reference 54, using 30 elements with independent rotations in each layer, appears to overestimate the maximum shear stress by three to four percent, based on graphical results presented therein.

7.2.2 Three-Layered Plate under Pressure

The square plate in Figure 16 is a $[0/90/0]$ graphite/epoxy laminate, with $E_L=25 \times 10^6$ and the remaining properties defined as in the previous example. The 0° direction is aligned with the x axis. For the sinusoidal pressure $q(x,y) = q_0 \sin(\pi x/a) \sin(\pi y/b)$, and simply supported edges, an analytical solution is possible.⁶² We consider the case $a=b=10$, for plate thicknesses between 0.1 and 2.5. In the finite element model, an 11×11 mesh of bilinear elements is used to represent the entire plate. The symmetry of the problem is not exploited, in the interest of obtaining stress values at suitable locations for comparison with other solutions.

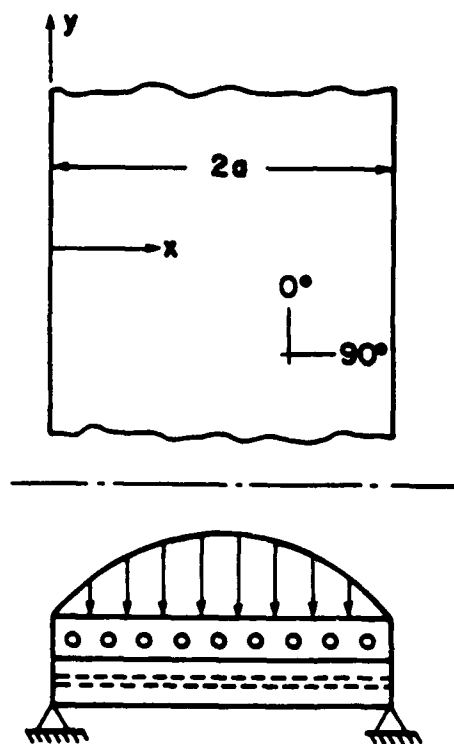


Figure 14. Semi-infinite Plate with Sinusoidal Pressure.

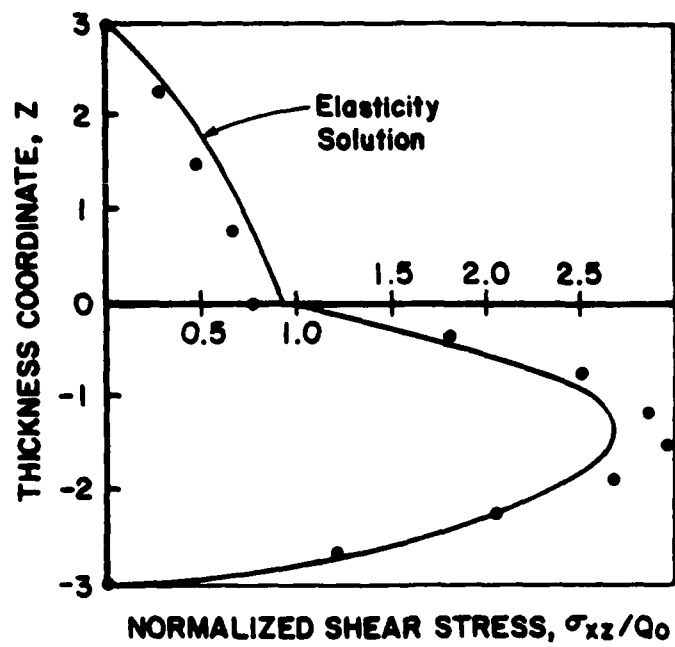


Figure 15. Transverse Shear Stresses in Unsymmetric Plate.

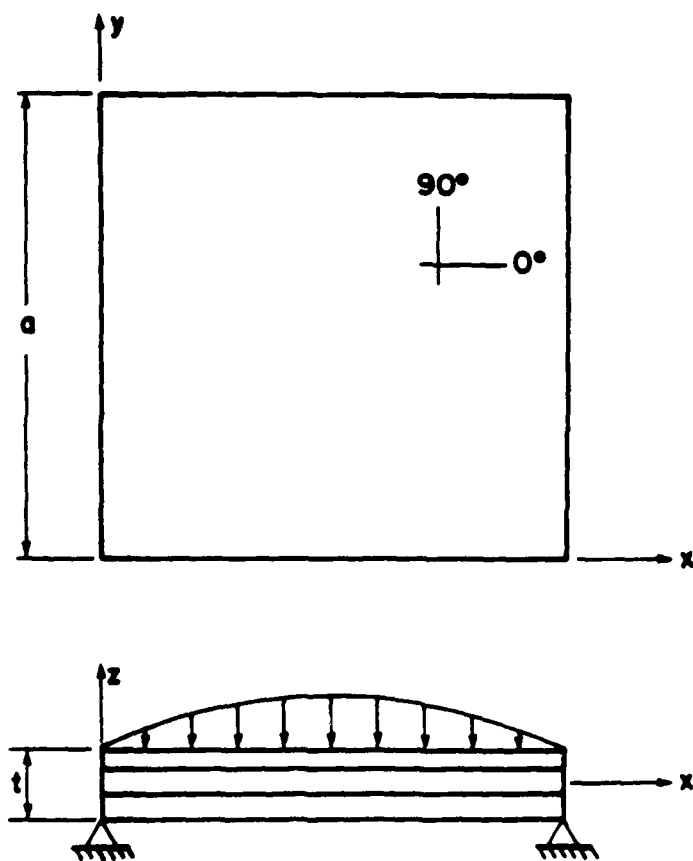


Figure 16. Square [0/90/0] Plate under Pressure Load.

Table 7 compares the normalized bending stresses (defined by $\bar{\sigma} = \sigma t^2 / q_0 a^2$) obtained using the present method with the elasticity solution⁶² and the finite element results of Engblom and Ochoa,⁶³ who use a 40-DOF plate element with higher-order displacement variations through the thickness. Results listed in the Table are limited to those values reported in Reference 62 which can be evaluated directly at element centers.

The bending stresses obtained from the present solution are in reasonable agreement with the remaining solutions. The trends predicted are quite similar to those of the higher-order element, but the accuracy obtained is generally lower. In this example, the deformation pattern is quite different from the cylindrical bending assumptions used to derive the shear corrections. As a result the deflections and overall load paths are reasonable, but pointwise stress accuracy is limited.

7.2.3 Circular Sandwich Plate

The finite element mesh in Figure 17 represents one quadrant of a circular sandwich panel with the following properties:

<u>Faces:</u>	$E = 1 \times 10^7$	$\nu = 0.30$	$t_f = 0.025$
<u>Core:</u>	$G = 260,000$	$t_c = 0.450$	

The radius of the panel is $a=20$, and the outer edge is completely fixed. A uniform static pressure $q = 10$ is applied. This case has been analyzed by Sharifi⁶⁴, using special-purpose elements with independent shear rotations in the sandwich core layer.

Figure 18 shows the radial distribution of moment resultants obtained from the present analysis. Though only graphical results are available in Reference 64, the two solutions appear to agree quite well. The shear force per unit length obtained from the finite element solution is shown in Figure 19, together with the exact solution $Q(r) = qr/2$.

Table 7. Normalized Stresses for Square [0/90/0] Plate

a/h	Stress Component	Present	Elasticity Solution [62]	Higher-Order Element [63]
4	$\bar{\sigma}_x^1$	0.357	0.755	0.391
	$\bar{\sigma}_y^2$	0.521	0.556	0.572
10	$\bar{\sigma}_x$	0.476	0.590	0.500
	$\bar{\sigma}_y$	0.273	0.285	0.279
20	$\bar{\sigma}_x$	0.506	0.552	0.531
	$\bar{\sigma}_y$	0.200	0.189	0.210
50	$\bar{\sigma}_x$	0.513	0.541	0.541
	$\bar{\sigma}_y$	0.176	0.185	0.164
100	$\bar{\sigma}_x$	0.514	0.539	0.542
	$\bar{\sigma}_y$	0.173	0.181	0.167

¹ $\bar{\sigma}_x$ at center of plate, $z = \frac{t}{2}$

² $\bar{\sigma}_y$ at center of plate, $z = \frac{t}{6}$ (top of 90° layer)

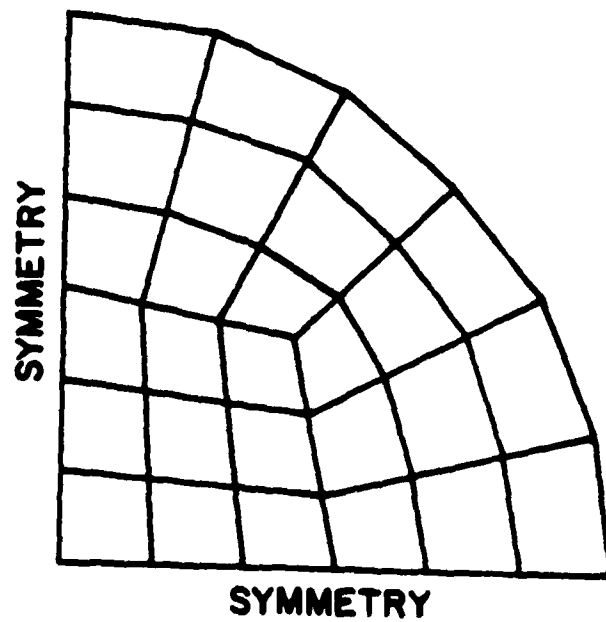


Figure 17. Circular Sandwich Plate.

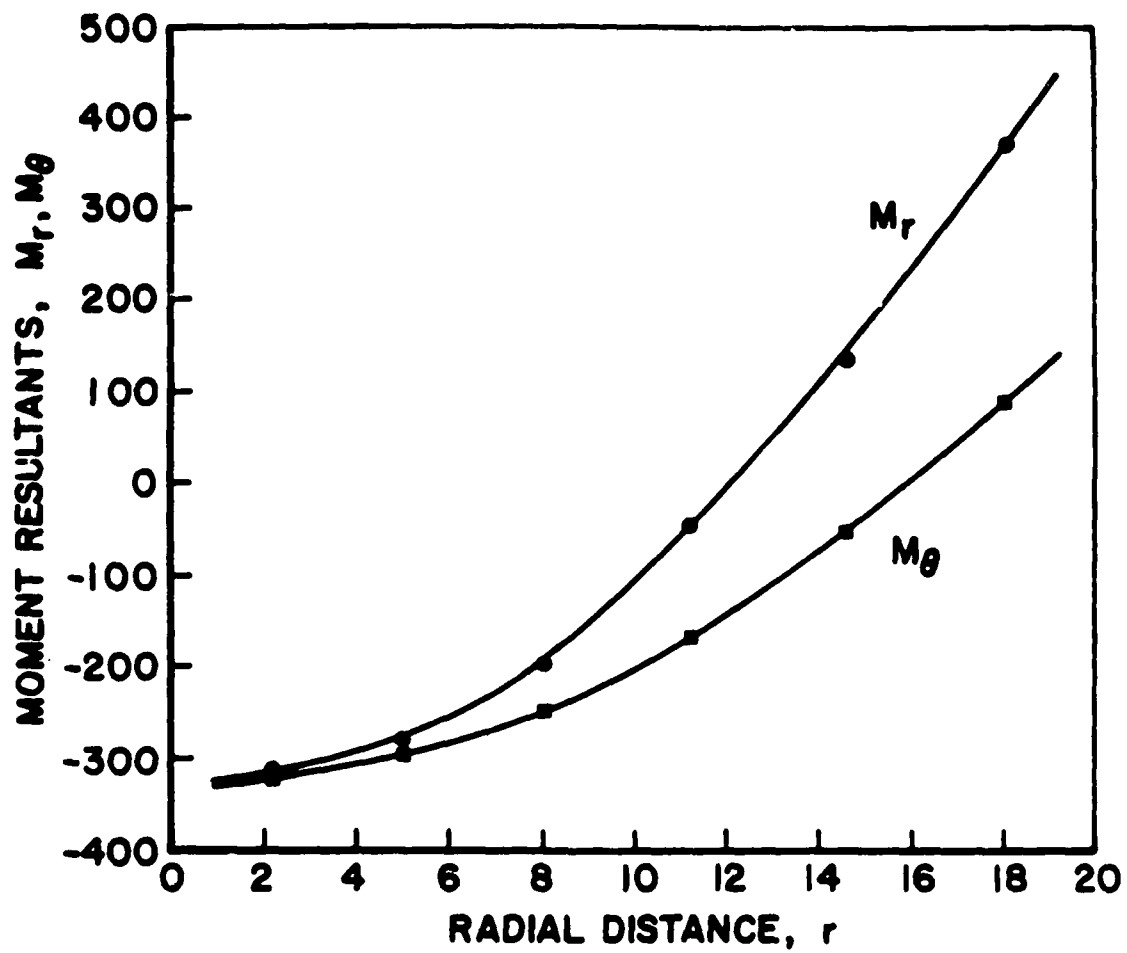


Figure 18. Moment Resultants in Circular Sandwich Plate.

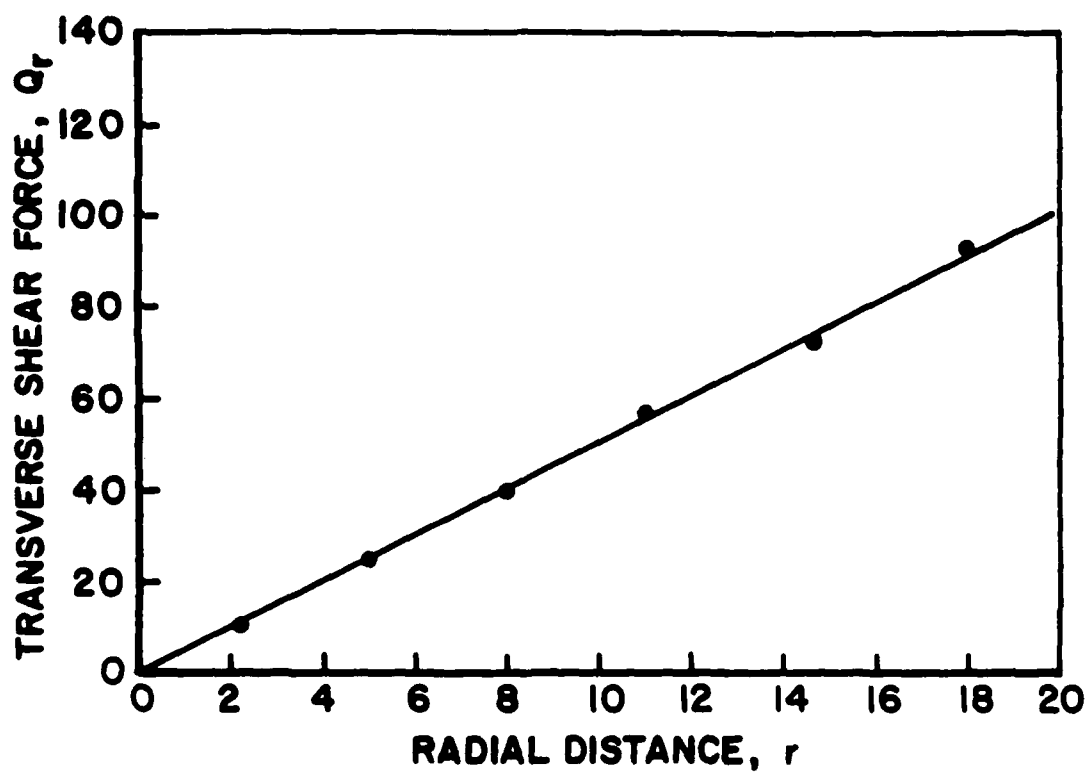


Figure 19. Shear Forces in Circular Sandwich Plate.

7.2.4 Rectangular Sandwich Plate

A square sandwich panel (Figure 20) is loaded by a uniform pressure q_0 . The three-layer plate is 50 inches on each side, with identical aluminum face sheets ($E=10.5 \times 10^6$, $\nu=0.3$, $t_f=0.015$) and a honeycomb core ($G=50,000$, $t_c=1.0$). All edges of the panel are completely fixed.

The present solution uses a 5×5 mesh of bilinear elements in one quadrant of the plate, and yields a transverse deflection at the center $w_c = 0.09285$. This value compares well (2.2 percent) with the analytic solution presented by Kan and Huang,⁶⁵ which gives $w_c = 0.09497$. The finite element solutions of References 66 and 67 achieve comparable accuracy, but with more than twice as many equations and considerably more complicated elements.

7.2.5 Vibrations of a Layered Panel

The natural frequencies of a rectangular $[0/90/0]$ laminate obtained using the present analysis have been compared with the analytical solution by Ashton and Whitney.³⁴ The plate (Figure 21) has dimensions 30×10 , and mechanical properties identical to those used in the first two examples; a density of $\rho = 0.0001$ is assumed. Each layer is 0.01 thick. In the finite element solution, a 15×5 element mesh is used to represent the entire plate. All four edges are simply supported.

Table 8 compares the computed natural frequencies with the analytical solution,

$$\bar{\omega} = \omega \frac{b^2}{\pi^2} \sqrt{\rho t / D_{22}} = \left[\frac{D_{11}}{D_{22}} \left(m \frac{b}{a} \right)^4 + \frac{2(D_{12} + 2D_{66})}{D_{22}} \left(n m \frac{b}{a} \right)^2 + n^4 \right]^{1/2} \quad (175)$$

in which (m,n) are mode numbers along the (x,y) axes. The seven lowest frequencies in the Table represent all modes below the first $n=3$ mode. The $n=1$ modes exhibit good accuracy; for $n=2$,

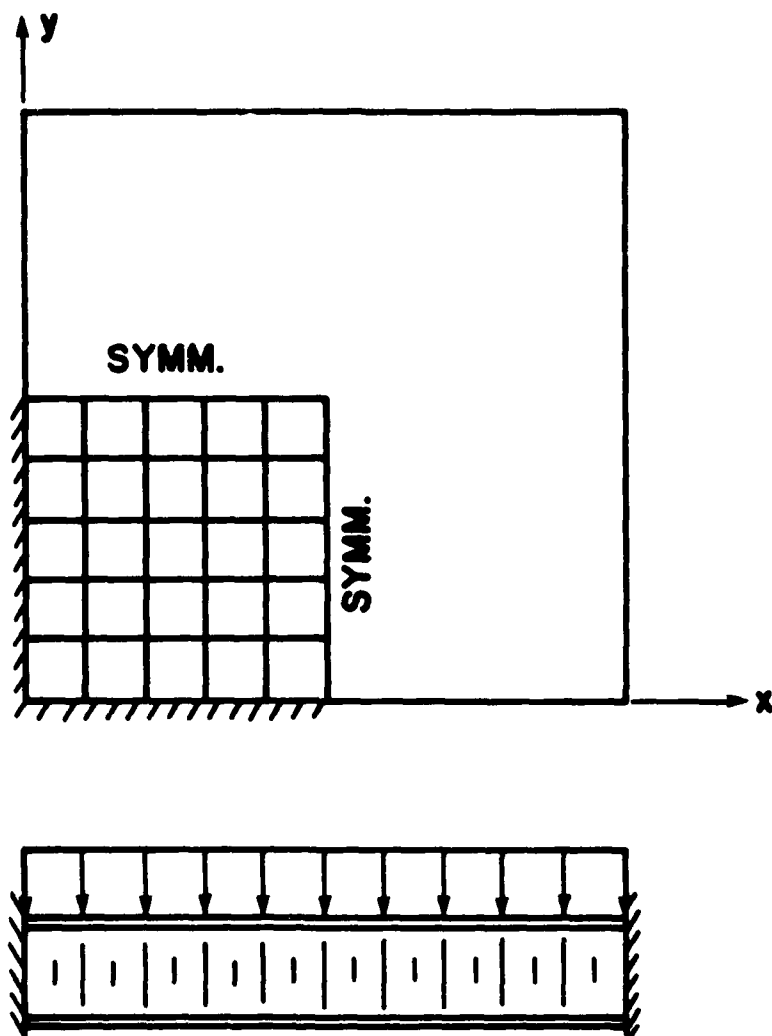


Figure 20. Clamped Sandwich Panel under Uniform Pressure.

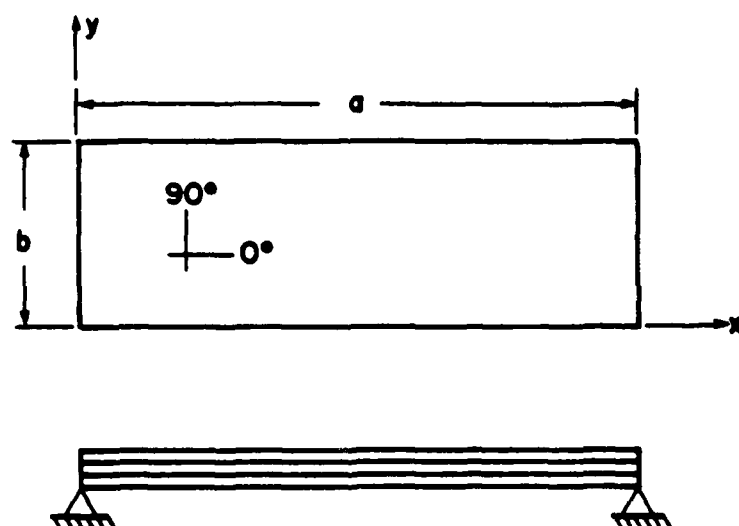


Figure 21. Rectangular [0/90/0] Laminate.

Table 8. Natural Frequencies of [0/90/0] Plate

Mode	m	n	$\bar{\omega}_{\text{exact}}$	$\bar{\omega}_{\text{comp.}}$	Error(%)
1	1	1	1.415	1.473	4.1
2	2	1	2.626	2.733	4.1
3	1	2	4.420	4.864	10.0
4	3	1	4.622	5.056	9.4
5	2	2	5.659	6.358	12.4
6	4	1	7.406	8.025	8.4
7	3	2	7.691	8.528	10.9

where the five elements across the width can be expected to give only marginal accuracy, the computed frequencies are still within 10-12 percent of the exact values.

7.3 SENSITIVITY ANALYSIS EXAMPLES

The examples of this Section are sensitivity calculations, in which material modulus and density, plate thickness, and arbitrary geometric variables appear as independent parameters. The first five problems have analytical solutions, so that errors in the finite element solution can be assessed conclusively. In these problems, we include both static and natural frequency results, and sensitivities with respect to intrinsic properties, shape (dimensions), and orientation. The final example deals with a twisted plate for which numerical results are available, and compares the sensitivity calculations for total angle of twist to approximations obtained using finite differences.

7.3.1 Static Analysis of a Tension Strip

The long, thin strip in Figure 12 (see Section 7.1.1) is subjected to a uniform load applied at the end. We choose as sensitivity variables the modulus E , thickness t , width b , and length L . The first two of these are intrinsic variables, and the remaining two are geometry parameters which affect the nodal positions. The exact inplane displacements are linear functions of position, as are the sensitivities, and therefore a single bilinear element should reproduce both results exactly. Data obtained for the displacement and stress resultant sensitivities from a single-element model are indeed exact, as shown in Table 9.

7.3.2 Statics of a Cantilever Beam

Figure 22 shows a cantilever beam subjected to a transverse force at the tip. Again, an analytical solution is possible both

Table 9. Sensitivity Data for Simple Tension Problem[†]

Quantity	Exact	Exact (x=L)	Computed
u	Px/Ebt	0.001	0.001
$\partial u/\partial E$	$-Px/E^2bt$	-1.0×10^{-10}	-1.0×10^{-10}
$\partial u/\partial t$	$-Px/Ebt^2$	-0.01	-0.01
$\partial u/\partial b$	$-Px/Eb^2t$	-0.001	-0.001
$\partial u/\partial L$	P/Ebt	0.0001	0.0001
N	P/b	100.0	100.0
$\partial N/\partial E$	0	0.0	0.0
$\partial N/\partial t$	0	0.0	0.0
$\partial N/\partial b$	$-P/b^2$	-100.0	-100.0
$\partial N/\partial L$	0	0.0	0.0

[†] $E=1 \times 10^7$; $\nu=0.3$; $t=0.1$; $L=10$; $b=1$; $P=100$

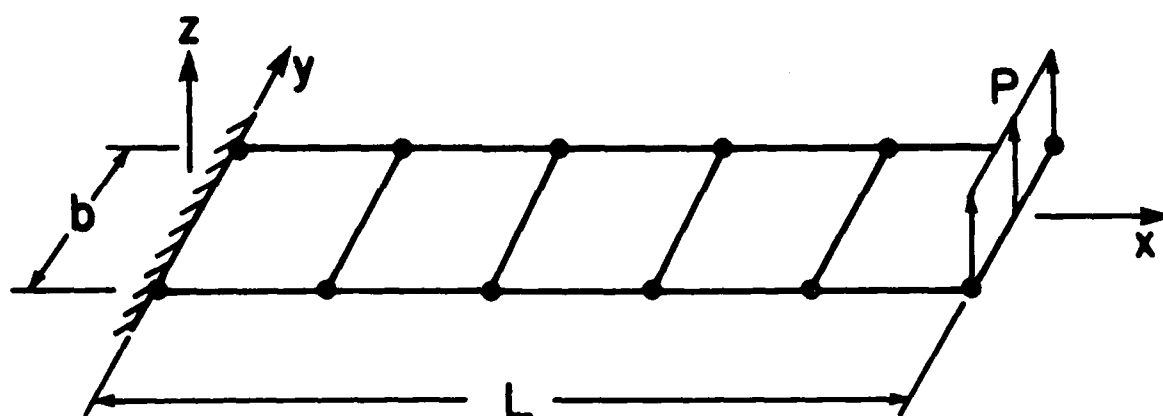


Figure 22. Cantilever Beam with Tip Load.

for the displacement and rotation, and for the sensitivities with respect to modulus E , thickness t , and width b . Five bilinear plate elements are used to model the beam; this number is sufficient for good accuracy but, since the elements have only linear displacement and rotation fields, does not reproduce the exact solution. Table 10 summarizes computed results for the displacements and rotations. Note that the displacement sensitivities are no less accurate than the displacements themselves (all are approximately 1 percent in error), and that the rotational results are exact. Table 11 shows moment and shear results, and the force sensitivities which are nonzero. In all cases, the moment and shear sensitivities are exact, despite small errors in the displacement solution. It is probably reasonable to expect exact results for the force sensitivities in a statically determinate problem.

7.3.3 Orientation Sensitivity of a Beam

Consider the bar shown in Figure 23, which is inclined with respect to the global X axis and subjected to a vertical force, producing both stretching and bending response. This problem is intended to test the sensitivity calculation for element local axis orientation; we select the orientation θ as the geometric control variable, which leads to $B'=0$, $|J|'=0$, and $A'\neq 0$ for all elements. Note that the nodal coordinate sensitivities are simply $X'=-Y$, $Y'=X$.

For $\theta=0$, the nonzero results and sensitivities are given in Table 12. Computed results are obtained from a model with five bilinear Mindlin plate elements, which exhibits a moderately small displacement error (1-3 percent). Again, the displacement sensitivities exhibit errors which are similar in magnitude to the displacement error in the original solution; both the computed moments and axial force sensitivities are exact.

Table 10. Displacement Sensitivity Data for Cantilever Beam[†]

Quantity	Exact	Exact (x=L)	Computed
w	$2P(3Lx^2 - x^3)/Ebt^3$	0.4	0.39602
$\partial w/\partial E$	$-2P(3Lx^2 - x^3)/E^2bt^3$	-4.0×10^{-8}	-3.96×10^{-8}
$\partial w/\partial t$	$-6P(3Lx^2 - x^3)/Ebt^4$	-12.0	-11.88
$\partial w/\partial b$	$-2P(3Lx^2 - x^3)/Eb^2t^3$	-0.4	-0.39602
θ	$6P(2Lx - x^2)/Ebt^3$	0.06	0.06
$\partial \theta/\partial E$	$-6P(2Lx - x^2)/E^2bt^3$	-6.0×10^{-9}	-6.0×10^{-9}
$\partial \theta/\partial t$	$-18P(2Lx - x^2)/Ebt^4$	-1.8	-1.8
$\partial \theta/\partial b$	$-6P(2Lx - x^2)/Eb^2t^3$	-0.06	-0.06

[†] $E=1 \times 10^7$; $\nu=0$; $t=0.1$; $b=1$; $L=10$; $P=1$

Table 11. Force Sensitivity Data for Cantilever Beam[†]

Quantity		Element Centers				
		x=1	x=3	x=5	x=7	x=9
M	Exact	-9.0	-7.0	-5.0	-3.0	-1.0
	Comp.	-9.0	-7.0	-5.0	-3.0	-1.0
$\partial M / \partial b$	Exact	9.0	7.0	5.0	3.0	1.0
	Comp.	9.0	7.0	5.0	3.0	1.0
Q	Exact	1.0	1.0	1.0	1.0	1.0
	Comp.	1.0	1.0	1.0	1.0	1.0
$\partial Q / \partial b$	Exact	-1.0	-1.0	-1.0	-1.0	-1.0
	Comp.	-1.0	-1.0	-1.0	-1.0	-1.0

[†]E=1×10⁷; v=0; t=0.1; b=1; L=10; P=1

Only nonzero values shown; $\frac{\partial M}{\partial E} = \frac{\partial M}{\partial t} = \frac{\partial Q}{\partial E} = \frac{\partial Q}{\partial t} = 0$ identically.

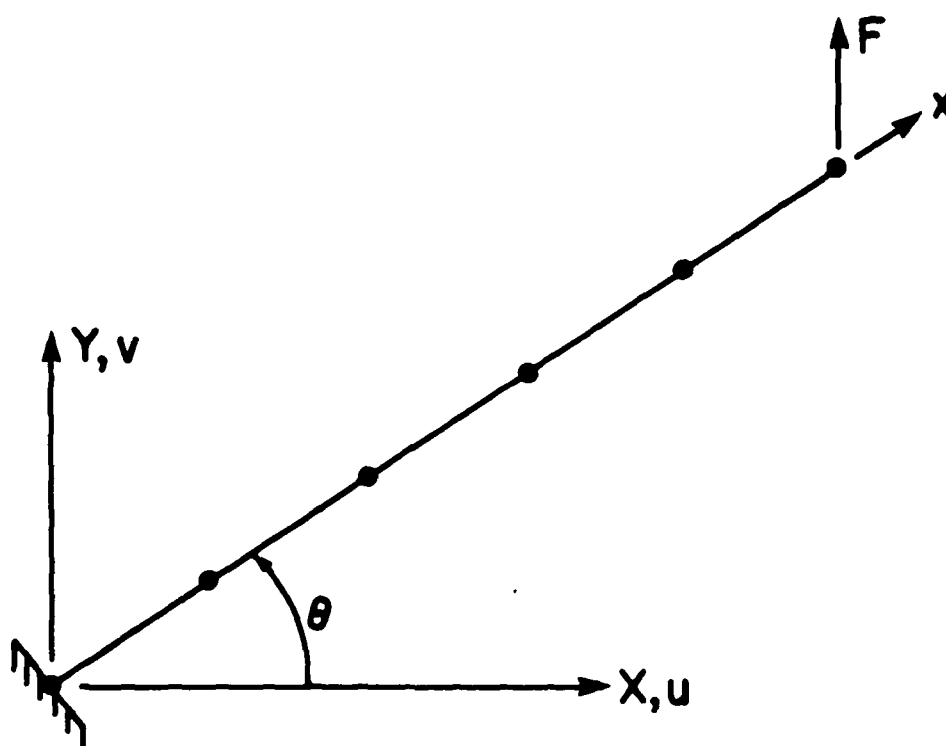


Figure 23. Cantilever with Specified Angular Orientation.

Table 12. Results for Angular Orientation Problem ($\theta=0$)[†]

		Nodal Positions				
Quantity		$x=L/5$	$x=2L/5$	$x=3L/5$	$x=4L/5$	$x=L$
v	Exact	0.07000	0.26000	0.54000	0.88000	1.2500
	Comp.	0.06756	0.25512	0.53268	0.87024	1.2378
$\partial u/\partial \theta$	Exact	-0.06998	-0.25995	-0.53993	-0.87990	-1.2499
	Comp.	-0.06754	-0.25507	-0.53260	-0.87014	-1.2377

		Element Centers				
Quantity		$x=L/10$	$x=3L/10$	$x=L/2$	$x=7L/10$	$x=9L/10$
M	Exact	-4.500	-3.500	-2.500	-1.500	-0.500
M	Comp.	-4.500	-3.500	-2.500	-1.500	-0.500
$\partial N/\partial \theta$	Exact	1.000	1.000	1.000	1.000	1.000
$\partial N/\partial \theta$	Comp.	1.000	1.000	1.000	1.000	1.000

[†]E=400,000; $\nu=0$; $t=0.1$; $b=1$; $L=5$; $F=1$.

Table 13 summarizes the results for a similar calculation with $\theta=26.565^\circ$ ($\tan\theta=1/2$). Computed and exact displacement values again compare well. Results for the axial force and moment resultants are exact as above (only one set of values is shown in the Table).

7.3.4 Frequency Sensitivity of a Flat Strip

The planar strip of Figure 12 is considered again, to determine parameter sensitivities of the fundamental frequency. Using a single bilinear element (which provides a poor estimate of the lowest frequency), we can make some interesting observations on the sensitivity solution. Since the first natural

frequency is $\omega = \sqrt{E\pi^2/4\rho L^2}$, we note that $\partial\omega/\partial E = \omega/2E$, $\partial\omega/\partial t = 0$, and $\partial\omega/\partial L = -\omega/L$.

The lowest natural frequency for a strip with $E=10^7$, $\nu=0.3$, $L=10$, and $\rho=0.000259$, as computed using a single element with consistent mass, is $\omega_c=39,669.4$ (see Section 7.1.1), and compares poorly with the exact value of $\omega=30,865.3$. The sensitivities, compared with exact results, are similarly poor. However, sensitivity values computed on the basis of the finite element model frequency (e.g., $\partial\omega/\partial E = \omega_c/2E$) are nearly exact, as shown in Table 14. That is, the sensitivity values are related to the model frequency in the correct manner, and the errors in the computed sensitivities are dominated by the discretization error in the original solution. This is true because parameters such as the modulus and density (and, in this problem, the length) enter the finite element solution in precisely the same way as for the analytical problem.

Table 13. Results for Angular Orientation Problem ($\theta=26.565^\circ$)[†]

Quantity		Nodal Positions				
		$x=L/5$	$x=2L/5$	$x=3L/5$	$x=4L/5$	$x=L$
u	Exact	-0.03912	-0.14532	-0.30184	-0.49189	-0.69872
	Comp.	-0.03775	-0.14258	-0.29772	-0.48641	-0.69186
v	Exact	0.07338	0.27254	0.56603	0.92241	1.3102
	Comp.	0.07553	0.28552	0.59553	0.97293	1.3839
$\partial u/\partial \theta$	Exact	-0.05868	-0.21798	-0.45275	-0.73784	-1.0480
	Comp.	-0.05662	-0.21387	-0.44659	-0.72961	-1.0378
$\partial v/\partial \theta$	Exact	-0.07824	-0.29064	-0.60367	-0.98378	-1.3974
	Comp.	-0.07550	-0.28516	-0.59545	-0.97281	-1.3837

Quantity		Element Centers ^{††}				
		$x=L/10$	$x=3L/10$	$x=L/2$	$x=7L/10$	$x=9L/10$
N		0.4472	0.4472	0.4472	0.4472	0.4472
M		-4.500	-3.500	-2.500	-1.500	-0.500
$\partial N/\partial \theta$		0.8944	0.8944	0.8944	0.8944	0.8944
$\partial M/\partial \theta$		2.250	1.750	1.250	0.750	0.250

[†] $E=400,000$; $\nu=0$; $t=0.1$; $b=1$; $L=5.59017$; $F_y=1$.

^{††} Only computed element results are shown; all values are exact.

Table 14. Frequency Sensitivities for Axial Vibration Problem¹

Quantity	Exact	Exact Value ²	Computed
$\partial\omega/\partial E$	$\omega/2E$	0.0019834	0.0019835
$\partial\omega/\partial t$	0	0.	-1.81×10^{-9}
$\partial\omega/\partial L$	$-\omega/L$	-3,966.94	-3,965.05

¹ $E=1 \times 10^7$; $\nu=0.3$; $t=0.1$; $\rho=0.000259$; $L=10$; $b=1$.

² Exact sensitivities computed using F. E. model frequency.

7.3.5 Frequency Sensitivity of a Beam

For the cantilever beam (Figure 22), an analytical solution for parameter sensitivities of the natural frequencies is quite simple. Defining

$$\beta = \left[\frac{EI}{\rho AL^4} \right]^{\frac{1}{2}} = \left[\frac{Et^2}{12\rho L^4} \right]^{\frac{1}{2}} \quad (176)$$

The bending frequencies are $\omega_i = \alpha_i \beta$, where α_i are independent of the geometry and properties of the beam. In particular, the first three natural frequencies have $\alpha = 3.52, 22.0$, and 61.7 , respectively.⁶⁸

Table 15 summarizes the results obtained for a particular case, using three different meshes. The sensitivity parameters are modulus E , density ρ , thickness t , width b , and length L . It is instructive to study the results from a relatively coarse model (five bilinear elements) first; this model is labeled Mesh 1 in the Table. All computed results for the first mode are quite good for Mesh 1, with the error in frequency sensitivities being similar in magnitude to the frequency error itself. For the next two modes, the sensitivities for intrinsic parameters E , ρ , and t are at least equal in accuracy to the frequencies, for reasons explained in the last example. The length sensitivity in Mesh 1 has been defined by attributing coordinate sensitivities only to the end nodes, however, and is rather poor: this "local" geometry parameter does not enter the finite element frequency equation in the same manner as in the analytical solution.

Meshes 2 and 3 represent the two obvious solutions to the poor accuracy of Mesh 1 for the length parameter in higher modes. Mesh 2 is a refined model, in which ten elements are used, and the coordinate sensitivities are defined for the end nodes only, as in Mesh 1. All results are much improved, as expected; but

Table 15. Frequency Sensitivities for Cantilever Beam[†]

Mode	ω	$\partial\omega/\partial E$	$\partial\omega/\partial \rho$	$\partial\omega/\partial t$	$\partial\omega/\partial b$	$\partial\omega/\partial L$
1 Exact	201.6	1.01×10^{-5}	-3.97×10^5	2016.	0.	-40.32
Mesh-1	202.3	1.01×10^{-5}	-3.98×10^5	2023.	3.9×10^{-10}	-40.67
Mesh-2	201.6	1.01×10^{-5}	-3.97×10^5	2016.	4.9×10^{-10}	-40.37
Mesh-3	201.6	1.01×10^{-5}	-3.97×10^5	2016.	4.9×10^{-10}	-40.32
2 Exact	1260.1	6.30×10^{-5}	-2.48×10^6	12601.	0.	-252.03
Mesh-1	1391.9	6.96×10^{-5}	-2.74×10^6	13904.	3.8×10^{-10}	-310.24
Mesh-2	1292.9	6.46×10^{-5}	-2.55×10^6	12917.	4.6×10^{-11}	-265.25
Mesh-3	1292.9	6.46×10^{-5}	-2.55×10^6	12917.	4.6×10^{-11}	-258.46
3 Exact	3534.1	1.77×10^{-4}	-6.96×10^6	35341.	0.	-706.82
Mesh-1	4727.9	2.36×10^{-4}	-9.31×10^6	47120.	1.5×10^{-10}	-1260.49
Mesh-2	3790.1	1.90×10^{-4}	-7.46×10^6	37809.	5.8×10^{-11}	-818.98
Mesh-3	3790.1	1.90×10^{-4}	-7.46×10^6	37809.	5.8×10^{-11}	-757.10

[†] $E=1 \times 10^7$; $\nu=0$; $t=0.1$; $\rho=0.000254$; $L=10$; $b=1$

the $\partial\omega/\partial L$ sensitivity is still less accurate (15.9 percent error for the third mode) than the frequency (7.2 percent error).

Mesh 3 is different from Mesh 2 only in the specification of the nodal coordinate sensitivities, which now are specified so that all nodes move proportionally when the length changes. Mesh 3 produces results which are essentially exact for Mode 1, and reduces the error in $\partial\omega/\partial L$ by half for the higher modes. For Mesh 3, the error in all of the sensitivity results is generally no larger than the frequency error for each case considered.

7.3.6 Twisted Plate Frequency Sensitivity

Figure 24 shows a twisted cantilever plate which has been used extensively for the comparison of natural frequency predictions.⁶⁹ We wish to compare natural frequency sensitivities obtained with the present analysis to those derived from finite differencing. For the case considered we take $E=10^7$, $\nu=0.30$, $\rho=0.00026$; the dimensions are length $a=3$, width $b=1$, and thickness $h=0.050$.

For the present analysis, we employ a 6×6 mesh of bilinear elements, which is adequate for the first few modes. As evidence of this, Table 16 summarizes the first several modes predicted for a twist angle of $\theta=30^\circ$. Frequencies obtained from NASTRAN⁶⁹ using a mesh of 128 TRIA2 elements are tabulated as well, and the two solutions are in reasonable agreement.

Table 17 lists the computed natural frequency sensitivities for modes 1-4, for a twist angle of 32° . The finite difference estimates shown for the sensitivities have been obtained from separate eigenvalue solutions performed for twist angles of 31.9° and 32.1° . The agreement of the predictions is reasonably good, and is quite accurate where the corresponding sensitivity is large in magnitude.

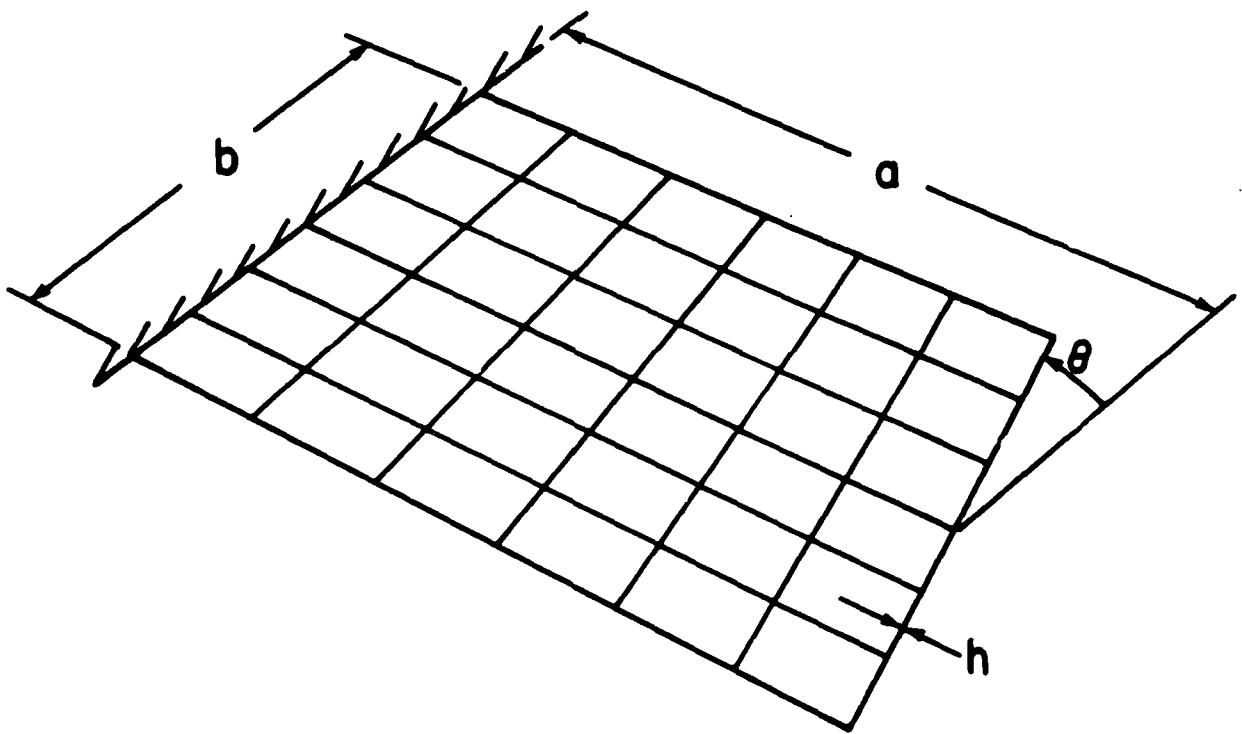


Figure 24. Twisted Cantilever Plate.

Table 16. Frequency Comparison for 30° Twisted Plate[†]

<u>Mode</u>	<u>Type</u>	<u>NASTRAN</u>	<u>Present</u>
1	1-B	3.42	3.20
2	2-B	19.10	19.08
3	1-T	26.04	26.52
4	3-B	60.15	61.62
5	1-EB	73.00	74.19
6	2-T	78.50	82.93

[†]Normalized frequencies are $\lambda = \omega a^2 \sqrt{\rho h/D}$

Table 17. Frequency Sensitivities for 32° Twisted Plate

Mode	Type	$\omega(31.9^\circ)$	$\omega(32^\circ)$	$\omega(32.1^\circ)$	$\partial\omega/\partial\theta^{1,2}$	$\Delta\omega/\Delta\theta^3$
1	1-B	921.16	920.23	919.29	-467.3	-535.1
2	2-B	5354.91	5346.21	5337.53	-4668.9	-4979.0
3	1-T	9006.48	9017.26	9028.02	4927.2	6170.8
4	3-B	17141.7	17119.2	17096.8	-12791.5	-12862.9

¹ Note that the variable θ is defined in radians.

² $\partial\omega/\partial\theta$ is computed directly by the sensitivity solution.

³ $\Delta\omega/\Delta\theta$ is computed by differencing values at 31.9° and 32.1°.

The relatively low accuracy of the sensitivities in torsion are thought to be an artifact of the bilinear element used in the frequency calculations. Since the element is integrated with a single point, the twisted undeformed geometry is not reflected in the stiffness computation (other than in "nodal offsets" which occur at each node, and which are taken into account). High accuracy for twisting modes (and presumably for the corresponding sensitivities) therefore requires a relatively fine mesh.

7.4 PROBABILISTIC ANALYSIS EXAMPLES

Probabilistic solutions obtained with the methods described herein are described in this Section. It should be recognized that the finite element calculations performed in the probabilistic analyses are limited to the basic (deterministic) solution and the sensitivity analyses, so that the numerical behavior reported for the sensitivity analyses of the previous Section is typical of the probabilistic solutions as well. The additional steps of performing variance and percentile calculations complete the process.

7.4.1 Forced Vibration of a Cantilever Beam

The cantilever beam shown in Figure 22 (see Sections 7.3.2 and 7.3.5) is subjected to a uniform pressure load which varies sinusoidally in time, $q = -0.01 \cdot \sin(\omega t)$. The finite element model used is the same as Mesh 1 of Section 7.3.5, so that the first resonant frequency is at $\omega = 202.3$ Hz. We consider forcing frequencies in the range $200 \leq \omega \leq 205$, to determine the steady-state response behavior of the beam near its first mode.

Figure 25 shows the amplitude of the end deflection versus forcing frequency. Note that the tip displacement and the forces are in phase for frequencies lower than the natural frequency,

Frequency Response of Cantilever Beam

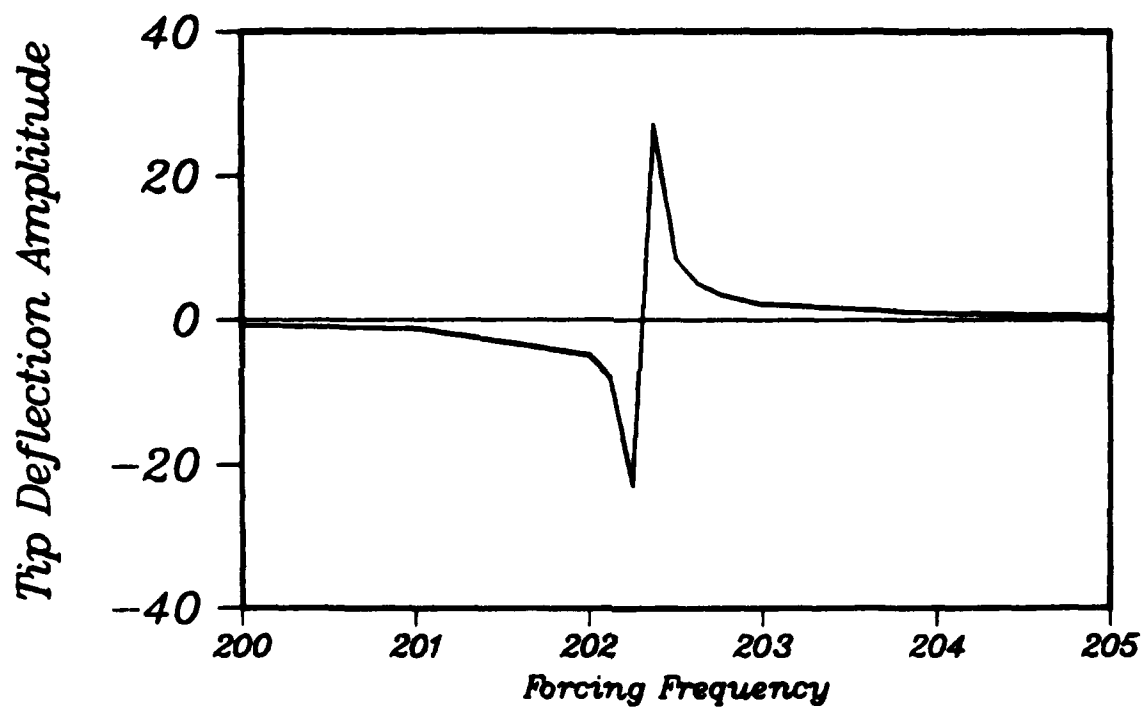


Figure 25. Frequency Response of Cantilever Beam.

and out of phase after crossing the resonance. In the neighborhood of the natural frequency, a step of 0.125 Hz. has been used for the forcing frequency in generating the results of Figure 25.

Statistical parameters selected for this analysis are the elastic modulus ($E=1 \times 10^7$; $\sigma_E=1 \times 10^5$), mass density ($\rho=2.54 \times 10^{-4}$; $\sigma_\rho=1 \times 10^{-5}$), thickness ($t=0.10$; $\sigma_t=0.005$), and beam width ($b=1$; $\sigma_b=0.001$). Figure 26 contains plots of amplitude sensitivity for each of these parameters, which is obtained as a by-product of the probabilistic solution.

Figure 27 depicts the variance of the tip displacement amplitude of the beam versus forcing frequency. The upper curve represents the total variance, and reflects the probabilistic variation of all four parameters (E , ρ , t , b). The remaining four curves show the contributions to this total from individual parameters. The relative magnitudes of these curves depend both upon the parameter sensitivities (Figure 26) and the variances in the statistical parameters. In this case the thickness variation is the most pronounced effect, followed by the density variation.

In Figures 28 and 29, we show the probabilistic solution in terms of percentile (confidence) levels. Figure 28 presents this data as a family of curves for discrete confidence levels. The same data are used to construct a continuous surface in Figure 29, with the second independent variable corresponding to the confidence level. Note that at a particular frequency, the plot should always indicate an amplitude which increases monotonically with the confidence level.

Figures 30 through 32 contain moment amplitude results for the beam, presented in forms similar to the displacement solutions above. Bending moment values are obtained from the element center nearest the root section ($x=1$).

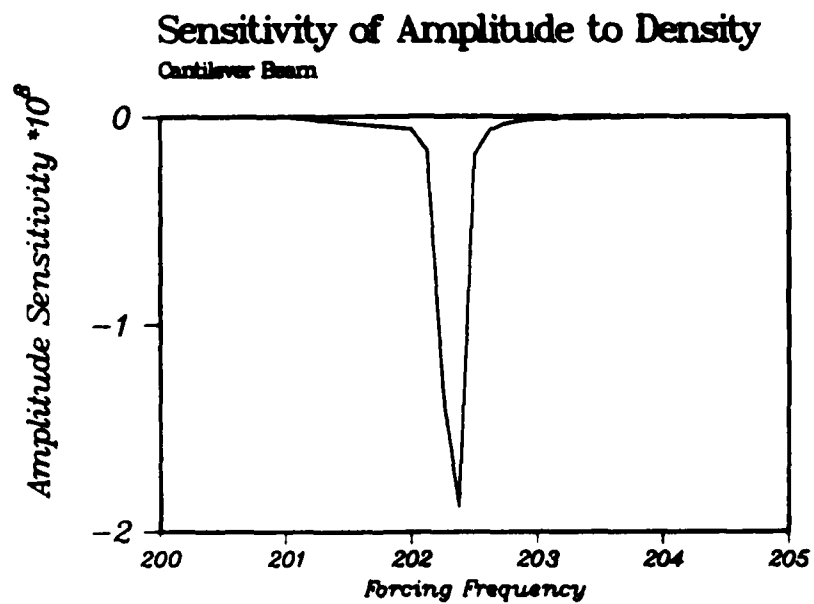
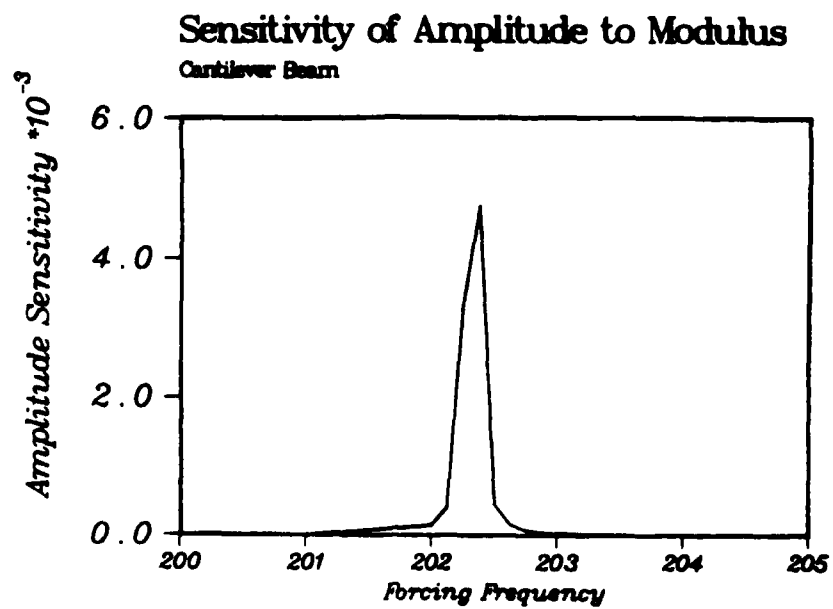
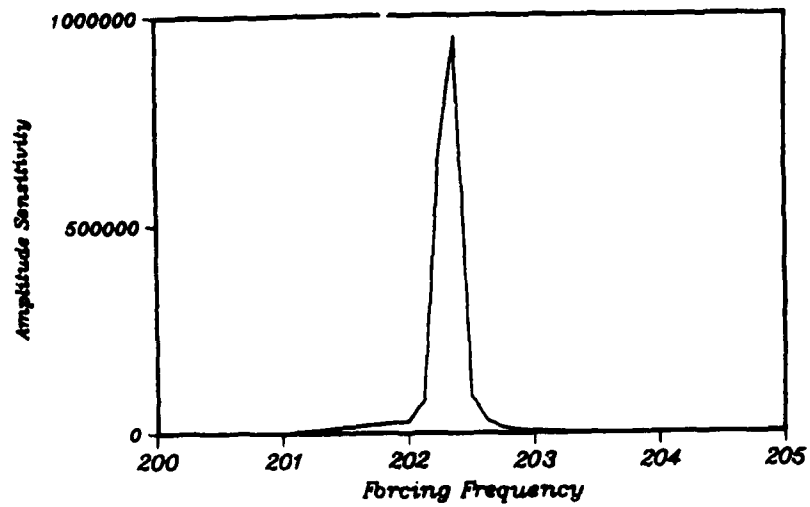


Figure 26. Amplitude Sensitivities for Cantilever Beam.

Sensitivity of Amplitude to Width

Cantilever Beam



Sensitivity of Amplitude to Thickness

Cantilever Beam

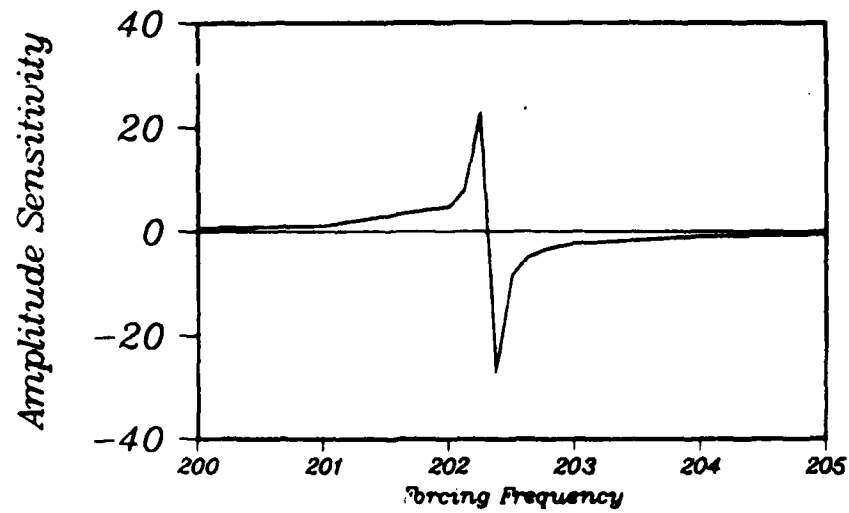


Figure 26. Amplitude Sensitivities for Cantilevered Beam (Concluded).

TIP DISPLACEMENT AMPLITUDE

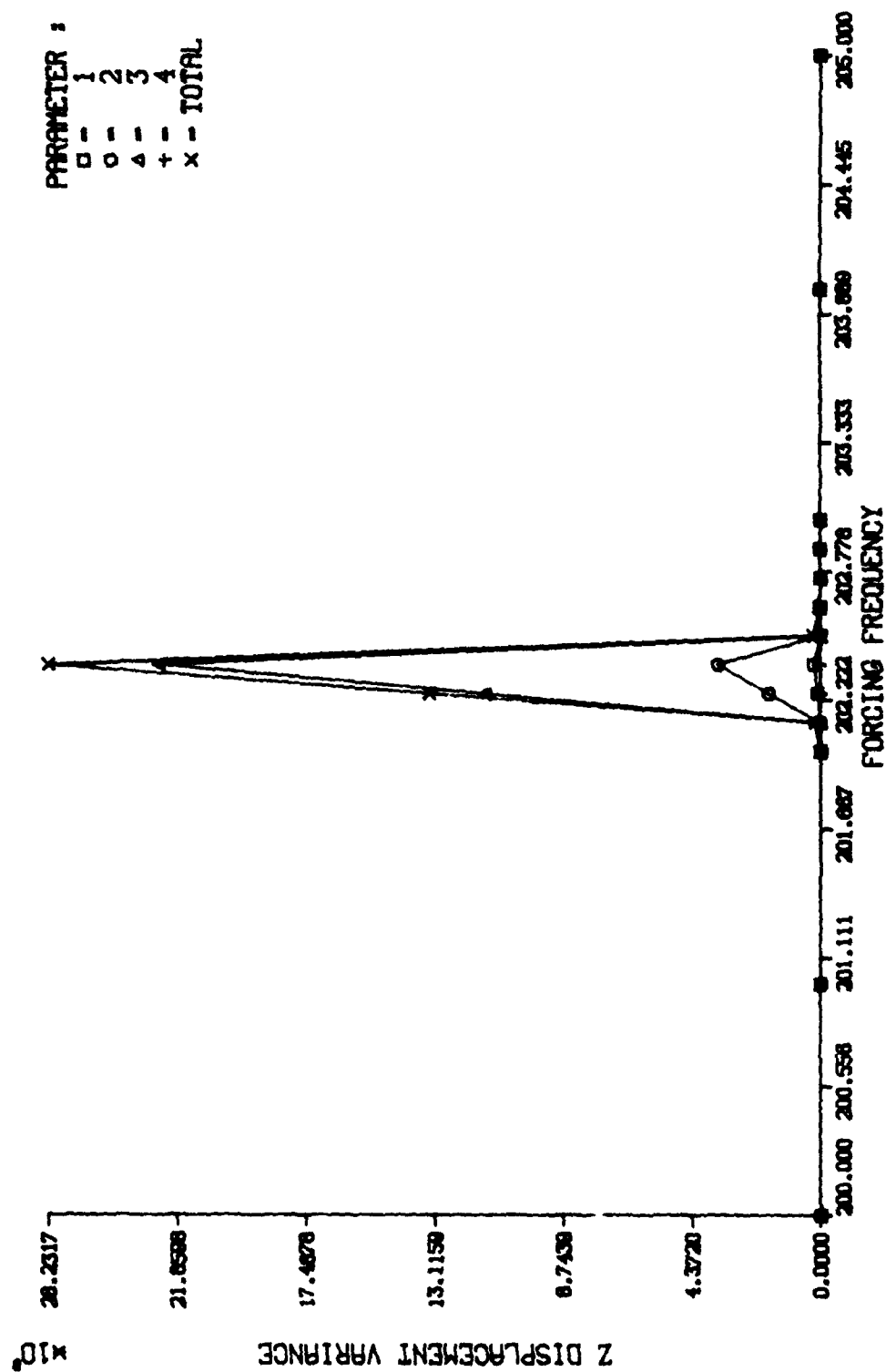


Figure 27. Displacement Amplitude Variance versus Frequency.

TIP DISPLACEMENT AMPLITUDE

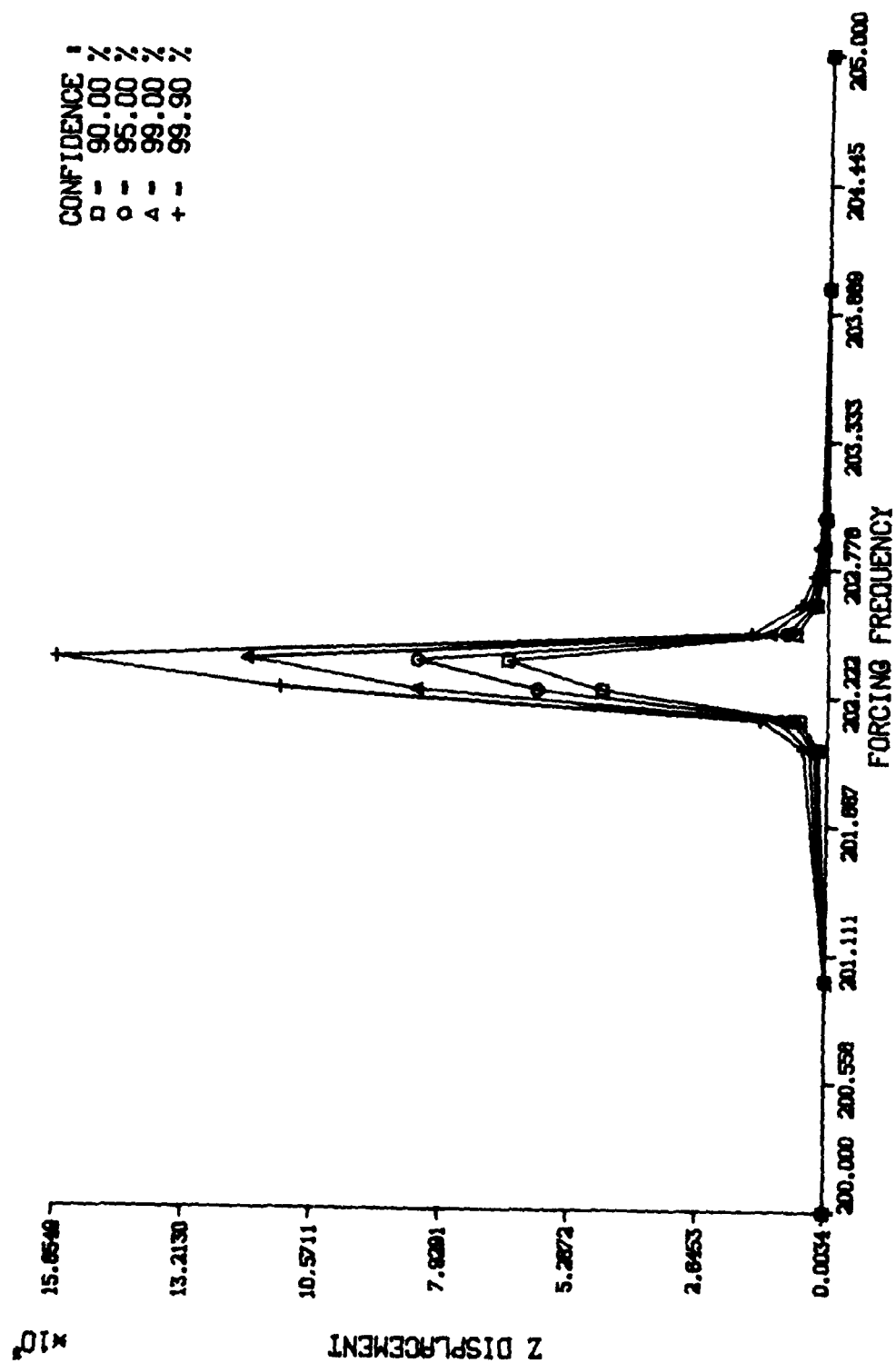


Figure 28. Tip Displacement versus Frequency and Confidence Level.

TIP DISPLACEMENT AMPLITUDE

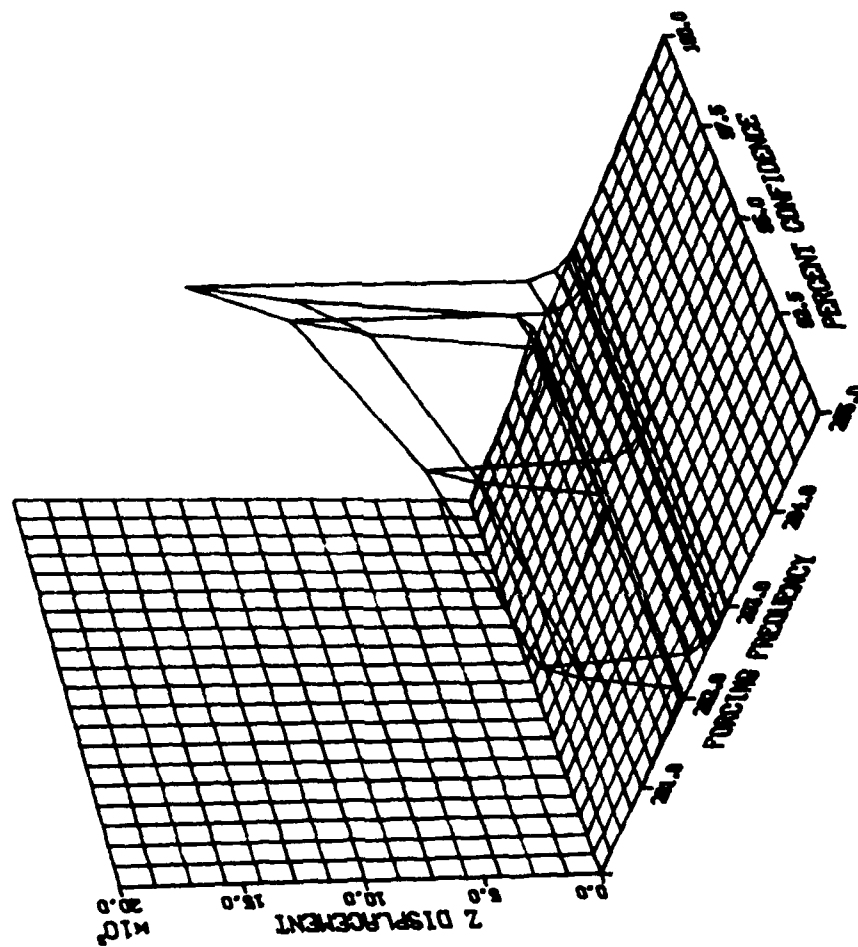


Figure 29. Displacement-Frequency-Confidence Level Surface.

ROOT SECTION BENDING MOMENT

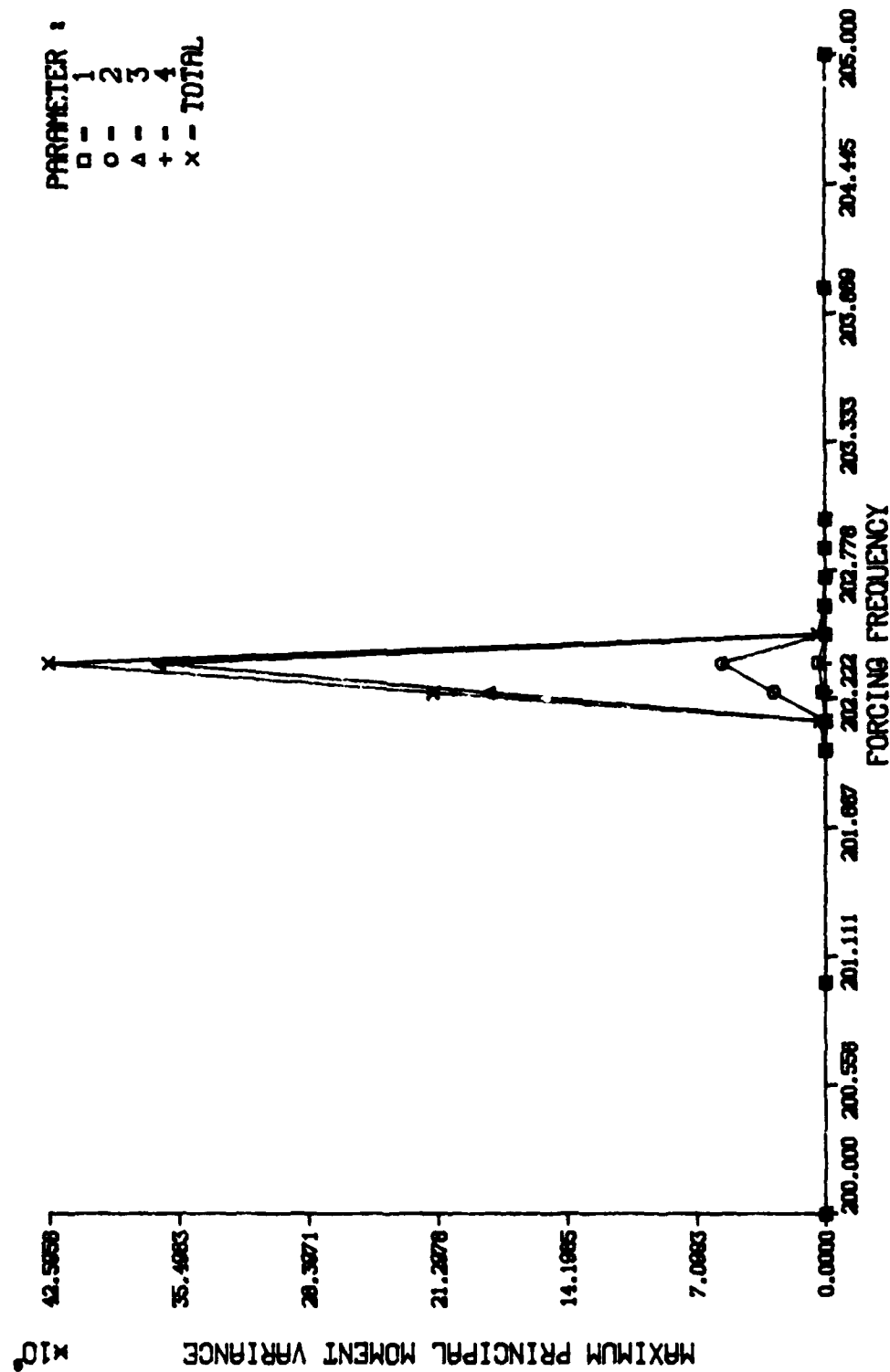


Figure 30. Moment Amplitude Variance versus Frequency.

ROOT SECTION BENDING MOMENT

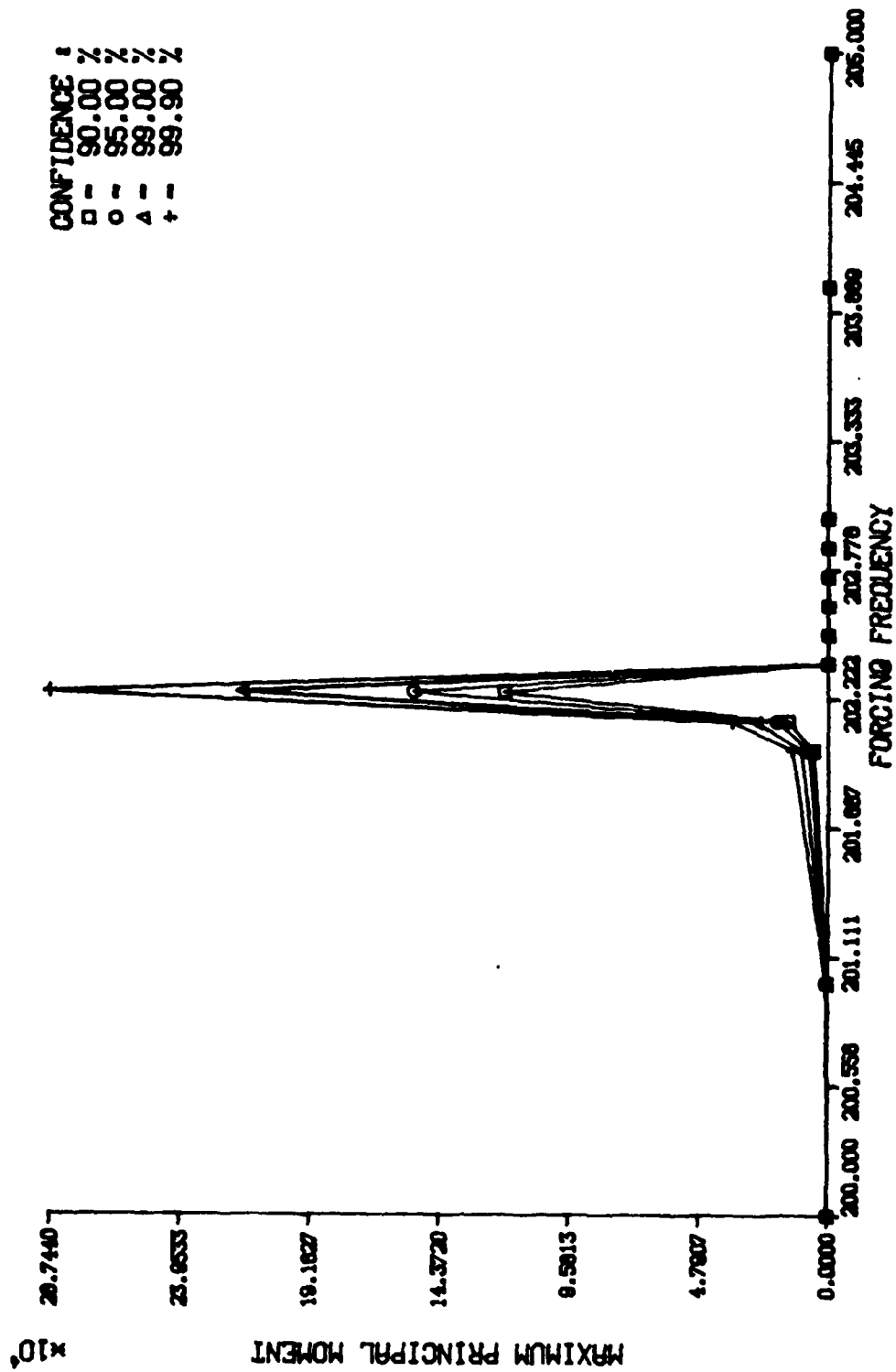


Figure 31. Root Moment versus Frequency and Confidence Level.

ROOT SECTION BENDING MOMENT

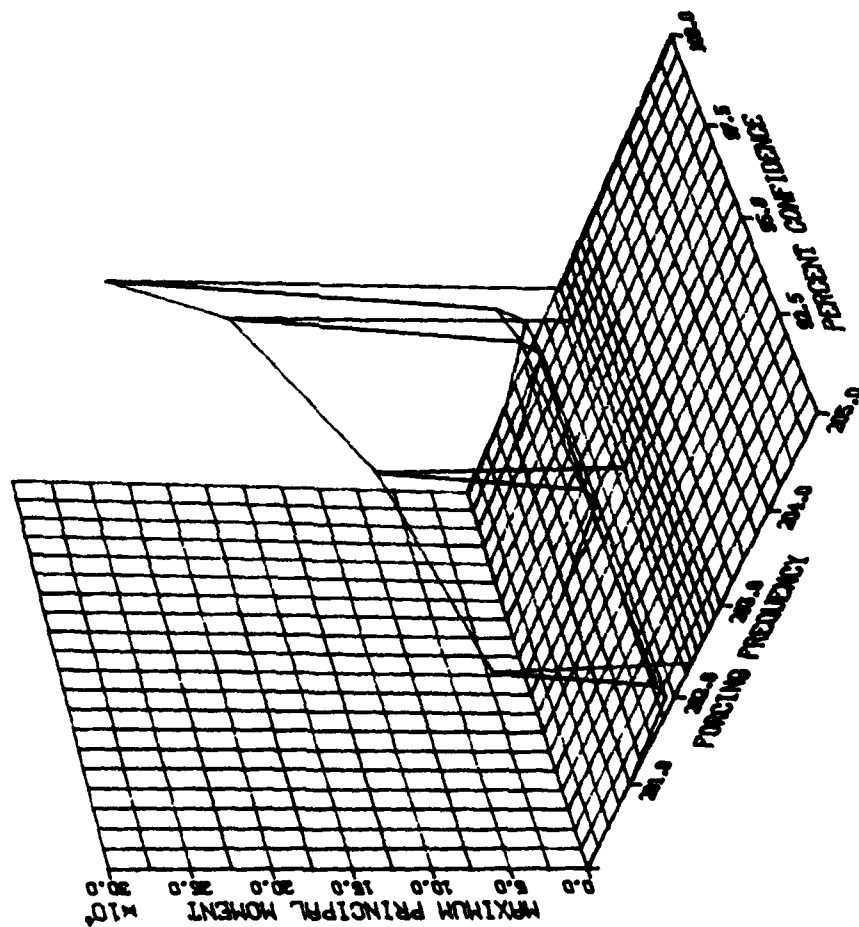


Figure 32. Moment-Frequency-Confidence Level Surface.

7.4.2 Natural Frequencies of a Twisted Blade

This problem considers a 2x2 inch blade with 45° twist, for which experimental results have been collected at the Air Force Wright Aero Propulsion and Power Laboratory, Wright Patterson Air Force Base. The finite element model of a single blade is shown in Figure 33. In the experiments, data were obtained from a twelve-bladed disk machined from flat stock and twisted to the final shape. Blade-alone frequencies have been measured by clamping the disk near the blade roots, and forcing each blade with a magnetic exciter.

The blade has inner and outer radii of 4 and 6 inches, and is a uniform 0.078 inch in thickness. The actual part contains 1/4-inch holes at either edge of the blade roots; in the model, we have simply moved the root nodes inward to obtain the correct area and moment of inertia there.

The first two statistical parameters used in this example are material properties. The part is made from steel, for which we take $E=29 \times 10^6$ and $\sigma_E=87000$. A density of $0.000751 \text{ lb-sec}^2/\text{in}^4$ is assumed, with $\sigma_\rho=3.7 \times 10^{-6}$.

The remaining parameters have to do with the twist angle of the blade. Let $\xi=x/S$, a normalized spanwise coordinate. For the angle of twist at the centerline of the blade, we assume that

$$\theta/\theta_{\max} = (1-C)\xi + C\xi^2 \quad (177)$$

For $C=0$ the angle of twist varies linearly with the spanwise coordinate. The distribution of the twist angle along the blade span is shown in Figure 34 for various values of the parameter C . The third and fourth statistical parameters are the maximum angle of twist, θ_{\max} , and the twist parameter C . The derivatives of θ with respect to these variables follow from equation (177), so

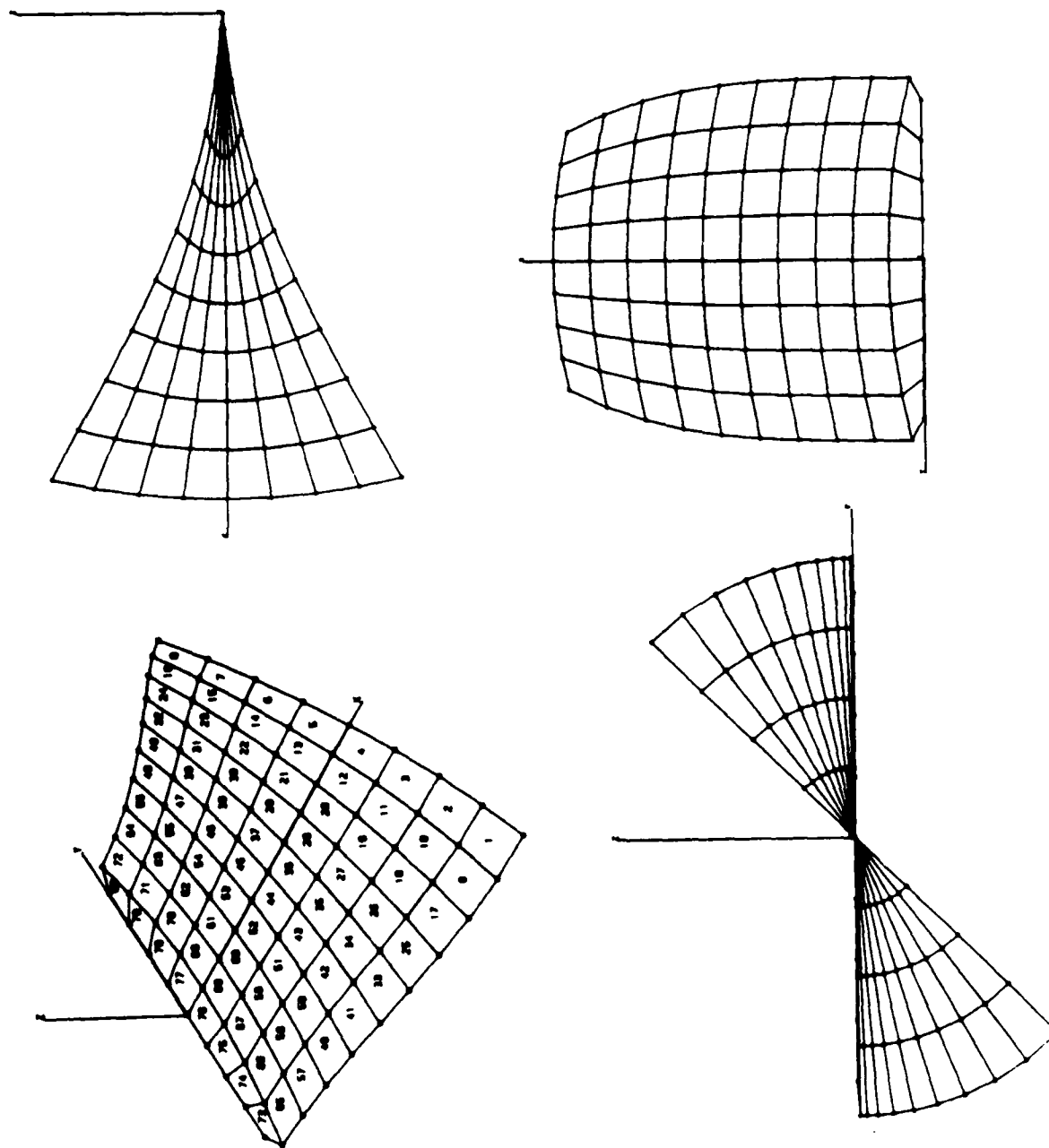


Figure 33. Finite Element Model of 45-Degree Twist Blade.

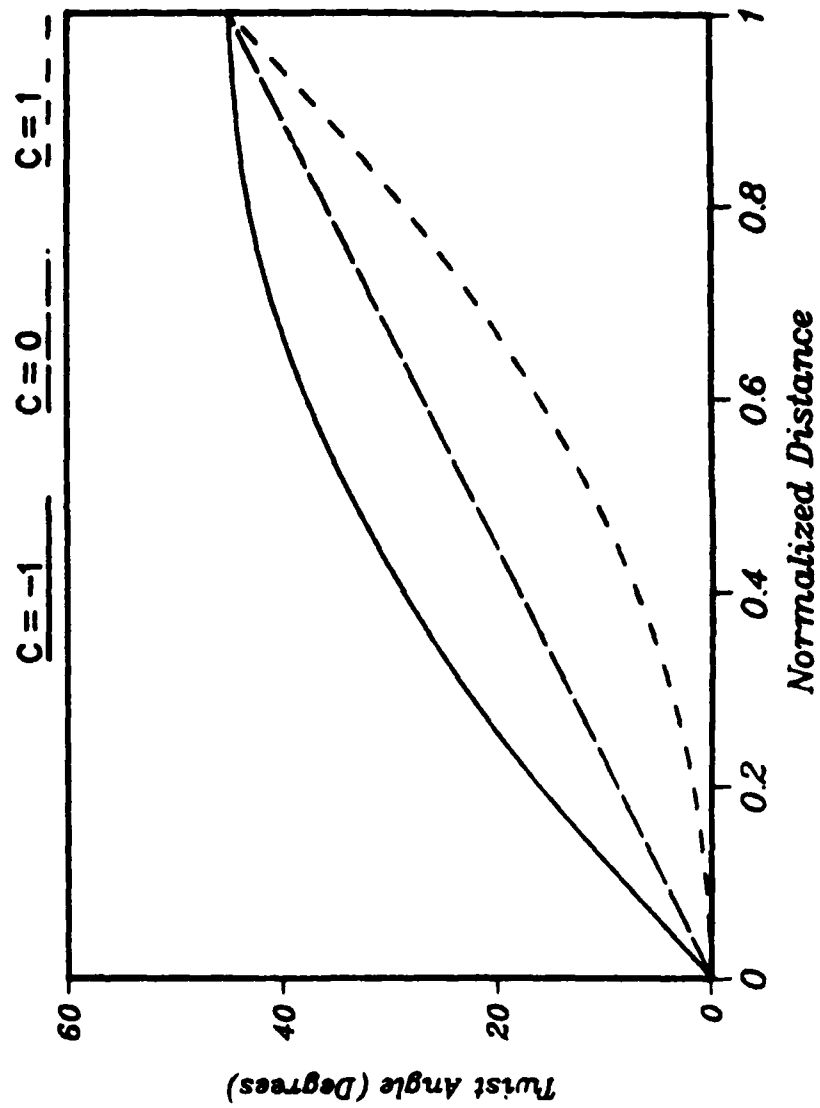


Figure 34. Twist Profiles versus Twist Parameter "C".

that the necessary coordinate sensitivities are relatively simple to define in equation form.

The nominal value of θ_{\max} is $\pi/4$ (45°). The standard deviation used for θ_{\max} has been computed from the tolerance of ± 0.005 inch on blade tip height above or below a fixed reference plane, giving an angular tolerance of 0.0087267 (0.5°). A nominal value of $C = -1.00$, with $\sigma_C = 0.001$, is used for the twist parameter.

The first three frequencies and corresponding standard deviations computed with the probabilistic model are summarized in Table 18. The experimental results for the lowest (1-B) mode are suspect, since other experiments using a bladed disk of the same design resulted in first bending frequencies in the neighborhood of 330 Hz. It is apparent that some details of the root conditions are not represented perfectly in the model. The remaining modes are more sensitive to the blade twist profile, as shown in Figure 35.

Figure 36 shows the variances of the first three natural frequencies, as well as the contribution of each statistical parameter to the total. Note that the frequency values are listed in radians per second. The second bending mode is quite sensitive to the total twist angle, while (from Figure 35) the twist profile is relatively unimportant. Conversely, the first torsion mode is influenced less by the total angle of twist than by the twist profile as determined by parameter C. The small variance assigned to parameter C prevents it from influencing the total variance of the natural frequency.

Table 18. Natural Frequencies for 45° Twisted Plate

<u>Mode</u>	<u>Type</u>	<u>$\omega \pm \Delta\omega$ (Experimental)</u>	<u>$\omega \pm 3\sigma$ (Computed)</u>
1	1-B	622.6 \pm 1.3 Hz.	552.0 \pm 29.4 Hz.
2	2-B	1932. \pm 6.	2266.7 \pm 278.3
3	1-T	3335. \pm 1.	3333.2 \pm 236.4

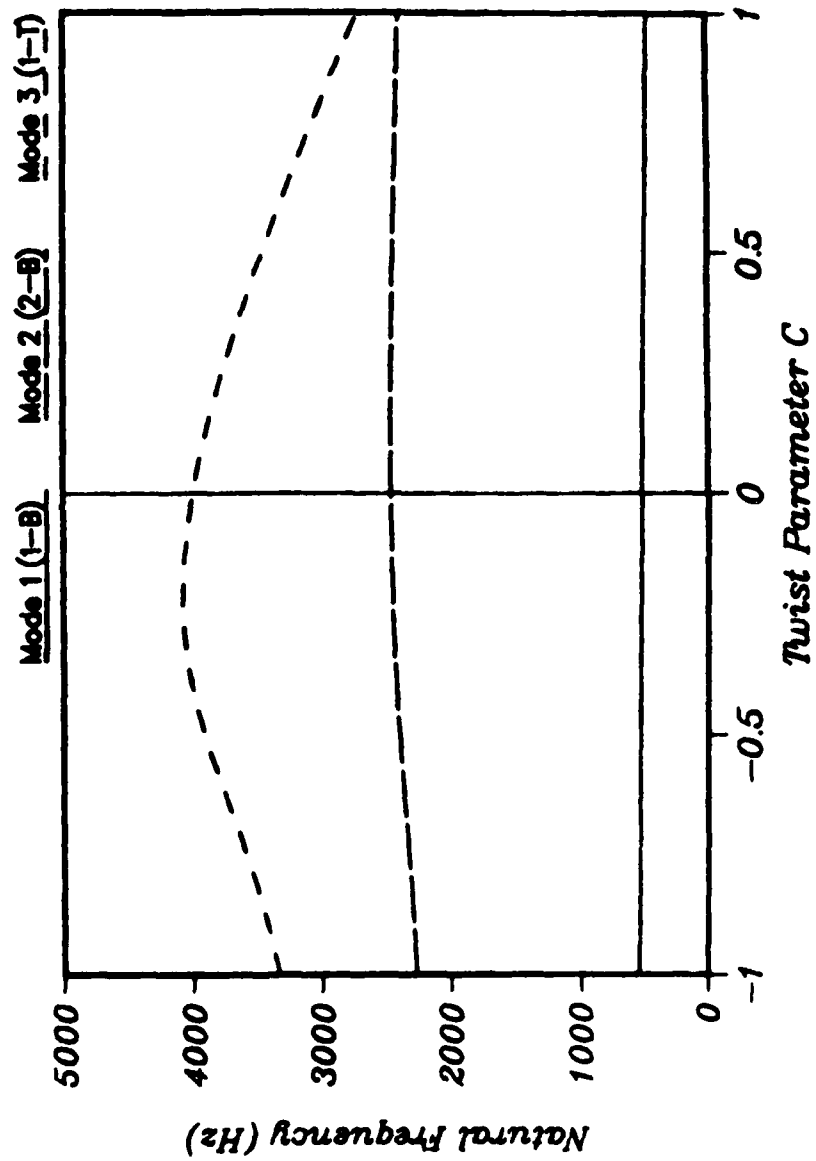


Figure 35. Blade Frequencies as Functions of Twist Parameter.

BLADED DISK FREQUENCIES

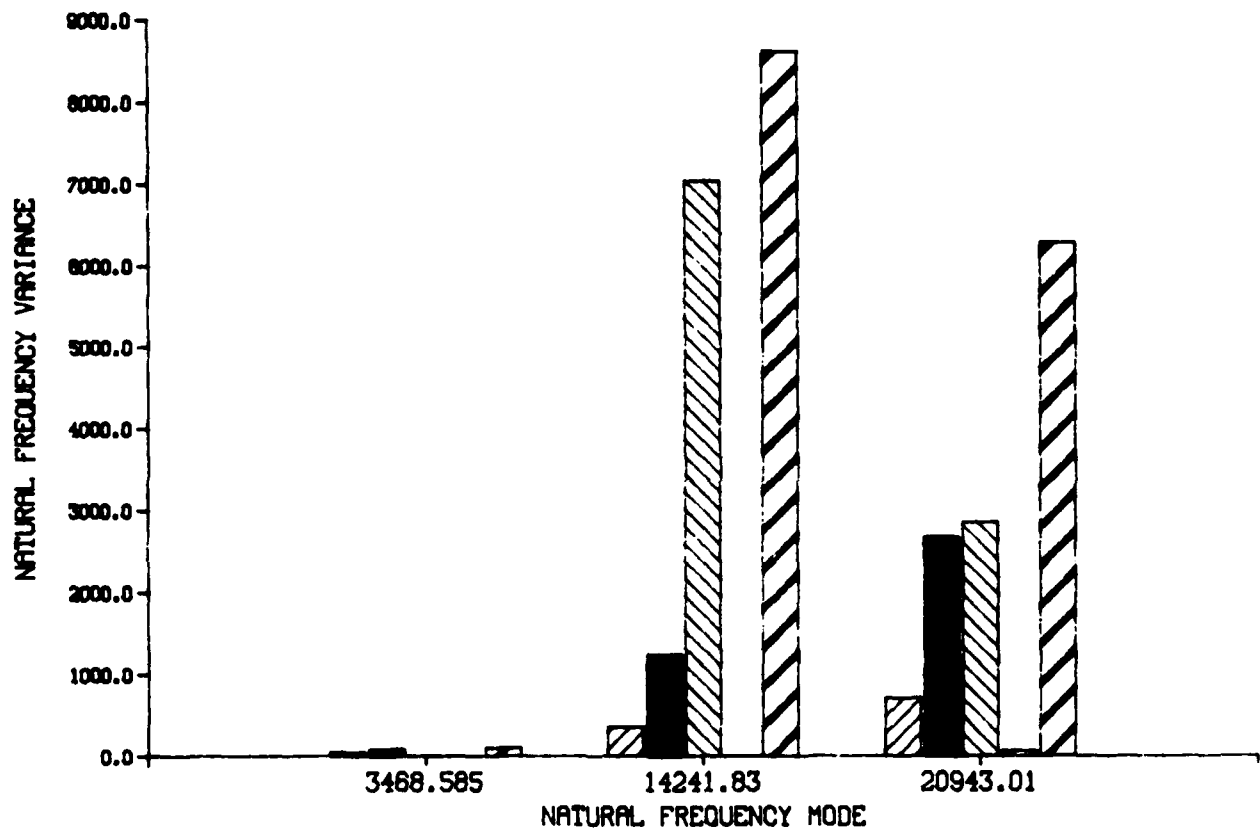


Figure 36. Frequency Variances for Twisted Blade.

REFERENCES

1. A. V. Srinivasan, "Vibrations of Bladed-Disk Assemblies -- A Selected Survey," J. Vib. Acous. Stress Reliab. Des. 106, 165-168 (1984).
2. D. J. Ewins, "Vibration Characteristics of Bladed Disk Assemblies," J. Mech. Engng. Sci. 15(3), 165-186 (1973).
3. D. Hoyniak and S. Fleeter, "Forced Response Analysis of an Aerodynamically Detuned Supersonic Turbomachine Rotor," J. Vib. Acous. Stress Reliab. Des. 108, 117-124 (1986).
4. N. A. Valero and O. O. Bendiksen, "Vibration Characteristics of Mistuned Shrouded Blade Assemblies," J. Engng. Gas Turb. Power 108, 293-299 (1986).
5. L. E. El-Bayoumy and A. V. Srinivasan, "Influence of Mistuning on Rotor-Blade Vibrations," AIAA J. 13(4), 460-464 (1975).
6. K. R. V. Kaza and R. E. Kielb, "Effects of Mistuning on Bending-Torsion Flutter and Response of a Cascade in Incompressible Flow," AIAA J. 20(8), 1120-1129 (1982).
7. W. A. Stange and J. C. MacBain, "An Investigation of Dual Mode Phenomena in a Mistuned Bladed Disk," J. Vib. Acous. Stress Reliab. Des. 105(3), 402-407 (1983).
8. R. A. Ibrahim, "Structural Dynamics with Parameter Uncertainties," Appl. Mech. Rev. 40(3), 309-328 (1987).
9. T. Belytschko, "A Review of Recent Developments in Plate and Shell Elements," in A. K. Noor (ed.), Computational Mechanics -- Advances and Trends, AMD Vol. 75, 217-231, ASME, New York (1986).
10. _____, PATRAN II Release Notes, Version 2.1, PDA Engineering, Santa Ana, California, 1986.
11. _____, DISSPLA (Display Integrated Software System and Plotting Language) User's Manual, Version 10.0, ISSCO, Inc., San Diego, California, 1985.
12. K. J. Bathe and E. L. Wilson, Numerical Methods in Finite Element Analysis, Prentice-Hall Co., New Jersey, 1976.
13. O. C. Zienkiewicz, The Finite Element Method, McGraw-Hill Co., New York, 1977.
14. R. D. Cook, Concepts and Applications of Finite Element Analysis, John Wiley and Sons, New York, 1981.

15. R. H. Gallagher, Finite Element Analysis: Fundamentals, Prentice-hall Co., New Jersey, 1975.
16. A. Ralston, A First Course in Numerical Analysis, McGraw-Hill Co., New York, 1965.
17. C. A. Felippa, "Solution of Linear Equations with Skyline-Stored Symmetric Matrix," Comp. Struc. 5, 13-29 (1975).
18. K. J. Bathe and E. L. Wilson, "Solution Methods for Eigenvalue Problems in Structural Mechanics," Int. J. Num. Meth. Engng. 6, 213-226 (1973).
19. N. S. Khot, L. Berke, and V. B. Venkayya, "Minimum Weight Design of Structures by the Optimality Criterion and Projection Methods," Proceedings of the AIAA/ASME/ASCE/AHS 20th Structures, Structural Dynamics, and Materials Conference, St. Louis, Mo. (1979).
20. U. Kirsch, "Multilevel Approach to Optimum Structural Design," Proc. ASCE, J. Struct. Div. 101, ST1 (1975).
21. R. T. Haftka and B. Prasad, "Programs for Analysis and Resizing of Complex Structures," Comp. Struc. 10, 323-330 (1979).
22. U. Kirsch, M. Reiss, and U. Shamir, "Optimum Design by Partitioning and Substructures," Proc. ASCE, J. Struct. Div. 98, ST1, 249-267 (1972).
23. O. C. Zienkiewicz and J. S. Campbell, "Shape Optimization and Sequential Linear Programming," in R. H. Gallagher and O. C. Zienkiewicz (eds), Optimum Structural Design, John Wiley and Sons, 1973.
24. C. V. Ramakrishnan and A. Francavilla, "Structural Shape Optimization Using Penalty Functions," J. Struct. Mech. 3(4), 403-422 (1974).
25. G. K. Smith and R. G. Woodhead, "An Optimal Design Scheme with Applications to Tanker Transverse Structure," Engineering Optimization 1, 79-98 (1974).
26. U. Kirsch and G. Toledano, "Approximate Reanalysis for Modifications of Structural Geometry," Comp. Struc. 16, 269-277 (1983).
27. S. Wang, Y. Sun, and R. H. Gallagher, "Sensitivity Analysis in Shape Optimization of Continuum Structures," Comp. Struc. 20, 855-867 (1985).
28. L. C. Rogers, "Derivatives of Eigenvalues and Eigenvectors," AIAA J. 8, 943-944 (1970).

29. H. Benaroya and M. Rehak, "The Decomposition Method in Structural Dynamics," AIAA Paper 85-0685, 26th AIAA/ASME/ASCE/AHS Struc. Dyn. Mat. Conf., 266-281 (1985).
30. F. S. Wong, "Stochastic Finite Element Analysis of a Vibrating String," J. Sound. Vib. 96(4), 447-459 (1984).
31. W. K. Liu, T. Belytschko, and A. Mani, "Random Field Finite Elements," Int. J. Num. Meth. Engng. 23, 1831-1845 (1986).
32. M. Shinozuka, "Simulation of Multivariate and Multidimensional Random Process," J. Acous. Soc. Amer. 49(1), Pt. 2, 357-367 (1971).
33. J. E. Freund, Mathematical Statistics, 2nd ed., Prentice-Hall Co., New Jersey, 1971.
34. J. E. Ashton and J. M. Whitney, Theory of Laminated Plates, Technomic Publ. Co., 1970.
35. _____, Stock Catalog and Metals Handbook, American Brass and Copper Co., Oakland, Calif., 1966.
36. R. D. Mindlin, "Influence of Rotatory Inertia and Shear on the Bending of Elastic Plates," J. Appl. Mech. 18, 1031-1036 (1951).
37. T. J. R. Hughes, M. Cohen, and M. Haroun, "Reduced and Selective Integration Techniques in Finite Element Analysis of Plates," Nucl. Eng. Des. 46, 203-222 (1978).
38. D. Kosloff and G. Frazier, "Treatment of Hourglass Patterns in Low Order Finite Element Codes," Num. Anal. Meth. Geomech. 2, 52-72 (1978).
39. D. Flanagan and T. Belytschko, "A Uniform Strain Hexahedron and Quadrilateral with Orthogonal Hourglass Control," Int. J. Num. Meth. Engng. 17, 679-706 (1981).
40. T. Belytschko, J. I. Lin, and C. S. Tsay, "Explicit Algorithms for the Nonlinear Dynamics of Shells," Comp. Meth. Appl. Mech. Engng. 42, 225-251 (1984).
41. R. H. MacNeal, "A Simple Quadrilateral Shell Element," Comp. Struct. 8, 175-183 (1978).
42. T. J. R. Hughes and T. E. Tezduyar, "Finite Elements Based upon Mindlin Plate Theory with Particular Reference to the Four-node Bilinear Isoparametric Element," J. Appl. Mech. 48, 587-596 (1981).
43. R. L. Taylor, "Finite Element for General Shell Analysis," 5th Intl. Seminar on Computational Aspects of the Finite Element Method, Berlin, August 1979.

44. T. Belytschko, C. S. Tsay, and W. K. Liu, "A Stabilization Matrix for the Bilinear Mindlin Plate Element," Comp. Meth. Appl. Mech. Engng. 29, 313-327 (1981).
45. T. Belytschko and C. S. Tsay, "A Stabilization Procedure for the Quadrilateral Plate Element with One-point Quadrature," Int. J. Num. Meth. Engng. 19, 405-419 (1983).
46. W. K. Liu, J. S. Ong, and R. A. Uras, "Finite Element Stabilization Matrices - A Unification Approach," Comp. Meth. Appl. Mech. Engng. 53, 13-46 (1985).
47. W. K. Liu, E. S. Law, D. Lam, and T. Belytschko, "Resultant-Stress Denerated-Shell Element," Comp. Meth. Appl. Mech. Engng. 55, 259-300 (1986).
48. K. C. Park, G. M. Stanley, and D. L. Flaggs, "A Uniformly Reduced, Four-noded C⁰ Shell Element with Consistent Rank Corrections," Comp. Struct. 20, 129-139 (1985).
49. J. M. Whitney, "Shear Correction Factors for Orthotropic Laminates under Static Load," J. Appl. Mech. 40, 302-304 (1973).
50. T. J. R. Hughes, "Recent Developments in Computer Methods for Structural Analysis," Nucl. Eng. Des. 57, 427-439 (1980).
51. R. M. Jones, Mechanics of Composite Materials, Scripta Book Co., Washington, D. C., 1975.
52. R. A. Brockman, "Current Problems and Progress in Aircraft Transparency Impact Analysis," in S. A. Morolo (ed.), Proc. 14th Conf. on Aerospace Transparent Materials and Enclosures, AFWAL-TR-83-4154, Air Force Wright Aeronautical Laboratories, Wright-Patterson Air Force Base, Ohio, 1058-1082 (1983).
53. R. A. Brockman, "On Vibration Damping Analysis Using the Finite Element Method," in L. Rogers (ed.), Vibration Damping 1984 Workshop Proceedings, AFWAL-TR-84-3064, Air Force Wright Aeronautical Laboratories, Wright-Patterson Air Force Base, Ohio, pp. II-1:II-10 (1984).
54. A. N. Palazotto and W. P. Witt, "Formulation of a Nonlinear Compatible Finite Element for the Analysis of Laminated Composites," Comput. Struct. 21, 1213-1234 (1985).
55. H. P. Huttelmaier and M. Epstein, "A Finite Element Formulation for Multilayered and Thick Shells," Comput. Struct. 21, 1181-1185 (1985).
56. S. T. Mau, P. Tong, and T. H. H. Pian, "Finite Element Solutions for Laminated Thick Plates," J. Comp. Mat. 6, 304-311 (1972).

57. R. L. Spilker, "Hybrid-stress Eight-node Elements for Thin and Thick Multilayer Laminated Plates," Int. J. Num. Meth. Engng. 18, 801-828 (1982).
58. R. L. Spilker, "An Invariant 8-node Hybrid-stress Element for Thin and Thick Multilayer Laminated Plates," Int. J. Num. Meth. Engng. 20, 573-582 (1984).
59. R. L. Spilker and D. M. Jakobs, "Hybrid Stress Reduced-Mindlin Elements for Thin Multilayer Plates," Int. J. Num. Meth. Engng. 23, 555-578 (1986).
60. J. M. Whitney and N. J. Pagano, "Shear Deformation in Heterogeneous Anisotropic Plates," Trans. ASME, J. Appl. Mech. 37, 1031-1036 (1970).
61. N. J. Pagano, "Exact Solutions for Composite Laminates in Cylindrical Bending," J. Comp. Mater. 3, 398-411 (1969).
62. N. J. Pagano, "Exact Solutions for Rectangular Bidirectional Composites and Sandwich Plates," J. Comp. Mater. 4, 20-34 (1970).
63. J. J. Engblom and O. O. Ochoa, "Finite Element Formulation Including Interlaminar Stress Calculations," Comp. Struct. 23(2), 241-249 (1986).
64. P. Sharifi, "Nonlinear Analysis of Sandwich Structures," Ph.D. Thesis, Univ. California, Berkeley, 1970.
65. H. P. Kan and J. C. Huang, "Large Deflection of Rectangular Sandwich Plates," AIAA J. 5, 1706-1708 (1967).
66. G. R. Monforton, "Discrete Element, Finite Displacement Analysis of Anisotropic Sandwich Shells," Ph.D. Thesis, Case Western Reserve Univ., 1970.
67. R. A. Brockman, "MAGNA: A Finite Element System for Three-Dimensional Static and Dynamic Structural Analysis," Comput. Struct. 13, 415-423 (1981).
68. T. R. Tauchert, Energy Principles in Structural Mechanics, McGraw-Hill Co., New York, 1974.
69. R. E. Kielb, A. W. Leissa, and J. C. MacBain, "Vibrations of Twisted Cantilever Plates - A Comparison of Theoretical Results," Int. J. Num. Meth. Engng. 21, 1365-1380 (1985).

APPENDIX A

PROTEC INPUT DATA DESCRIPTIONS

The computer program in which the analysis techniques reported herein are implemented is called **PROTEC** (**P**robabilistic **R**esponse **O**f **T**urbine **E**ngine **C**omponents). **PROTEC** is written in ANSI FORTRAN 77, and has been executed successfully on CDC Cyber, CRAY X/MP, and DEC VAX machines. This Appendix summarizes input requirements for **PROTEC**. The remaining Appendices of this report describe **PROTEC** file output (Appendices B and C), data conversion between **PROTEC** and the **PATRAN**¹⁰ modeling package (Appendix D), and plotting of probabilistic data using **DISSPLA**¹¹ (Appendix E).

Input to **PROTEC** is arranged in a series of input "blocks". Each input block begins with a header line identifying the block, followed by the data, and ends with a blank line signifying the end of the block. Input block types are:

<u>Block Name</u>	<u>Status</u>	<u>Data Description</u>
BOUNDARY	Optional	Nodal boundary conditions
COORDINATE	Required	Nodal coordinates
DERIVATIVES	Optional	Coordinate derivative data for sensitivity analysis
DIAGNOSTICS	Optional	Diagnostic output selection
ELEMENT	Required	Element connections
FORCE	Optional	Nodal forces, moments, and prescribed displacements
GRAVITY	Optional	Self-weight loading
LAMINATE	Optional	Laminate section definitions
MATERIAL	Required	Material properties
OPTION	Optional	Analysis options
PARAMETERS	Optional	Statistical and sensitivity parameter definitions
PRESSURE	Optional	Element surface pressures
PROPERTY	Required	Element thicknesses, areas
TITLE	Required	Alphanumeric problem title

Input blocks may appear in any order on the input file. While data within a block is highly structured, comments and extra lines may be inserted between blocks.

Formats for individual input blocks are described on the following several pages. The description of each block includes:

- Header: Four-character block title (see above);
- Format: Typical record format and a sample data line;
- Variables: Definitions of input variable names; and
- Notes: Rules, hints, or clarifications.

BOUNDARY
Input Block

BOUNDARY Input Block: Nodal Displacement Constraints

Header: **BOUN**

Format:

5	10	15	20	25	30	35	40	45
IBEG	IEND	INCR	ID1	ID2	ID3	ID4	ID5	ID6

Example:

27	45	2	3	4	5			
----	----	---	---	---	---	--	--	--

Variables:

IBEG = First node number to be constrained.
IEND = Last node in a series of nodes to be constrained.
INCR = Node number increment.
ID1-ID6 = List of nodal degrees of freedom to be fixed; the numeric values 1-6 refer to u , v , w , θ_x , θ_y , θ_z , respectively.

Notes:

- ⊙ If IBEG, IEND, and INCR are all present, each of the nodes IBEG, IBEG+INCR, IBEG+2*INCR, ..., IEND are constrained.
- ⊙ If IEND is omitted, the default is IBEG (single node).
- ⊙ If INCR is omitted, a default of INCR = 1 is assumed.
- ⊙ Only one degree-of-freedom value (IDn) is required.

COORDINATE
Input Block

COORDINATE Input Block: Nodal Coordinate Data

Header: COOR

Format:

5	10	20	30	40
NODE	INCR	XCOORD	YCOORD	ZCOORD

Example:

12		10.28	-67.42875	1.257E-2
----	--	-------	-----------	----------

Variables:

NODE = Current node number.
 INCR = Increment for node number generation.
 XCOORD = Cartesian coordinate X at the current node.
 YCOORD = Cartesian coordinate Y at the current node.
 ZCOORD = Cartesian coordinate Z at the current node.

Notes:

- Valid node numbers are from one to the maximum number in the model. Intermediate node numbers may be omitted, but must be constrained.
- INCR is used for generating a series of nodes along a line from two successive lines of data. For example, the input

10		2.50	-5.0	3.10
20	2	3.00	-5.0	2.10

would generate the following coordinate data:

Node	X	Y	Z
10	2.50	-5.0	3.10
12	2.60	-5.0	2.90
14	2.70	-5.0	2.70
16	2.80	-5.0	2.50
18	2.90	-5.0	2.30
20	3.00	-5.0	2.10

DERIVATIVES
Input Block

DERIVATIVES Input Block: Coordinate Derivatives for Sensitivity Analysis

Header: DERI <value>

Format:

NODE	INCR	XDERIV	YDERIV	ZDERIV
------	------	--------	--------	--------

Example:

5		0.5	0.0	0.2
---	--	-----	-----	-----

Variables:

<value> = Integer value in header line, specifying IDENT (parameter i.d., see **PARA** input block) for the sensitivity parameter being defined.

NODE = Current node number.

INCR = Increment for node number generation.

XDERIV = Derivative of Cartesian coordinate X at the current node, with respect to this parameter.

YDERIV = Derivative of Cartesian coordinate Y at the current node, with respect to this parameter.

ZDERIV = Derivative of Cartesian coordinate Z at the current node, with respect to this parameter.

Notes:

- ⊙ This block is used to define a geometric parameter for use in sensitivity analysis (that is, a parameter which controls the placement of nodes in the model). A **DERI** block is required for each such parameter; multiple **DERI** blocks are distinguished from one another by the <value> appearing in the header line.
- ⊙ NODE numbers are as defined in the **COOR** input block, and INCR is used to generate data exactly as the **COOR** block.
- ⊙ If the sensitivity parameter is p, then $XDERIV = \partial X / \partial p$, the derivative of coordinate X.
- ⊙ Nodes for which all derivatives are zero for the current parameter may be omitted.

DIAGNOSTICS
Input Block

DIAGNOSTICS Input Block: Selection of Diagnostic Output Options

Header: **DIAG**

Format:

5	10	15	20																80
IDSW1	IDSW2	IDSW3	IDSW4	IDSWn

Example:

2	10																		
---	----	--	--	--	--	--	--	--	--	--	--	--	--	--	--	--	--	--	--

Variables:

IDSWi = Number of a diagnostic output switch to be
activated during the present analysis.

Notes:

- ⊙ Continue input on additional lines until all selections have been made. Each input line may contain from one to sixteen switch values.
- ⊙ Valid diagnostic output options are as follows:

<u>IDSWi</u>	<u>Description of Diagnostic Output</u>
1	Element data (nodes, properties, coordinates)
2	Element stiffness matrices
3	Element mass matrices
4	Element harmonic stiffness matrices (K-λM)
5	Element stabilization (artificial) forces
6	Element transformation matrices
7	Element local coordinates
8	Element shape functions
9	Element strain-displacement matrices
10	Element stress-strain matrices
11	Element local displacements
12	Element displacement sensitivities

ELEMENT
Input Block

ELEMENT Input Block: Finite Element Connections and Properties

Header: **ELEM**
Format:

5	10	15	20	25	30	35	40	45	50
ETYP	IDEL	MATL	IPR	INGEN	IEGEN	N1	N2	N3	N4

Example:

SHELL	21	1	2			264	288	295	276
-------	----	---	---	--	--	-----	-----	-----	-----

Variables:

ETYP = Mnemonic for element type.
 IDEL = Element number for current element.
 MATL = Material number for current element. A negative value refers to a laminate number, as defined in the LAMI input block.
 IPR = Physical property set number for this element.
 INGEN = Node increment for element generation.
 IEGEN = Element increment for element generation.
 N1-N4 = Nodes connected to the current element, listed in counterclockwise order around the boundary.

Notes:

- At present, the only acceptable element type mnemonic (ETYP) is "SHELL", designating the bilinear, 24-D.O.F. Mindlin plate/shell element.
- Valid element numbers are from one to the total number of elements in the model.
- Elements may be generated in any pattern which involves equal increments in all node numbers N1-N4. INGEN and IEGEN appear on the second input line of a pair, and specify node and element number increments, respectively. For instance, the data

SHELL	20	1	1			10	14	16	12
SHELL	26	1	1	3	2				

generates the element data:

Element	N1	N2	N3	N4
20	10	14	16	12
22	13	17	19	15
24	16	20	22	18
26	19	23	25	21

FORCE
Input Block

FORCE Input Block: Imposed Nodal Forces, Moments, Displacements, and Rotations

Header: **FORC**

Format:

	5	10	20	25
	NODE	KODE	VALUE	ICASE

Example:

258	1	275.5	1
-----	---	-------	---

Variables:

NODE = Node at which load or displacement is specified.
KODE = Code for type and direction of prescribed value:

1 = F_x ; 2 = F_y ; 3 = F_z ; 4 = M_x ; 5 = M_y ; 6 = M_z ;

7 = u_x ; 8 = u_y ; 9 = u_z ; 10 = θ_x ; 11 = θ_y ; 12 = θ_z

VALUE = Value of prescribed force, moment, displacement, or rotation.

ICASE = Static load case number.

Notes:

- ⊙ The first three values must be provided. There are no default values for NODE or KODE. ICASE, if omitted, is assumed to be 1.
- ⊙ If a nodal displacement or rotation is set to zero in this input block, the effect is the same as a constraint specified in the BOUNDARY input block.

GRAVITY
Input Block

GRAVITY Input Block: Self-Weight Body Force on Entire Model

Header: **GRAV**

Format:

10	20	30
GX	GY	GZ

Example:

0.0	0.0	-386.
-----	-----	-------

Variables:

GX,GY,GZ = Cartesian components of gravity vector, defining both the magnitude and direction of the local gravitational acceleration.

Notes:

- ⊙ The gravitational force per unit volume at any point is determined from $\mathbf{F} = \rho (GX\mathbf{i} + GY\mathbf{j} + GZ\mathbf{k})$, in which ρ is the material density at the point.
- ⊙ By default, gravity loads become part of load case 1.

LAMINATE
Input Block

LAMINATE Input Block: Laminate Definitions for Layered Shells

Header: **LAMI**

Format:

(1) Sizing Data (one per laminate):

	5	10
LAM	NLAY	

(2) Layer Data (one per layer):

	5	15	25
MATL	THICK	ANGLE	

Example:

1	3
---	---

3	0.060	0.0
2	0.500	45.0
3	0.060	0.0

Variables:

LAM = Laminate number.
 NLAY = Number of layers in current laminate.
 MATL = Material number for a specific layer.
 THICK = Layer thickness.
 ANGLE = Angle from local 'x' axis of an element to the material '1' axis (fiber direction).

Notes:

- ⊙ Laminate definitions must be numbered sequentially and input in ascending order.
- ⊙ The layers of a laminate are numbered from bottom (layer 1) to top (layer NLAY).
- ⊙ MATL may reference either an isotropic or orthotropic material, as defined in the MATERIAL input block.
- ⊙ ANGLE is positive counterclockwise when viewing an element from the top.
- ⊙ ANGLE is measured in degrees.

MATERIAL
Input Block

MATERIAL Input Block: Material Properties Data

Header: MATE

Format:

(1) For isotropic materials (one line/material):

5	10	20	30	40	50
MAT	////	E	XNU	RHO	SY

(2) For orthotropic materials (two lines/material):

5	10	20	30	40	50	60	70
MAT	////	E1	E2	XNU12	G12	G13	G23
////	////	RHO	C1	C2	////////	////////	////////

Examples:

1		1.E7	0.3	2.5E-4	10000.
---	--	------	-----	--------	--------

2		25.E6	1.E6	0.25	0.5E6	0.5E6	0.2E6
		9.2E-5	70000.	20000.			

Variables:

MAT = Material number for current material.
 E = Extensional modulus.
 XNU = Poisson's ratio.
 RHO = Mass density.
 SY = Yield stress.
 E1 = Extensional modulus in material direction '1'.
 E2 = Extensional modulus in material direction '2'.
 XNU12 = Major inplane Poisson's ratio.
 G12 = Shear modulus in material (1,2) plane.
 G13 = Shear modulus in material (1,3) plane.
 G23 = Shear modulus in material (2,3) plane.
 C1, C2 = Failure stress constants.

Notes:

- ⊙ Materials may be entered in any order, but should be numbered from 1 to the total number of materials, with few gaps.
- ⊙ The relationship $E = 2G(1+\nu)$ is assumed for isotropic materials.
- ⊙ Mass densities must be entered in units consistent with force, length, and time units used elsewhere in input.
- ⊙ Constants C1, C2 are currently not used.

OPTION
Input Block

OPTION Input Block: Selection of Solution Options

Header: **OPTI**

Format:

(Enter keywords and values as described below.
All input in this block may be in free format.)

Examples:

HARMONIC ANALYSIS
FREQUENCY 10, 20.2, 23, 24.
STATIC
SENSITIVITY STATIC

Valid Options and Keywords:

EIGENVALUE Selects natural frequency solution
FREQUENCY <values> Defines forcing frequencies for steady-
state harmonic solution
HARMONIC Selects steady-state forced harmonic
vibration solution
LOAD_CASES Defines number of static loading cases
MODES Requests a specified number of natural
frequencies in an eigenvalue analysis
SENSITIVITY <name> Requests sensitivity analysis following
a basic solution, to determine response
derivatives
SSITERATIONS Defines the maximum number of iteration
cycles for eigenvalue solutions
SSTOLERANCE Defines the relative accuracy tolerance
used to test eigenvalue convergence
STATIC Selects linear static solution

Notes:

- ⊙ Linear static analysis normally requires the **STATIC** and **LOAD_CASES** options.
- ⊙ Steady-state harmonic analysis normally requires the use of **HARMONIC** and **FREQUENCY** options.
- ⊙ Natural frequency analysis normally requires the use of **EIGENVALUE** and **MODES** options.
- ⊙ Valid names for the **SENSITIVITY** option are: **STATIC**, **HARMONIC**, and **EIGENVALUE**.
- ⊙ The first four characters of each keyword (shown in bold above) must be present.

Defaults:

- **LOAD_CASFS**= 1, if **STATIC** option is specified.
- **SSITERATIONS**= max(2***MODES**, 10) if **EIGENVALUE** specified.
- **SSTOLERANCE**= 1.E-6, if **EIGENVALUE** specified.

PARAMETERS
Input Block

PARAMETERS Input Block: Definition of Control Parameters for Statistical or Sensitivity Analysis

Header: **PARA**
Format:

(1) Sizing Data (one line only):

5
NPAR

(2) Control Parameter Data (one line/parameter):

5	10	15	25
IPAR	ITYPE	IDENT	STDDEV

Example:

2			
1	1	4	100000.
2	4	999	0.05

Variables:

NPAR = Number of control parameters to be defined.
 IPAR = Sequence number of current parameter.
 ITYPE = Parameter type: 1 = modulus; 2 = density; 3 = thickness; 4 = geometric.
 IDENT = I.D. of material, property set, or other data corresponding to the current parameter.
 STDDEV = Standard deviation of current parameter.

Notes:

- ⊙ Valid sequence numbers IPAR are from 1 to NPAR; numbers outside this range are ignored.
- ⊙ For ITYPE = 1,2,3, the parameter being defined is simply a property value defined elsewhere in the **MATERIAL** data or **PROPERTY** data. When ITYPE = 4, the parameter controls the positions of nodes in the model, and requires some additional data for its definition (see **DERI** block).
- ⊙ IDENT refers to a material number if ITYPE = 1 or 2. If ITYPE = 3, IDENT refers to a physical property number as defined in the **PROPERTY** input block.

PARAMETERS
Input Block
(Continued)

- ⊙ When $ITYPE = 4$, the geometric parameter is defined by the derivatives $\partial X/\partial p$, $\partial Y/\partial p$, $\partial Z/\partial p$ of coordinates at certain nodes. These derivatives must be specified in a DERIVATIVE input block, with the value of IDENT specified in the block header.
- ⊙ STDDEV is unnecessary for sensitivity analysis alone, but must be defined when probabilistic information about the response is to be computed.
- ⊙ The units of STDDEV must be the same as those of the mean values defined elsewhere (e.g., a modulus value defined in MATERIAL data). For $ITYPE = 4$, STDDEV might have the same units as the nodal coordinate data (if the parameter is a key dimension), or different units (if the parameter is an angle, for instance).

PRESSURE
Input Block

PRESSURE Input Block: Element Pressure Loading

Header: **PRES**

Format:

5	10	15	25
IEBEG	IEEND	IENCR	PRESS ICASE

Example:

5	35	2	-250.0	1
---	----	---	--------	---

Variables:

IEBEG = First element number to which the specified pressure is to be applied.
IEEND = Last element to which pressure is applied.
IENCR = Element number increment.
PRESS = Surface pressure, positive outward
ICASE = Static loading condition number.

Notes:

- ⊙ Pressures are applied to elements IEBEG, IEBEG+IENCR, IEBEG+2*IENCR, ..., IEEND.
- ⊙ If IEEND is not given, its default is IEBEG (one element loaded).
- ⊙ If IENCR is not specified, the increment is set to one (all elements from IEBEG to IEEND loaded).
- ⊙ The "outward" direction for an element is determined by the ordering of its nodes. When the element is viewed from the top (nodes N1-N4 arranged counterclockwise), a positive (outward) pressure acts upward, toward the viewer.
- ⊙ If ICASE is omitted, load case 1 is assumed.

PROPERTY
Input Block

PROPERTY Input Block: Element Thicknesses and Areas

Header: PROP

Format:

		5	15
IPR	VALUE		

Example:

4	0.375
---	-------

Variables:

IPR = Property set number.

VALUE = Property value (area for 1-D elements, thickness for 2-D elements and shells).

Notes:

- Property sets may be entered in any order, but should be numbered from 1 to the total number of distinct element properties (or with few gaps).

TITLE
Input Block

TITLE Input Block:

Header: **TITL**

Format:

1		80
	TITLE	

Example:

Sensitivity Analysis of Blade with Variable Twist
--

Variables:

TITLE = Alphanumeric problem title.

Notes:

- ◎ **TITLE** may include any valid alphanumeric characters.

APPENDIX B

POSFIL Results File Description

This Appendix documents the results file output written from PROTEC. The results file POSFIL is a formatted, card-image file whose structure is rigid (and therefore simple to read from other programs). The PATRAN translator PROPAT (see Appendix D) is an example of a program which reads this results file and transmits data to other programs for analysis and display.

Data on POSFIL are arranged in blocks, similar in concept to the input data blocks (Appendix A). Each data block begins with a header line identifying the block, followed by the data, and ends with an empty line signifying the end of the block. Types of data blocks generated as output include:

<u>Block Name</u>	<u>Description</u>
BOUN	Nodal boundary conditions
CORD	Nodal coordinates
DISP	Nodal displacement
DSEN	Nodal displacement sensitivities
ELEM	Element connections
ESEN	Eigenvalue (frequency) sensitivities
FREQ	Harmonic forcing frequencies or system natural frequencies
LOAD	Nodal forces and prescribed displacements
MATL	Material properties
MSEN	Mode shape sensitivity coefficients
PATR	Patran neutral file title
PVAR	Sensitivity parameter variances
REAC	Nodal force reactions
SSEN	Element stress sensitivities
STRS	Element stress resultants
TITL	Alphanumeric problem title

Formats for the individual data blocks and block headers are summarized on the following pages.

Record Descriptions for Postprocessor File Output

BLOCK	VARIABLE	DESCRIPTIONS	FORMAT
BOUN	'BOUN'	Block identifier	A8, I8
	NUMDOF	Number of degrees of freedom	
	DOFKOD	'1'=fixed, '0'=free D.O.F. (Repeated for all DOF in model)	80A1
CORD	'CORD'	Block identifier	A8, I8
	NUMNOD	Number of nodes	
	NODE XYZ(3)	Node number Cartesian coordinates X,Y,Z	I8, 3E16.8
DISP	'DISP'	Block identifier	A8, 2I8
	ICASE	Load case/mode number	
	NUMNOD	Number of nodes	
	NODE DISP(6)	Node number Nodal displacements and rotations	I8, 8X, 3E16.8, 16X,3E16.8
DSEN	'DSEN'	Block identifier	A8, 3I8
	ICASE	Load case/mode number	
	NUMNOD	Number of nodes	
	IPARAM	Sensitivity parameter number	
	NODE DISP(6)	Node number Nodal displacement and rotation sensitivities	I8, 8X, 3E16.8, 16X,3E16.8
ELEM	'ELEM'	Block identifier	A8, I8
	NUMELT	Number of elements	
	ELTYPE	Element type	A8, 7I8
	IELT	Element number	
	MATLNO	Material number	
	IPROP NCON(4)	Property number List of connected node points	
ESEN	'ESEN'	Block identifier	A8, 2I8
	NUMMOD	Number of vibration modes	
	NUMPAR	Number of sensitivity param's.	
	MODE	Mode number	2I8,
	IPARAM	Sensitivity parameter number	2E16.8
	FREQ FRSENS	Natural frequency Frequency sensitivity	

Record Descriptions for Postprocessor File Output

BLOCK	VARIABLE	DESCRIPTIONS	FORMAT
FREQ	'FREQ'	Block identifier	A8, 2I8
	NUMMOD IANAL	Number of frequencies '2' = Natural frequencies '3' = Harmonic forcing freq's.	
	FREQS(.)	List of frequencies (5/record)	5E16.8
LOAD	'LOAD'	Block identifier	4A8
	'FORC'	'FORC' for nodal force	
	'GRAV'	'GRAV' for gravity loading	
	'PRES'	'PRES' for pressure loading	
	NODE CODE(6	Node number '1' = loading/imposed displ. '0' = no prescribed values	I8, 2X, 6A1, 3E16.8,/,
	FORCE	Applied force or displ. value for each direction	16X,3E16.8
MATL	'MATL'	Block identifier	A8, I8
	NUMMAT	Number of materials	
	I ELMAT(9)	Material number Material property list (E ₁ , E ₂ , ν ₁₂ , G ₁₂ , G ₁₃ , G ₂₃ , ρ, C ₁ , C ₂)	I8, 8X, 4E16.8, / 5E16.8
MSEN	'MSEN'	Block identifier	A8, 2I8
	NUMMOD	Number of vibration modes	
	NUMPAR	Number of sensitivity param's.	
	MODE IPARAM INDEX COEFF	Mode number Sensitivity parameter number Coefficient number Mode shape sensitivity coefficient	3I8, E16.8
PATR	'PATR'	Block identifier	A8
	DATE	Date neutral file generated	
	TIME	Time neutral file generated	
	PATVER	Patran version number	
PVAR	'PVAR'	Block identifier	A8, I8
	NUMPAR	Number of sensitivity param's.	
	IPARAM ITYPE	Sensitivity parameter number '1' = material modulus '2' = material density '3' = thickness '4' = geometric parameter	
	IDENT VAR	Material, property, or DERIV block i.d. for this parameter Parameter standard deviation	

Record Descriptions for Postprocessor File Output

BLOCK	VARIABLE	DESCRIPTIONS	FORMAT
REAC	'REAC'	Block identifier	A8, 2I8
	ICASE	Applied loading case number	
	NUMNOD	Number of nodes	
	NODE FORC(6)	Node number Nodal reaction force and nodal reaction moments	I8, 8X, 3E16.8, /, 16X, 3E16.8
SSEN	'SSEN'	Block identifier	A8, 3I8
	NCASE	Number of load cases or modes	
	NUMELT	Number of elements	
	NPARAM	Number of sensitivity param's.	
	IDEL ELTYPE ICASE IANAL	Element number Element type Load case/mode number '4' = Static sensitivity '5' = Frequency sensitivity '6' = Harmonic sensitivity	I8, A8, 3I8
	IPARAM	Sensitivity parameter number	
	EPSS(8)	Generalized strain sensitivity	5E16.8
	SIGS(8) SIGVMS(3)	Generalized stress sensitivity von Mises stress sensitivities	
STRS	'STRS'	Block identifier	A8, 2I8
	NCASE	Number of load cases or modes	
	NUMELT	Number of elements	
	IDEL ELTYPE ICASE IANAL	Element number Element type Load case/mode number '1' = Static solution '2' = Natural frequency '3' = Steady state harmonic	I8, A8, 2I8
	EPS(8) SIG(8) SIGVM(3)	Generalized strains Generalized stresses von Mises stresses	5E16.8
	'TITL'	Block identifier	A8
	TITLE	Alphanumeric problem title	80A1

The example below shows the POSFIL output for a very simple finite element model. For larger models, the nodes, elements, degrees of freedom, and other data are repeated as required in the same formats.

```

TITL
Natural frequencies of square plate, inplane motions only, one element

MATL      1
1          0.10000000E+08 0.10000000E+08 0.25000000E+00 0.40000000E+07
0.40000000E+07 0.40000000E+07 0.25900000E-03 0.10000000E+06

CORD      4
1          0.00000000E+00 0.00000000E+00 0.00000000E+00
2          0.10000000E+01 0.00000000E+00 0.00000000E+00
3          0.10000000E+01 0.10000000E+02 0.00000000E+00
4          0.00000000E+00 0.10000000E+02 0.00000000E+00

ELEM      1
SHEL      1      1      1      1      2      3      4

BOUN      24
111111011111001111101111
FREQ      2      2
0.15426565E+10 0.16475772E+12

DISP      1      4
1          0.00000000E+00 0.00000000E+00 0.00000000E+00
           0.00000000E+00 0.00000000E+00 0.00000000E+00
2          -0.25236442E-01 0.00000000E+00 0.00000000E+00
           0.00000000E+00 0.00000000E+00 0.00000000E+00
3          -0.25236442E-01 0.10000000E+01 0.00000000E+00
           0.00000000E+00 0.00000000E+00 0.00000000E+00
4          0.00000000E+00 0.10000000E+01 0.00000000E+00
           0.00000000E+00 0.00000000E+00 0.00000000E+00

DISP      2      4
1          0.00000000E+00 0.00000000E+00 0.00000000E+00
           0.00000000E+00 0.00000000E+00 0.00000000E+00
2          0.10000000E+01 0.00000000E+00 0.00000000E+00
           0.00000000E+00 0.00000000E+00 0.00000000E+00
3          0.10000000E+01 0.25236442E-01 0.00000000E+00
           0.00000000E+00 0.00000000E+00 0.00000000E+00
4          0.00000000E+00 0.25236442E-01 0.00000000E+00
           0.00000000E+00 0.00000000E+00 0.00000000E+00

STRS      2      1
1          1      2
-0.25236442E-01 0.10000000E+00 0.69388939E-17 0.00000000E+00 0.00000000E+00
0.00000000E+00 0.00000000E+00 0.00000000E+00 -0.12610265E+03 0.49968474E+05
0.00000000E+00 0.00000000E+00 0.00000000E+00 0.00000000E+00 0.00000000E+00
0.00000000E+00 0.10006329E+07 0.10006329E+07 0.10006329E+07

STRS      2      1
1          2      2
0.10000000E+01 0.25236442E-02 -0.13010426E-17 0.00000000E+00 0.00000000E+00
0.00000000E+00 0.00000000E+00 0.00000000E+00 0.53366982E+06 0.13467928E+06
-0.11368684E-12 0.00000000E+00 0.00000000E+00 0.00000000E+00 0.00000000E+00
0.00000000E+00 0.96139007E+07 0.96139007E+07 0.96139007E+07

```


APPENDIX C

LAYSTR Layer Stress File Description

The usual stress output from PROTEC consists of reference surface strains and curvatures, as well as force and moment resultants at the center of each element. For layered elements, the program generates much more detailed stress data defining point stress distributions throughout the element thickness. However, this data is quite lengthy for large models, and often must be plotted for correct interpretation.

When layered elements are present in a finite element model, SAFE generates a separate output file containing detailed layer stresses, which may be printed or read as input for graphical postprocessing. The name of this lamina stress file is LAYSTR (**L**Ayer **S**Tresses). On VAX computers, the file is saved automatically on the current directory; on CDC and CRAY systems, LAYSTR is a local file which must be saved at the end of an analysis job.

The LAYSTR file is a formatted, 80-column card image file, with a simple, highly structured format. For each element and loading case (or mode), the file contains the following data:

<u>Line</u>	<u>Format</u>	<u>Data Description</u>
1	4I8	1. IDEL - element i.d. number 2. ICASE - load case or mode number 3. LAMNO - laminate i.d. number 4. NLAYER - number of layers
2	2I8, E16.9	1. LAYER - current layer number 2. MATL - material i.d. for layer 3. Z - thickness coordinate
3	5E16.9	1. SXX - stress component σ_{xx} 2. SYX - stress component σ_{yx} 3. SXY - stress component σ_{xy} 4. SXZ - stress component σ_{xz} 5. SYZ - stress component σ_{yz}

The following points should be noted concerning the data items described above:

- ⊙ Elements appear in sequential order on the file.
- ⊙ For each element, all load cases or modes will appear together, in ascending order.
- ⊙ Within an element and case, layers will appear sequentially, in decreasing order (top to bottom).
- ⊙ For each layer, three "Z" stations are output, since the computed transverse shear stresses vary parabolically within each layer.
- ⊙ Stress components are referred to the element local axes.

A segment of a typical LAYSTR file corresponding to a single element with three layers is listed below.

IDEL	ICASE	LAMMO	NLAYER			
LAYER	MATL		Z			
	SXX	SYX		SXY	SXZ	SYZ
1	1	1	3			
3	1 0.250000000					
-28358.0728	-28302.5974	269.531802		0.000000000E+00	0.000000000E+00	
3	1 0.237500000					
-26940.1691	-26887.4675	256.055212		7.42952757	8.23334692	
3	1 0.225000000					
-25522.2655	-25472.3377	242.578622		14.4780537	16.0444709	
2	2 0.225000000					
-0.178805642	-0.178156580	0.315352208E-02		14.4780537	16.0444709	
2	2 0.000000000E+00					
0.000000000E+00	0.000000000E+00	0.000000000E+00		14.4786154	16.0450934	
2	2-0.225000000					
0.178805642	0.178156580	-0.315352208E-02		14.4780537	16.0444709	
1	1-0.225000000					
25522.2655	25472.3377	-242.578622		14.4780537	16.0444709	
1	1-0.237500000					
26940.1691	26887.4675	-256.055212		7.42952757	8.23334692	
1	1-0.250000000					
28358.0728	28302.5974	-269.531802		0.000000000E+00	0.000000000E+00	

APPENDIX D

PATRAN INTERFACES (PATPRO/PROPAT)

This Appendix describes the data translation performed by **PATPRO** (**PATRAN-to-PROTEC**) and **PROPAT** (**PROTEC-to-PATRAN**). **PATPRO** converts a finite element neutral file from the geometric modeling program **PATRAN** into a standard input file for finite element analysis by **PROTEC**. **PROPAT** transforms a **PROTEC** results file into a **PATRAN** results file for postprocessing. **PATRAN**¹⁰ is a product of PDA Engineering in Santa Ana, California.

The modeling-analysis-postprocessing cycle begins in **PATRAN**, where the finite element model is generated. The completed model is written (by **PATRAN**) to a **PATRAN Neutral File**. A Neutral File is a card-image text file which contains geometric data, node and element definitions, properties data, loads, constraints, and model identification parameters. From the Neutral File, **PATPRO** generates most of the data required to perform a finite element analysis with **PROTEC**.

When the analysis is complete, the results file **POSFIL** (see Appendix B) may be processed using **PROPAT** to create plotting data files compatible with **PATRAN**. Results files, together with the original **PATRAN Neutral File**, are then used within **PATRAN** for the graphical display of stress and displacement results.

Both **PATPRO** and **PROPAT** are written in ANSI FORTRAN-77, and are operational on the DEC VAX under VMS and CDC Cyber under NOS. Important features and limitations for each of the programs are noted in the paragraphs below.

PATPRO (PATRAN-to-PROTEC): **PATPRO** uses the **PATRAN Neutral File** to generate most of the **PROTEC** input needed for an analysis. **PATRAN** data types which can be translated are shown in the Table below.

<u>PATRAN Packet</u>	<u>PROTEC Data Block</u>	<u>Description</u>	<u>Notes and Restrictions</u>
25	TITL	Problem title	
26	PATR	Model identification	
1	COOR	Nodal coordinates	
2	ELEM	Element connections	QUAD/4 (SHELL) only
3	MATE	Material properties	Isotropic materials
4	PROP	Physical properties	Element thicknesses
6	PRES	Pressure loads	Element avg. only
7	FORC	Nodal forces	
8	FORC	Nodal displacements	

All nodes present in the PATRAN model are translated into PROTEC format, without resequencing. The model should be fully equivalenced (i.e, duplicate nodes eliminated) in PATRAN before writing the Neutral File. We also recommend the node renumbering facilities in PATRAN, which are extremely effective; the RMS WAVEFRONT criterion is most appropriate when the analysis is to be performed using PROTEC.

When data blocks other than those listed above are needed, these must be entered manually using a text editor. Examples are the OPTIOns, SENSitivity, and LAMInate input blocks.

PROPAT (PROTEC-to-PATRAN): PROPAT processes the results file (POSFIL) generated by PROTEC, and produces PATRAN-compatible files containing nodal or element results "columns". The PATRAN results files are binary files and cannot be listed or printed; PROPAT will, at the user's option, generate formatted versions of the results files for printing. For postprocessing, both the binary results files from PROPAT and the original PATRAN neutral file must be supplied to PATRAN. Postprocessing options include plots of deformed geometry, stress or displacement contours, and color-coded plots of key element or nodal results from PROTEC.

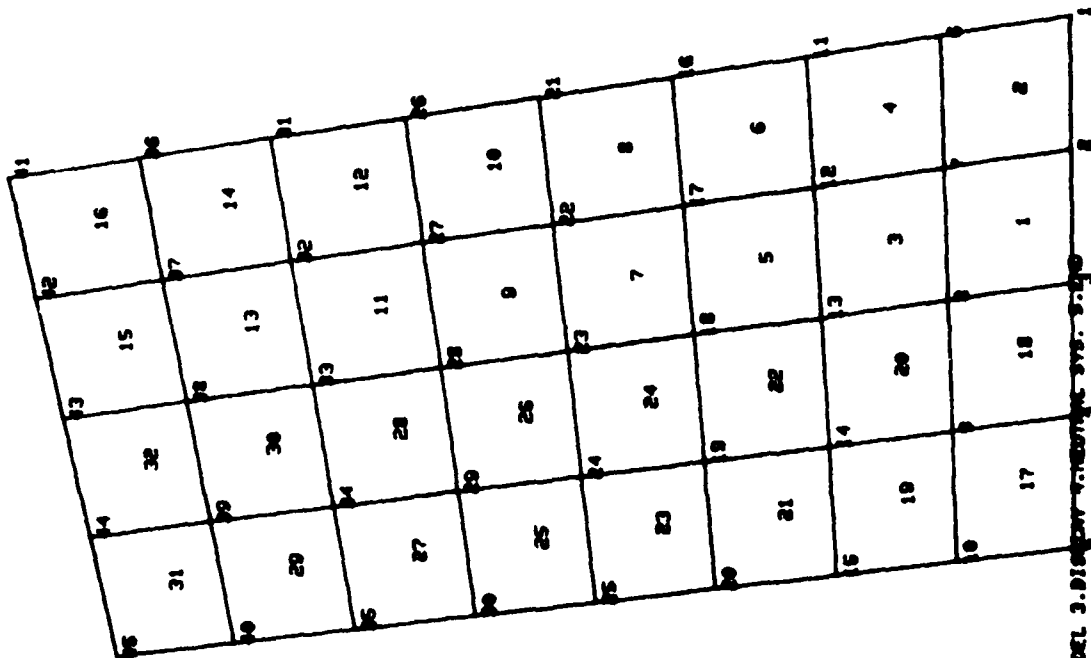
The listings which follow demonstrate the operation of the PATRAN interface programs, and show the types of data which are generated at each stage of the process. The table below gives a summary of the sample listings.

<u>Listing</u>	<u>Title</u>	<u>Description</u>
D.1	PATRAN Session File	Keyboard input to PATRAN
D.2	PATRAN Neutral File	Model as output from PATRAN
D.3	PATPRO Execution	Change PATRAN data to PROTEC format
D.4	PROTEC Input Data	Final PROTEC input file
D.5	POSFIL Results File	Results file output by PROTEC
D.6	PROPAT Execution	Change results file to PATRAN format
D.7	Element Results File	Element results as used in PATRAN
D.8	Nodal Results File	Nodal results as used in PATRAN
D.9	PATRAN Session	Interactive postprocessing

```

00
1 1
1 1
00.1..0/0/0
00.2..-7/1.8/1.7
00.3..-8/2/1.7
00.4..-85/1.9/0
00.5..-5/0/0
00.6..-5/0/0
00.1.0..1/4/3/6
00.2.0..5/8/4/1
00.7.1.180.18.5E8..0.3.0.000000
END
8
SET,PML,OFF
SET,RADN,10
CFEQ,PIT2..3/0
CFEQ,PIT2,QUAD..1
3 M 2 Y 1 Y 7 3 2 1 8 4 1
1
SIMPLIFIED BLADE/DISC SECTOR
Y Y Y S ,

```



MODEL 1.GEOMETRY MODEL 2.ANALYSIS MODEL 3.DISPLAY-INTERACTIVE SYS. 5.30
 ,

Listing D.1. PATRAN Session File.

PATPRO

```
*****
PAT - PRO
PATRAN TO PROTEC TRANSLATOR
PAT_PRO TRANSLATES A PATRAN NEUTRAL
FILE INTO A PROTEC INPUT FILE
*****
```

PLEASE ENTER THE PATRAN NEUTRAL FILENAME :
? NEUTRAL

PLEASE ENTER THE PROTEC INPUT FILENAME ...:
? INPRO

THE TITLE OF PATRAN NEUTRAL FILE IS

SIMPLIFIED BLADE/DISC SECTOR

THIS PATRAN NEUTRAL FILE WAS CREATED AT 08.40.5
ON 87/10/15 FROM PATRAN VERSION NUMBER 1.5

THE FILE PARAMETERS ARE . . .

NUMBER OF NODES	•	45
NUMBER OF ELEMENTS	•	32
NUMBER OF MATERIAL PROPERTIES	•	1
NUMBER OF PHYSICAL PROPERTIES	•	0

PROCESSING PLEASE WAIT . . .

1.006 CP SECONDS EXECUTION TIME.

Listing D.3. PATPRO Execution.

11	0 9940393E-01	-0 20401233E+00	0 10000000E+01	-0 23010329E-01	-0 23010329E-01	-0 16113469E+00	-0 70304124E+00
12	0 14060823E-02	0 11800033E-01	0 19077333E-01	0 9883444E+00	0 18513550E-01	0 48551070E+00	-0 64263490E+00
13	0 7527934E-02	0 89162403E-02	0 78498333E-01	0 45989713E-01	0 34895585E-01	0 53579211E+00	-0 53579211E+00
14	0 47758133E-02	0 91113034E-03	0 32022993E-01	0 32022993E-01	0 94345523E-01	0 64818005E+00	-0 64818005E+00
15	0 91430484E-02	0 41681160E-03	0 32022993E-01	0 32022993E-01	0 13742788E-01	0 50456474E+00	-0 50456474E+00
16	0 13049703E-02	0 41681160E-03	0 32022993E-01	0 32022993E-01	0 23347084E+00	0 63199246E+00	-0 63199246E+00
17	0 80923632E-02	0 75223323E-02	0 49251939E-01	0 44294932E-01	0 23347084E+00	0 63199246E+00	-0 63199246E+00
18	0 17989333E-02	0 37491094E-01	0 23046110E-01	0 23046110E-01	0 23347084E+00	0 63199246E+00	-0 63199246E+00
19	0 12892319E-02	0 11843292E-01	0 84148858E-01	0 84148858E-01	0 23347084E+00	0 63199246E+00	-0 63199246E+00
20	0 7844437E-01	0 92174540E-01	0 96205862E-01	0 96205862E-01	0 23347084E+00	0 63199246E+00	-0 63199246E+00
21	0 96581787E-02	0 38290038E-01	0 79178227E-01	0 79178227E-01	0 23347084E+00	0 63199246E+00	-0 63199246E+00
22	0 30243448E-01	0 10895359E+00	0 11964493E+00	0 11964493E+00	0 23347084E+00	0 63199246E+00	-0 63199246E+00
23	0 23702624E-01	0 23480243E-01	0 65698636E+00	0 65698636E+00	0 23347084E+00	0 63199246E+00	-0 63199246E+00
24	0 37753978E-01	0 39464674E-01	0 12253256E+00	0 12253256E+00	0 23347084E+00	0 63199246E+00	-0 63199246E+00
25	0 27152733E-01	0 31644441E-02	0 44769993E+00	0 44769993E+00	0 23347084E+00	0 63199246E+00	-0 63199246E+00
26	0 15268343E+00	0 57839124E-02	0 11594913E+00	0 11594913E+00	0 23347084E+00	0 63199246E+00	-0 63199246E+00
27	0 24760142E-01	0 18014381E-01	0 62118297E+00	0 62118297E+00	0 23347084E+00	0 63199246E+00	-0 63199246E+00
28	0 56673703E-01	0 16928108E-01	0 86548390E-01	0 86548390E-01	0 23347084E+00	0 63199246E+00	-0 63199246E+00
29	0 99489684E-02	0 35933630E-01	0 7646442E+00	0 7646442E+00	0 23347084E+00	0 63199246E+00	-0 63199246E+00
30	0 78487251E-02	0 53154779E-01	0 19362104E+00	0 19362104E+00	0 23347084E+00	0 63199246E+00	-0 63199246E+00
31	0 33815560E-01	0 7615362E-01	0 69513647E+00	0 69513647E+00	0 23347084E+00	0 63199246E+00	-0 63199246E+00
32	0 39004843E-01	0 72487411E-01	0 21305944E+00	0 21305944E+00	0 23347084E+00	0 63199246E+00	-0 63199246E+00
33	0 51598883E-01	0 44163433E-01	0 59277038E+00	0 59277038E+00	0 23347084E+00	0 63199246E+00	-0 63199246E+00
34	0 99928186E-01	0 36572743E-01	0 21305944E+00	0 21305944E+00	0 23347084E+00	0 63199246E+00	-0 63199246E+00
35	0 56957217E-01	0 70336229E-02	0 21509461E+00	0 21509461E+00	0 23347084E+00	0 63199246E+00	-0 63199246E+00
36	0 17201733E-01	0 78070592E-02	0 47946210E+00	0 47946210E+00	0 23347084E+00	0 63199246E+00	-0 63199246E+00
37	0 98267213E-01	0 31315268E-01	0 20403098E+00	0 20403098E+00	0 23347084E+00	0 63199246E+00	-0 63199246E+00
38	0 34856031E-01	0 12970123E-01	0 63124895E+00	0 63124895E+00	0 23347084E+00	0 63199246E+00	-0 63199246E+00
39	0 70755292E-01	0 12970123E-01	0 63124895E+00	0 63124895E+00	0 23347084E+00	0 63199246E+00	-0 63199246E+00
40	0 16245240E+00	0 13639969E-01	0 30905642E+00	0 30905642E+00	0 23347084E+00	0 63199246E+00	-0 63199246E+00
41	0 90555207E-01	0 69400079E-01	0 54799720E+00	0 54799720E+00	0 23347084E+00	0 63199246E+00	-0 63199246E+00
42	0 15203164E+00	0 15760711E-01	0 32209504E+00	0 32209504E+00	0 23347084E+00	0 63199246E+00	-0 63199246E+00
43	0 97620985E-01	0 12377933E-02	0 50306250E+00	0 50306250E+00	0 23347084E+00	0 63199246E+00	-0 63199246E+00
44	0 17703439E+00	0 70943967E-02	0 30791736E+00	0 30791736E+00	0 23347084E+00	0 63199246E+00	-0 63199246E+00
45	0 92198199E-01	0 46252481E-01	0 30791736E+00	0 30791736E+00	0 23347084E+00	0 63199246E+00	-0 63199246E+00
46	0 16487172E+00	0 52499020E-02	0 52943584E+00	0 52943584E+00	0 23347084E+00	0 63199246E+00	-0 63199246E+00
47	0 71833756E-01	0 10372427E-02	0 27800997E+00	0 27800997E+00	0 23347084E+00	0 63199246E+00	-0 63199246E+00
48	0 16284481E+00	0 13816946E-02	0 52896525E+00	0 52896525E+00	0 23347084E+00	0 63199246E+00	-0 63199246E+00
49	0 11718648E+00	0 17201352E-02	0 43479939E+00	0 43479939E+00	0 23347084E+00	0 63199246E+00	-0 63199246E+00
50	0 13897523E+00	0 87275897E-02	0 30476767E+00	0 30476767E+00	0 23347084E+00	0 63199246E+00	-0 63199246E+00
51	0 21102164E+00	0 97975646E-01	0 43195123E+00	0 43195123E+00	0 23347084E+00	0 63199246E+00	-0 63199246E+00
52	0 18735353E+00	0 28321730E-02	0 43968133E+00	0 43968133E+00	0 23347084E+00	0 63199246E+00	-0 63199246E+00
53	0 18735353E+00	0 19278274E-01	0 43968133E+00	0 43968133E+00	0 23347084E+00	0 63199246E+00	-0 63199246E+00
54	0 10692115E+00	0 42049874E-02	0 43183144E+00	0 43183144E+00	0 23347084E+00	0 63199246E+00	-0 63199246E+00
55	0 1927813E+00	0 87779977E-03	0 51193137E+00	0 51193137E+00	0 23347084E+00	0 63199246E+00	-0 63199246E+00
56	0 11858816E+00	0 14230310E+00	0 39098997E+00	0 39098997E+00	0 23347084E+00	0 63199246E+00	-0 63199246E+00
57	0 24525814E+00	0 14230310E+00	0 48303327E+00	0 48303327E+00	0 23347084E+00	0 63199246E+00	-0 63199246E+00
58	0 17084852E+00	0 22736233E+00	0 36707038E+00	0 36707038E+00	0 23347084E+00	0 63199246E+00	-0 63199246E+00
59	0 29049085E+00	0 37949573E-01	0 44859374E+00	0 44859374E+00	0 23347084E+00	0 63199246E+00	-0 63199246E+00
60	0 19473439E+00	0 12880427E+00	0 54795274E+00	0 54795274E+00	0 23347084E+00	0 63199246E+00	-0 63199246E+00
61	0 22455737E+00	0 11148449E-01	0 49193189E+00	0 49193189E+00	0 23347084E+00	0 63199246E+00	-0 63199246E+00
62	0 20480192E+00	0 24499704E-01	0 34291793E+00	0 34291793E+00	0 23347084E+00	0 63199246E+00	-0 63199246E+00
63	0 17437093E+00	0 64100148E-02	0 32101728E+00	0 32101728E+00	0 23347084E+00	0 63199246E+00	-0 63199246E+00
64	0 19491759E+00	0 78155041E-01	0 34272727E+00	0 34272727E+00	0 23347084E+00	0 63199246E+00	-0 63199246E+00
65	0 22186967E+00	0 10901162E-01	0 49269814E+00	0 49269814E+00	0 23347084E+00	0 63199246E+00	-0 63199246E+00
66	0 17232220E+00	0 18258871E+00	0 30953404E+00	0 30953404E+00	0 23347084E+00	0 63199246E+00	-0 63199246E+00
67	0 26777946E+00	0 14372277E-01	0 47134470E+00	0 47134470E+00	0 23347084E+00	0 63199246E+00	-0 63199246E+00
68	0 22917554E+00	0 28370108E+00	0 70294657E+00	0 70294657E+00	0 23347084E+00	0 63199246E+00	-0 63199246E+00
69	0 30944347E+00	0 45467563E-01	0 43970263E+00	0 43970263E+00	0 23347084E+00	0 63199246E+00	-0 63199246E+00

Listing D.5. POSFIL Results File (continued).

28	0.38063346E+00	0.73927362E-01	0.69405515E+00	0.17	0.28556101E-02	0.14620863E-01	0.34069134E-02
29	0.78810802E-01	0.49418038E-02	0.73501899E-01	18	-0.15972304E+00	0.21328339E+00	-0.40187671E+00
29	0.76511011E+00	0.23576826E-02	0.55961603E+00	14	0.20364841E-01	0.13169767E-01	0.54182602E-01
30	0.32044686E-01	0.20977441E-01	0.77267099E-01	15	0.39273665E+00	0.19145882E+00	0.49968253E+00
30	0.39037295E+00	0.36771771E-02	0.69569082E+00	15	0.25619482E+00	0.31491199E+00	0.13260893E+00
31	0.85463851E-02	0.39067587E-01	0.10087788E+00	16	-0.05619482E+00	0.37780367E-01	0.13821450E-02
31	0.48304788E+00	0.23335076E-01	0.82099368E+00	16	-0.06042606E+00	0.43282242E+00	0.11687826E+00
31	0.35031451E-01	0.16672996E-01	0.72393825E-01	17	-0.26710189E+00	0.29554292E-01	0.91408647E-01
32	0.22524071E+00	0.26279587E-01	0.60371250E+00	17	-0.4780788E-01	0.3943636E+00	0.16504340E-01
32	0.77999779E-01	0.33716450E-02	0.49921251E-01	18	-0.4449337E-02	0.22916087E-01	0.63530284E-02
33	0.85542721E-01	0.11097217E-01	0.41520407E-01	19	0.4976713E-01	0.19696901E-01	0.91630295E-01
33	0.24000019E+00	0.14897405E-01	0.53596251E+00	20	0.29159467E+00	0.3779783E+00	0.38907532E+00
34	0.78318217E-01	0.20577884E-01	0.46568805E-01	20	0.11292359E+00	0.16702590E-01	0.20432386E+00
34	0.2212593E+00	0.10532496E-01	0.57117041E+00	21	0.10718112E+00	0.32438605E+00	0.2141771E+00
35	0.52864327E-01	0.10489853E-01	0.67438412E-01	21	-0.19286703E+00	0.5695997E-01	0.24515703E+00
35	0.26644587E+00	0.10779601E-02	0.63030236E+00	22	-0.2845307E+00	0.40266632E+00	0.1550042E+00
36	0.1173737E+00	0.88996060E-02	0.23532056E-01	22	-0.85073204E-01	0.41965035E-01	0.1158717E+00
37	0.3462497E-01	0.62339027E-01	0.39956305E+00	23	-0.2645307E+00	0.45152731E+00	0.2456712E+00
37	0.1349592E+00	0.13700609E-01	0.57658429E-02	23	-0.2645307E+00	0.45152731E+00	0.2456712E+00
38	0.14409125E+00	0.23066847E-01	0.46373428E+00	24	-0.8766537E-01	0.3779507E-01	0.32417834E-02
38	0.13360477E+00	0.49285027E-02	0.50160575E+00	24	0.8766537E-01	0.3779507E-01	0.32417834E-02
39	0.13483865E+00	0.19546678E-01	0.53016394E-02	25	0.1813735E-01	0.3283284E-01	0.14830345E+00
40	0.9707737E-01	0.13730339E-01	0.48782226E-01	25	0.643737E-01	0.1507031E+00	0.34509831E+00
40	0.10968134E+00	0.3572947E-01	0.38243737E+00	26	0.2747803E+00	0.77904837E-01	0.32597432E+00
41	0.18143440E+00	0.36381023E-01	0.28634423E-01	26	-0.13323687E+00	0.82808505E+00	0.32355943E+00
41	0.1987297E+00	0.11326920E-01	0.29794758E+00	27	-0.33134215E+00	0.52944897E-01	0.13434643E+00
42	0.39629934E-02	0.33690066E-01	0.4014200E-01	28	0.74543940E-02	0.58072305E+00	0.24822434E+00
43	0.20978252E+00	0.2742242E-01	0.5025725E-01	28	-0.53134215E+00	0.58072305E+00	0.24822434E+00
43	0.0897126E+00	0.20519919E-03	0.49322780E+00	29	0.19801076E+00	0.58072305E+00	0.17384943E-01
44	0.19878245E+00	0.18372034E-01	0.41828780E-01	29	0.32430291E+00	0.14294052E-01	0.31791751E+00
45	0.20455894E-01	0.17047005E-01	0.4058059E+00	30	0.29072715E+00	0.65025571E+00	0.49225778E+00
45	0.17002768E+00	0.94720491E-02	0.19993134E-01	31	-0.20495988E+00	0.80637279E+00	0.34017965E+00
45	0.19701423E+00	0.43077907E-01	0.29307613E+00	31	-0.41796815E+00	0.10320813E+00	0.70259037E-01
45	0.19701423E+00	0.43077907E-01	0.29307613E+00	32	-0.48992124E+00	0.80373005E+00	0.15120504E+00
45	0.19701423E+00	0.43077907E-01	0.29307613E+00	32	-0.48992124E+00	0.80373005E+00	0.15120504E+00
45	0.19701423E+00	0.43077907E-01	0.29307613E+00	33	-0.75795653E+00	0.42394003E+00	0.41684285E+00
45	0.19701423E+00	0.43077907E-01	0.29307613E+00	33	-0.75795653E+00	0.42394003E+00	0.41684285E+00
45	0.19701423E+00	0.43077907E-01	0.29307613E+00	34	0.1166769E-01	0.40260419E-01	0.22636382E-01
45	0.19701423E+00	0.43077907E-01	0.29307613E+00	34	0.1166769E-01	0.40260419E-01	0.22636382E-01
45	0.19701423E+00	0.43077907E-01	0.29307613E+00	35	0.22759934E+00	0.26104203E-01	0.18546615E+00
45	0.19701423E+00	0.43077907E-01	0.29307613E+00	35	0.22759934E+00	0.26104203E-01	0.18546615E+00
45	0.19701423E+00	0.43077907E-01	0.29307613E+00	36	0.35464796E+00	0.73885698E+00	0.12900295E+00
45	0.19701423E+00	0.43077907E-01	0.29307613E+00	36	0.35464796E+00	0.73885698E+00	0.12900295E+00
45	0.19701423E+00	0.43077907E-01	0.29307613E+00	37	0.17257187E+00	0.13720339E-01	0.34963480E+00
45	0.19701423E+00	0.43077907E-01	0.29307613E+00	37	0.17257187E+00	0.13720339E-01	0.34963480E+00
45	0.19701423E+00	0.43077907E-01	0.29307613E+00	38	-0.23946259E+00	0.12902504E+00	0.11189916E+00
45	0.19701423E+00	0.43077907E-01	0.29307613E+00	38	-0.23946259E+00	0.12902504E+00	0.11189916E+00
45	0.19701423E+00	0.43077907E-01	0.29307613E+00	39	-0.31938331E+00	0.98327029E+00	0.70148333E-01
45	0.19701423E+00	0.43077907E-01	0.29307613E+00	39	-0.31938331E+00	0.98327029E+00	0.70148333E-01
45	0.19701423E+00	0.43077907E-01	0.29307613E+00	40	-0.61099982E+00	0.80579962E+00	0.23617105E+00
45	0.19701423E+00	0.43077907E-01	0.29307613E+00	40	-0.61099982E+00	0.80579962E+00	0.23617105E+00
45	0.19701423E+00	0.43077907E-01	0.29307613E+00	41	0.16907654E-01	0.41981174E-01	0.32395016E-01
45	0.19701423E+00	0.43077907E-01	0.29307613E+00	41	0.16907654E-01	0.41981174E-01	0.32395016E-01
45	0.19701423E+00	0.43077907E-01	0.29307613E+00	42	0.25864541E+00	0.25068092E-01	0.17603948E+00
45	0.19701423E+00	0.43077907E-01	0.29307613E+00	42	0.25864541E+00	0.25068092E-01	0.17603948E+00
45	0.19701423E+00	0.43077907E-01	0.29307613E+00	43	0.19454103E+00	0.85545209E+00	0.17481562E-01
45	0.19701423E+00	0.43077907E-01	0.29307613E+00	43	0.19454103E+00	0.85545209E+00	0.17481562E-01
45	0.19701423E+00	0.43077907E-01	0.29307613E+00	44	0.32551353E+00	0.14411767E-01	0.4133899E+00
45	0.19701423E+00	0.43077907E-01	0.29307613E+00	44	0.32551353E+00	0.14411767E-01	0.4133899E+00
45	0.19701423E+00	0.43077907E-01	0.29307613E+00	45	0.92090949E-02	0.93498354E+00	0.22103943E+00
45	0.19701423E+00	0.43077907E-01	0.29307613E+00	45	0.92090949E-02	0.93498354E+00	0.22103943E+00
45	0.19701423E+00	0.43077907E-01	0.29307613E+00	46	-0.6589984E+00	0.15636570E+00	0.42352914E+00
45	0.19701423E+00	0.43077907E-01	0.29307613E+00	46	-0.6589984E+00	0.15636570E+00	0.42352914E+00
45	0.19701423E+00	0.43077907E-01	0.29307613E+00	47	-0.26499801E+00	0.10000000E+01	0.33668493E-01
45	0.19701423E+00	0.43077907E-01	0.29307613E+00	47	-0.26499801E+00	0.10000000E+01	0.33668493E-01
45	0.19701423E+00	0.43077907E-01	0.29307613E+00	48	-0.75446043E+00	0.81049099E+00	0.33115186E+00
45	0.19701423E+00	0.43077907E-01	0.29307613E+00	48	-0.75446043E+00	0.81049099E+00	0.33115186E+00
45	0.19701423E+00	0.43077907E-01	0.29307613E+00	49	0.25490782E-01	0.42215803E-01	0.43823489E-01
45	0.19701423E+00	0.43077907E-01	0.29307613E+00	49	0.25490782E-01	0.42215803E-01	0.43823489E-01
45	0.19701423E+00	0.43077907E-01	0.29307613E+00	50	-0.41591330E+00	0.81132384E+00	0.27625852E+00
45	0.19701423E+00	0.43077907E-01	0.29307613E+00	50	-0.41591330E+00	0.81132384E+00	0.27625852E+00
45	0.19701423E+00	0.43077907E-01	0.29307613E+00	51	0.23771784E-01	0.23771784E-01	0.24928607E+00
45	0.19701423E+00	0.43077907E-01	0.29307613E+00	51	0.23771784E-01	0.23771784E-01	0.24928607E+00

Listing D.5. POSFIL Results File (continued).

43

0 23514083E+00 0 16326341E+01 0 14070926E+01 -0 44035013E-03 0 16753934E-01 -0 13033714E+03 -0 49618617E+07
0 18434084E+00 0 17442343E-01 0 12172122E+02 0 82127753E+02 0 72430019E+06 0 13751234E+07
0 18627280E+00 0 94024083E+00 -0 12079403E+00

STRS 3 32
1 SHELL
0 21662340E-03 -0 27823438E-03 0 50032871E-03 0 10480318E+00 0 28894324E+00
0 17972810E-03 -0 19443727E-03 0 27752081E-03 0 37648002E+03 -0 5756532E+03
0 48031544E+03 0 24039424E+03 0 42482353E+03 -0 89494431E+02 -0 15372581E+03
0 22201663E+04 0 38432383E+06 0 73754359E+05 0 34621990E+06

STRS 3 32
1 SHELL
0 33763471E-03 0 16276732E-02 0 78637083E-03 -0 12545872E+00 -0 34903012E+00
0 62373140E-01 -0 93088840E-03 0 21598499E-02 0 17736601E+03 0 39507573E+04
0 79492369E+03 -0 49043542E+03 0 51929301E+03 -0 31933047E+02 -0 74711077E+03
0 1278799E+04 0 46386153E+06 0 79617454E+05 0 38841663E+06

STRS 3 32
1 SHELL
0 48298706E-03 -0 16806679E-01 0 11839415E-01 -0 30264527E-01 0 51457311E+00
0 68309338E+00 0 40642271E-02 0 79555988E-02 -0 95198280E+04 -0 42715988E+05
0 11363839E+03 0 13431704E+03 0 69223295E+03 0 34973281E+03 0 32513817E+04
0 63444790E+04 0 11282344E+07 0 59173444E+06 0 82162143E+06

STRS 3 32
1 SHELL
0 13178012E-03 -0 11676043E-03 0 87123122E-03 0 59603362E-01 0 76358402E+01
0 32315655E+00 -0 44436979E-04 0 23955083E-02 0 26283043E+03 -0 1456747E+03
0 83640117E+03 0 90375459E+02 0 56325670E-02 0 18486020E+03 -0 35349380E+02
0 20761668E+04 0 26231426E+06 0 70015914E+05 0 29840199E+06

STRS 3 32
1 SHELL
0 33486866E-03 0 20002674E-02 0 12373448E-02 -0 49227744E-01 -0 23370059E+00
0 14132396E+00 -0 63036135E-03 0 1277930E-03 0 4117734E+03 0 49050885E+04
0 11878310E+04 -0 13517407E+03 0 36407028E+03 0 72257869E+02 -0 50428911E+03
0 11499136E+04 0 38176577E+06 0 76096397E+05 0 26081122E+06

STRS 3 32
1 SHELL
0 47808485E-02 0 19403813E-01 0 10077387E-01 -0 55167592E-01 0 70803162E+00
0 17603423E+00 0 16758443E-02 0 17628249E-01 0 17946785E+03 0 46614017E+04
0 96742919E+04 0 16635263E+03 0 94786865E-03 0 69650611E+02 0 13406754E+04
0 14102613E+05 0 28113943E+06 0 77054229E+06 0 14356318E+07

STRS 3 32
1 SHELL
0 47699131E-03 0 32939842E-05 0 17483213E-03 0 15751861E+00 0 19440110E+00
0 17570013E+00 -0 93184867E-03 0 18426984E-02 0 12248459E+04 0 31882704E+03
0 16782884E+03 0 28142098E+03 0 31918865E-03 -0 89958464E+02 -0 76149494E+03
0 14741587E+04 0 30959834E+06 0 55750941E+05 0 32807667E+06

STRS 3 32
1 SHELL
0 22803094E-03 0 27323409E-03 0 14313833E-02 -0 10304009E+00 -0 11704673E+00
0 19327813E+00 0 72929380E-03 0 10985670E-02 -0 40887304E+03 0 35375704E+03
0 13763200E+04 -0 18063602E-03 -0 19497883E+03 -0 10003360E+03 0 56343664E+03
0 87885340E+03 0 22228552E+06 0 46366147E+05 0 26003963E+06

STRS 3 32
1 SHELL
0 26210910E-03 -0 19316745E-01 0 75811000E-02 -0 75779635E-01 0 17996748E+00
-0 71868213E-02 0 23143414E-01 0 21746370E-02 0 48097597E-02 -0 17922838E-01

Listing D.5. POSFIL Results File (continued).

0	88911482E+00	-0	13572794E-01	-0	12029554E-01	-0	33864781E-04	0	34647574E+05
0	20871707E+04	0	1761944E+00	-0	22897181E+02	0	49322679E+03	0	26861917E+03
0	96238468E+04	0	10058631E+07	0	77398349E+06	0	10412498E+07		
STRS	3	32							
7	SHEL								
0	17244315E-03	0	32013442E-03	0	59567352E-04	0	48045033E-01	0	10771673E+00
0	47293740E-02	-0	44075417E-03	-0	49717294E-03	-0	10836075E+03	0	12212304E+04
0	51184648E-02	-0	10236460E+03	0	16346861E+03	0	24215415E+01	-0	35260332E+03
0	39773836E-03	0	12292094E+06	0	23560495E+05	0	14623163E+06		
STRS	3	32							
7	SHEL								
0	21210045E-05	0	26249989E-03	0	16711141E-02	0	11596930E+00	0	18133748E+00
0	11327644E-01	-0	26192548E-04	-0	59534980E-03	0	17537016E-03	0	72184224E+03
0	16049396E-04	0	19004774E+03	0	20417383E+03	0	57997548E+03	-0	20954039E+02
0	22835984E-03	0	24463883E+06	0	34446622E+05	0	28212333E+04		
STRS	3	32							
7	SHEL								
0	16938688E-02	-0	18627846E-01	-0	31992513E-02	0	10859710E+00	0	12239231E+00
0	31524119E-01	-0	53866524E-01	-0	51204121E-05	0	27408350E+03	-0	63370494E+03
0	35926110E+03	0	29291574E+05	0	75390417E+02	0	16140389E+02	-0	43002979E+03
0	40963297E-01	0	72142113E+05	0	18914390E+03	0	64112310E+03		
STRS	3	32							
8	SHEL								
0	18010065E-03	0	29217341E-03	0	37423024E-03	0	81992915E-02	0	53177732E-01
0	31524119E-01	-0	53866524E-01	-0	51204121E-05	0	27408350E+03	-0	63370494E+03
0	35926110E+03	0	29291574E+05	0	75390417E+02	0	16140389E+02	-0	43002979E+03
0	40963297E-01	0	72142113E+05	0	18914390E+03	0	64112310E+03		
STRS	3	32							
8	SHEL								
0	35047769E-03	0	97457005E-03	0	72277644E-04	0	24985982E-02	0	10927321E+00
0	14112410E+00	0	18318630E-04	0	83366490E-03	-0	27251481E-03	0	22751184E+04
0	67286540E-02	0	7112387E+02	0	15725281E+03	0	72255337E+02	0	14654904E+02
0	66653321E-03	0	15364241E+06	0	37271798E+03	0	19504020E+06		
STRS	3	32							
8	SHEL								
0	64928890E-02	0	209734450E-01	0	17685982E-02	0	684333498E-01	0	12691483E-01
0	80033647E+00	-0	70363663E-03	-0	10120480E-01	-0	32364920E+04	0	49438404E+05
0	14978934E+04	0	97766363E+02	0	40686735E+02	0	40977135E+03	-0	56290920E+03
0	80763638E+04	0	90853306E+06	0	69233624E+06	0	94473975E+06		
STRS	3	32							
9	SHEL								
0	19089354E-03	0	35410377E-03	0	17922334E-04	0	17371078E-01	0	64271244E-01
0	15981402E-01	-0	16337515E-05	-0	15623670E-03	0	26205042E+03	0	78437627E+03
-0	17205440E+02	0	45655231E+02	0	93681003E+02	0	81824779E+01	-0	13086017E+01
0	12498926E+03	0	69296452E+05	0	12473805E+05	0	86034131E+05		
STRS	3	32							
9	SHEL								
-0	23178252E-03	0	66017118E-03	0	11793104E-02	0	91369524E-01	0	18013335E+00
-0	11805153E-01	-0	31193431E-03	-0	35796414E-03	-0	17083536E+03	0	15416974E+04
0	11321382E+04	0	18725150E+03	0	28124882E+03	-0	60442281E+01	-0	24954745E+03
-0	28437133E+03	0	21923453E+06	0	34206505E+06	0	24949283E+06		
STRS	3	32							
9	SHEL								
0	34066424E-03	-0	13170862E-01	-0	79970727E-02	0	16474094E+00	0	10954039E+00

Listing D.5. POSFIL Results File (continued).

0	80813210E+00	0	64324522E-02	0	79928592E-02	0	62316032E+04	0	39416035E+03	0	81624376E+00	0	23133798E-02	0	12714382E-01	0	69468803E+03	0	32626866E+05
-0	43667624E+04	0	20401200E+03	0	41267648E+03	0	41376364E+03	0	51467617E+04	0	98718966E+04	0	46151706E-02	0	35163707E+02	0	41899721E+03	0	18507039E+04
-0	63920866E+04	0	79417612E+06	0	53971300E+06	0	96801309E+06	0	6801309E+06	0	10171505E+05	0	11026485E+07	0	76702463E+06	0	81496417E+06	0	
STRS	3	32	STRS	3	32	STRS	3	32	STRS	3	32	STRS	3	32	STRS	3	32	STRS	3
19	SMEL	19	SMEL	19	SMEL	19	SMEL	19	SMEL	19	SMEL	19	SMEL	19	SMEL	19	SMEL	19	SMEL
0	36952703E-03	0	50542366E-03	0	42106286E-03	0	53625985E-01	0	806277120E-01	0	70591473E-04	0	2513812E-03	0	61242281E-03	0	92030354E-01	0	16681616E+00
0	19391743E+00	0	36995930E-03	0	10390186E-02	0	62321810E+03	0	10373873E+04	0	60563636E-01	0	49864454E-03	0	60393535E-03	0	19630160E+02	0	59837402E+03
0	40422035E+03	0	10073770E+03	0	12638720E+03	0	94295737E+02	0	34959640E+03	0	58792599E+03	0	18259416E+01	0	23947746E+03	0	42477382E+03	0	39871565E+03
0	84721668E+03	0	19241671E+06	0	36064089E+05	0	19966808E+06	0	19966808E+06	0	31887484E+03	0	27627981E+06	0	23177749E+05	0	21820087E+06	0	
STRS	3	32	STRS	3	32	STRS	3	32	STRS	3	32	STRS	3	32	STRS	3	32	STRS	3
19	SMEL	19	SMEL	19	SMEL	19	SMEL	19	SMEL	19	SMEL	19	SMEL	19	SMEL	19	SMEL	19	SMEL
-0	21132849E-03	0	19679760E-02	0	15967189E-04	0	75091661E-01	0	11099732E-01	0	25144599E-01	0	13689211E-07	0	17322020E-02	0	64611683E-01	0	94943712E-01
0	36465884E+00	0	11703396E-02	0	21557296E-02	0	18005036E+04	0	51732689E+04	0	16629137E+04	0	12667942E+03	0	39899130E-03	0	73091171E+03	0	30416313E+03
-0	13328502E+02	0	10630030E+03	0	40731510E+02	0	18660293E+03	0	93627187E+03	0	31887484E+03	0	2476481E+06	0	40281156E+05	0	19817786E+06	0	
0	17265897E+04	0	31734807E+06	0	85406744E+05	0	32334010E+06	0	32334010E+06	0	16529137E+04	0	12667942E+03	0	13168336E+03	0	11019430E+03	0	38194768E+03
STRS	3	32	STRS	3	32	STRS	3	32	STRS	3	32	STRS	3	32	STRS	3	32	STRS	3
19	SMEL	19	SMEL	19	SMEL	19	SMEL	19	SMEL	19	SMEL	19	SMEL	19	SMEL	19	SMEL	19	SMEL
0	66327987E-02	0	21178727E-01	0	14502897E-01	0	43644738E-02	0	28327892E-01	0	36791010E-01	0	32796274E-01	0	40568872E-02	0	76346381E-01	0	70828236E-01
0	10599877E+01	0	10248914E-03	0	15261492E-01	0	34076352E+04	0	28977031E+03	0	36791010E-01	0	32796274E-01	0	40568872E-02	0	76346381E-01	0	70828236E-01
0	13922781E+03	0	37785798E-01	0	37460425E+02	0	58217352E+03	0	81999311E+02	0	14366407E+05	0	1319471E+07	0	81832838E+04	0	13687279E+07	0	63668036E+03
0	12209194E+05	0	13643450E+07	0	81663504E+06	0	84487182E+06	0	84487182E+06	0	1366407E+05	0	1319471E+07	0	81832838E+04	0	13687279E+07	0	
STRS	3	32	STRS	3	32	STRS	3	32	STRS	3	32	STRS	3	32	STRS	3	32	STRS	3
20	SMEL	20	SMEL	20	SMEL	20	SMEL	20	SMEL	20	SMEL	20	SMEL	20	SMEL	20	SMEL	20	SMEL
0	36799112E-04	0	41602088E-03	0	72820170E-03	0	14404118E+00	0	22915294E+00	0	13628812E-03	0	14343868E-03	0	19028991E-03	0	16386608E-01	0	40488171E-01
0	24187704E+00	0	11020483E-03	0	11519868E-02	0	17307420E+03	0	10417187E+04	0	29104124E-01	0	21408784E-03	0	10174172E-03	0	44069836E+03	0	43448742E+03
0	99703632E+03	0	27688163E+03	0	36203966E+03	0	12384104E+03	0	88165656E+02	0	18277047E+02	0	36192431E-02	0	60872967E+02	0	12853312E+02	0	17127028E+03
0	82178992E+03	0	36766627E+06	0	35764903E+09	0	36705941E+06	0	36705941E+06	0	81993378E+02	0	51033646E+05	0	92143866E+04	0	57482002E+05	0	
STRS	3	32	STRS	3	32	STRS	3	32	STRS	3	32	STRS	3	32	STRS	3	32	STRS	3
20	SMEL	20	SMEL	20	SMEL	20	SMEL	20	SMEL	20	SMEL	20	SMEL	20	SMEL	20	SMEL	20	SMEL
-0	28777186E-03	0	31975426E-03	0	12890657E-02	0	12412486E+00	0	10367372E+00	0	36196279E-04	0	10474831E-02	0	27863023E-04	0	23797312E-01	0	95777344E-01
0	96918714E-01	0	10322170E-02	0	96078191E-03	0	94133773E+03	0	10027447E+04	0	11203120E+00	0	90321256E-03	0	84607700E-03	0	57772674E+03	0	26583912E+03
0	12735319E+04	0	20554178E+03	0	18664781E+03	0	49622381E+02	0	82377105E+03	0	24770904E+02	0	63813016E+02	0	13854823E+03	0	57360026E+02	0	72257004E+03
0	76862553E+03	0	20312896E+06	0	46991951E+05	0	20376420E+06	0	20376420E+06	0	67686160E+03	0	17012326E+06	0	44165012E+05	0	12490432E+06	0	
STRS	3	32	STRS	3	32	STRS	3	32	STRS	3	32	STRS	3	32	STRS	3	32	STRS	3
20	SMEL	20	SMEL	20	SMEL	20	SMEL	20	SMEL	20	SMEL	20	SMEL	20	SMEL	20	SMEL	20	SMEL
0	99423207E-03	0	21001336E-01	0	43496406E-03	0	91765194E-01	0	39387069E-01	0	63255062E-02	0	20475138E-01	0	55532046E-02	0	65375061E-01	0	42929839E-01
0	14973631E+01	0	30409919E-02	0	16406715E-01	0	10998021E+05	0	53152713E+05	0	65655532E+00	0	31559721E-03	0	10548700E-01	0	30880737E+04	0	48568303E+05
0	41756550E+03	0	11184596E+02	0	22453959E+02	0	76473932E+03	0	24327534E+04	0	53331076E+04	0	10390396E+03	0	16407092E+03	0	33613632E+03	0	25247777E+03
0	13123372E+05	0	14029292E+07	0	74623721E+06	0	13715996E+07	0	13715996E+07	0	84389761E+04	0	62938971E+06	0	69260724E+06	0	74514871E+06	0	
STRS	3	32	STRS	3	32	STRS	3	32	STRS	3	32	STRS	3	32	STRS	3	32	STRS	3
21	SMEL	21	SMEL	21	SMEL	21	SMEL	21	SMEL	21	SMEL	21	SMEL	21	SMEL	21	SMEL	21	SMEL
-0	24525298E-03	0	95528879E-04	0	20461951E-03	0	22453262E-01	0	54846669E-01	0	45415807E-04	0	23688669E-04	0	33425117E-03	0	50492322E-01	0	10749603E+00
0	18731316E-01	0	89968434E-03	0	39144968E-03	0	54230915E+03	0	14807987E+02	0	20971363E-01	0	86731980E-04	0	27828917E-03	0	13562110E+03	0	10560761E+04
0	19643472E+03	0	50059850E+02	0	85278698E+02	0	95903544E+01	0	71987674E+03	0	32960112E+03	0	10590396E+03	0	16407092E+03	0	10737339E+02	0	67385588E+02
0	31315976E+03	0	71748182E+05	0	26861877E+05	0	71867103E+05	0	71867103E+05	0	22570814E+03	0	14775462E+06	0	16085306E+05	0	12517908E+06	0	
STRS	3	32	STRS	3	32	STRS	3	32	STRS	3	32	STRS	3	32	STRS	3	32	STRS	3
21	SMEL	21	SMEL	21	SMEL	21	SMEL	21	SMEL	21	SMEL	21	SMEL	21	SMEL	21	SMEL	21	SMEL
0	94992851E-03	0	19857612E-02	0	37043156E-03	0	14694886E-02	0	67476206E-01	0	19359477E-03	0	21936001E-07	0	16740200E-02	0	11380601E+00	0	18586546E+00
0	32863735E+00	0	94498763E-03	0	15413780E-02	0	11607554E+04	0	44753888E+04	0	98866377E-01	0	41996311E-03	0	3277278E-04	0	29982021E+03	0	42638897E+03
0	35561430E+03	0	21024881E+02	0	91623202E+02	0	18625232E+03	0	75399010E+03	0	26962222E+02	0	2758867E+06	0	37482957E+05	0	2492264E+06	0	33397049E+03
0	12331026E+04	0	29985321E+06	0	80112684E+05	0	28277401E+06	0	28277401E+06	0	31887484E+03	0	27627981E+06	0	23177749E+05	0	21820087E+06	0	
STRS	3	32	STRS	3	32	STRS	3	32	STRS	3	32	STRS	3	32	STRS	3	32	STRS	3
21	SMEL	21	SMEL	21	SMEL	21	SMEL	21	SMEL	21	SMEL	21	SMEL	21	SMEL	21	SMEL	21	SMEL
-0	57724603E-02	0	22004391E-01	0	42415589E-02	0	29188110E-01	0	18457641E-01	0	19145005E-02	0	2063962E-01	0	57002037E-02	0	10515721E+00	0	18821159E-02

Listing D.5. POSFIL Results File (continued).

0 10463953E+01	0 10637371E+02	-0 13367494E+01	-0 83172913E+04	-0 51648837E+05	0 28487971E+05
0 94721973E+04	-0 14293222E+03	-0 33323944E+02	0 9460913E+03	0 85260570E+07	0 71156704E+03
0 12293993E+03	0 99346611E+06	0 73123932E+06	0 11879698E+07	0 77918675E+06	0 29590143E+03
STRS	3	32	3	32	3
26	26	26	26	26	26
0 14460974E+03	0 19213794E+03	0 61929720E+04	0 53112349E+02	0 27231143E+01	0 30173131E+01
0 57932318E+01	0 32411424E+03	-0 13852904E+03	0 24800044E+03	0 39411209E+03	0 52950633E+03
0 96452331E+02	0 14580833E+02	0 79129703E+02	-0 29641347E+02	0 26727301E+03	0 14831893E+02
0 12482325E+03	0 56627499E+03	0 11997350E+03	0 5972483E+03	0 36457396E+04	0 75163208E+03
STRS	3	32	3	32	3
26	26	26	26	26	26
0 41124201E+03	-0 44574823E+03	-0 10572834E+03	0 78929164E+01	0 95598544E+01	0 12743204E+00
0 81640713E+02	-0 14772709E+03	-0 23493343E+04	0 75494413E+03	-0 92910474E+03	0 71232784E+02
0 10149923E+03	0 72128923E+02	0 14039837E+03	-0 41823443E+01	-0 11818167E+03	0 14548492E+02
0 20394875E+02	0 12485707E+06	0 18862403E+04	0 10570402E+06	0 14425375E+06	0 12263624E+03
STRS	3	32	3	32	3
26	26	26	26	26	26
0 54032448E+02	0 17058937E+01	-0 84717744E+03	-0 10501713E+00	-0 53624077E+01	0 42177645E+01
0 62149375E+00	-0 10393594E+02	0 79223341E+02	-0 34242449E+04	0 40084563E+05	0 42959875E+02
0 65129034E+03	0 16148716E+03	0 10906332E+03	0 32574378E+03	-0 84764736E+03	0 42959875E+02
0 63378489E+04	0 78887834E+06	0 56359634E+06	0 74638691E+06	0 64724806E+05	0 42959875E+02
STRS	3	32	3	32	3
26	26	26	26	26	26
0 94887697E+04	-0 32402367E+03	-0 30375510E+04	0 18740163E+01	0 60983639E+01	0 93193494E+02
0 18220307E+01	0 13993714E+03	-0 18846203E+03	0 35537372E+02	-0 73877234E+01	0 11673575E+03
0 29160490E+02	0 46430374E+02	0 89649468E+02	-0 73288383E+01	0 10876571E+03	0 13424854E+02
0 13076944E+03	0 82498764E+05	0 11761213E+05	0 64724806E+05	0 29316147E+05	0 66563421E+02
STRS	3	32	3	32	3
26	26	26	26	26	26
0 23755734E+03	-0 63704663E+03	-0 14075841E+02	0 74330423E+01	0 18309493E+09	0 41491999E+01
0 29982191E+01	0 47087916E+04	0 19004477E+03	0 19916444E+03	-0 14838891E+04	0 17794393E+03
0 13512807E+04	0 19126914E+03	0 28218380E+03	0 14838892E+02	0 37667133E+02	0 32304494E+02
0 13203393E+03	0 25337653E+06	0 37522344E+05	0 22107323E+06	0 73549503E+05	0 17877638E+02
STRS	3	32	3	32	3
26	26	26	26	26	26
0 52921595E+03	-0 16817937E+01	0 72382914E+04	-0 11962582E+00	0 45450915E+01	0 10934904E+01
0 10465444E+01	0 21937668E+02	0 11762530E+01	-0 94034847E+04	-0 42702420E+05	0 15003963E+05
0 69487503E+04	0 17684303E+03	0 10288799E+03	0 54607084E+03	0 17598134E+04	0 23110444E+03
0 94100244E+04	0 97047043E+06	0 59605282E+06	0 11723827E+07	0 76311618E+06	0 13534535E+00
STRS	3	32	3	32	3
26	26	26	26	26	26
0 41277723E+04	0 99404104E+04	0 32094540E+04	-0 83131620E+03	0 17254744E+01	0 11878415E+01
0 36604823E+01	-0 12499339E+03	0 20082987E+01	0 16934800E+03	0 28090505E+03	0 22611810E+03
0 50010758E+03	0 47543962E+01	0 23274724E+02	-0 19765449E+02	0 9494715E+02	0 35622211E+01
-0 16066390E+03	0 37398230E+05	0 69512628E+04	0 38472734E+05	0 22151504E+05	0 437620149E+01
STRS	3	32	3	32	3
26	26	26	26	26	26
0 81937040E+04	-0 22777145E+04	-0 22920810E+03	0 12827500E+01	0 73484015E+01	0 437620149E+01
-0 9995337E+01	0 36164768E+03	-0 31623884E+03	-0 22433300E+03	-0 11073644E+03	0 51515232E+02
-0 22003978E+03	0 42397149E+02	0 10471139E+03	-0 49129100E+02	0 28733414E+03	0 10392623E+04
-0 25349104E+03	0 11449494E+06	0 13574031E+05	0 11957817E+06	0 68860012E+05	0 58462431E+02
STRS	3	32	3	32	3
26	26	26	26	26	26
0 60548937E+02	0 12641828E+01	0 63322049E+02	-0 15034889E+00	-0 38537423E+01	0 22757237E+01

Listing D.5. POSFIL Results File (continued).

```

1 0 94763230E+00 0 34403678E+02 -0 32910284E+02 -0 29887988E+04 -0 16057349E+11
0 10579555E+05 -0 13167925E+03 -0 61999101E+02 0 48518774E+03 0 27522945E+14
-0 26328257E+04 0 59429827E+06 0 31867380E+06 0 10409367E+07

STRS 3 32
J1 SHEL 1 2
0 5088191E+05 0 4388110E+05 0 13254827E+04 -0 88603710E+02 0 4806328E+02
0 5089307E+02 -0 50325236E+04 0 56697617E+04 0 15803168E+02 0 14262005E+02
0 12726634E+02 -0 10456800E+02 0 37379003E+01 -0 18860232E+01 -0 40260189E+02
0 14548097E+02 0 12344038E+03 0 1997679E+04 0 12076677E+03

STRS 3 32
J1 SHEL 2
0 2573451E+04 0 4076562E+04 0 18892894E+04 -0 20957382E+01 0 14746459E+01
0 2215132E+01 -0 41970745E+04 -0 18187116E+03 -0 59265678E+02 0 88069073E+02
0 1813717E+02 -0 2780334E+02 0 12989779E+02 -0 11341492E+02 -0 7376597E+02
0 14549592E+03 0 34391466E+03 0 50659585E+04 0 36213974E+03

STRS 3 32
J1 SHEL 3
0 23279881E+02 0 93197198E+03 0 79794949E+02 -0 11376420E+00 0 49700169E+02
0 25279492E+00 0 20533749E+02 0 10230807E+02 0 65737594E+04 0 39281728E+04
0 76603170E+04 0 15363257E+03 -0 32046468E+02 0 12943231E+03 -0 16427159E+04
0 81846458E+03 0 20367862E+06 0 19627015E+06 0 38309670E+06

STRS 3 32
J1 SHEL 1 2
0 37341389E+05 0 40312573E+04 0 11899812E+04 -0 21621349E+01 0 54574910E+02
0 36441395E+02 -0 21321494E+04 0 3024542E+04 -0 1875231E+02 0 13093834E+03
0 11423819E+03 0 27729136E+02 0 3473875E+01 -0 18746892E+01 -0 1217189E+02
0 24197074E+02 0 26683774E+05 0 13318236E+04 0 23770800E+03

STRS 3 32
J1 SHEL 2
0 91979315E+04 -0 17541149E+03 0 16136264E+03 -0 45389377E+01 0 2497242E+01
0 96044124E+02 -0 26797578E+04 -0 13973473E+03 0 12309888E+03 -0 39021789E+03
0 13570813E+03 0 53447709E+02 0 18602773E+02 -0 49175615E+01 -0 21438063E+02
0 11178779E+03 0 65905154E+03 0 74808414E+04 0 56975120E+03

STRS 3 12
J1 SHEL 1
0 11225452E+01 0 43641820E+02 0 79469647E+02 -0 59414970E+01 0 56256420E+02
0 47260179E+03 0 38259741E+02 -0 49681028E+03 0 27816078E+03 -0 4900314E+03
0 7629091E+03 0 87041459E+02 -0 27961184E+02 0 24197211E+03 0 3060339E+03
0 55744923E+03 0 45953459E+06 0 40366027E+06 0 63119369E+06

ESEN 3
J1 1 0 21504509E+04 0 25942883E+04
1 0 21504509E+04 -0 14336604E+07
2 0 21504509E+04 0 14802774E+04
3 0 1066471E+05 0 12531773E+03
4 0 1066471E+05 -0 71098077E+07
5 0 1066471E+05 0 66442819E+03
6 0 1965782E+05 0 25578134E+03
7 0 1965782E+05 -0 13105189E+00
8 0 1965782E+05 0 43883681E+03

PSEN 3
J1 1 0 26600000E+00
1 0 26797202E+07
2 0 1787742E+08
3 0 24591768E+09
4 -0 12689078E+08
5 0 19730471E+08
6 1 -0 43358546E+08

```

Listing D.5. POSFIL Results File (concluded).

run pro-pat

```

*****
P R O - P A T
*****
Translation module results files to
input from a PROTEC results file and
from the terminal in order to generate
a node1 results file and/or a neutral
element results file.
*****
ENTER NAME OF PROTEC RESULTS FILE ..... outpro
THE TITLE OF THIS PROTEC RESULTS FILE IS ....
SIMPLIFIED BLADE/DISC SECTION
IS THIS THE CORRECT FILE (Y/N) ..... Y
ENTER CASE NUMBER
FROM PROTEC RESULTS FILE ..... 1
OUTPUT OPTIONS FOR PATRON:
(1) NORMAL RESULTS FILE
(2) NEUTRAL ELEMENT RESULTS FILE
ENTER OPTION (1-2) ..... 1
OPTIONS FOR NORMAL RESULT FILES:
(1) DISPLACEMENT RESULTS
(2) REACTION FORCES AND MOMENTS
ENTER OPTION (1-2) ..... 1
PROCESSING PLEASE WAIT ...
ENTER NAME OF PATRON
NORMAL DISPLACEMENTS FILE ..... address
DO YOU DESIRE TO HAVE A FORMATTED
NORMAL DISPLACEMENT FILE WRITTEN (Y/N) ..... Y
ENTER THE NAME OF THE FORMATTED
NORMAL DISPLACEMENT FILE ..... nodlist
ENTER THE TITLE OF THE
NORMAL DISPLACEMENT FILE ..... Example Problem
ENTER THE FIRST SUBTITLE OF THE
NORMAL DISPLACEMENT FILE ..... PROTEC analysis
ENTER THE SECOND SUBTITLE OF THE
NORMAL DISPLACEMENT FILE ..... Eigenvalue res
*****

```

```

CONTINUATION OPTIONS:
ENTER A NEW PROTEC RESULTS FILE ... (1)
ENTER A NEW CASE NUMBER ... (2)
SELECT PATRON RESULTS FILE
(NAMES OR ELEMENTS) ... (3)
END ..... (4)
ENTER A SELECTION (1-4) ..... 3
OUTPUT OPTIONS FOR PATRON:
(1) NORMAL RESULTS FILE
(2) NEUTRAL ELEMENT RESULTS FILE
ENTER OPTION (1-2) ..... 2
ENTER NAME OF PATRON NEUTRAL
ELEMENT RESULTS FILE ..... elenres
DO YOU DESIRE TO HAVE A FORMATTED NEUTRAL
ELEMENT RESULTS FILE WRITTEN (Y/N) ..... Y
ENTER NAME OF FORMATTED PATRON
NEUTRAL ELEMENT RESULTS FILE ..... elenlist
ENTER THE TITLE OF THE
NEUTRAL ELEMENT RESULTS FILE ..... Example Problem
ENTER THE FIRST SUBTITLE OF THE
NEUTRAL ELEMENT RESULTS FILE ..... PROTEC analysis
ENTER THE SECOND SUBTITLE OF THE
NEUTRAL ELEMENT RESULTS FILE ..... Eigenvalue results
PROCESSING PLEASE WAIT ...
CONTINUATION OPTIONS:
ENTER A NEW PROTEC RESULTS FILE ... (1)
ENTER A NEW CASE NUMBER ... (2)
SELECT PATRON RESULTS FILE
(NAMES OR ELEMENTS) ... (3)
END ..... (4)
ENTER A SELECTION (1-4) ..... 4
CONTIN STOP

```

Listing D.6. PROPAT Execution.

P D A / P A T R A N - G

RELEASE 1.5

CUSTOMER - WRIGHT PATTERSON AIR FORCE BASE

FOR INFORMATION ON NEW FEATURES IN RELEASE 1.5
OBTAIN A PRINTOUT OF FILE INFO15

PLEASE INPUT THE DEVICE NAME (OR "REPORT"):
>4C14

INPUT GO, SES, HELP, OR PDA/PATRAN-G EXECUTIVE DIRECTIVE
>GO

PATRAN DATA FILE? 1.NEW 2.OLD 3.LAST
>1

PREPARING THE DATA BASE SUB-SYSTEM
222 PARTITIONS TO BE INITIALIZED:
220
200
180
160
140
120
100
80
60
40
20

MODE? 1.GEOMETRY MODEL 2.ANALYSIS MODEL 3.DISPLAY 4.NEUTRAL SYS. 5.END
>SET,PH1,OFF

"PH1" IS NOW OFF (WAS ON).

MODE? 1.GEOMETRY MODEL 2.ANALYSIS MODEL 3.DISPLAY 4.NEUTRAL SYS. 5.END
>SET,LABE,OFF

PHASE1 LABELS - F F F F PHASE2 LABELS - F F F F F F F F F
PHASE3 LABELS - T T T LOAD LABELS - T T T T

Listing D.9. PATRAN Session.

MODE? 1.GEOMETRY MODEL 2.ANALYSIS MODEL 3.DISPLAY 4.NEUTRAL SYS. 5.END
>4

NEUTRAL FILE? 1.CREATE OUTPUT 2.INPUT MODEL 3.POST-PROCESSING 4.END
>2

INPUT NEUTRAL FILE NAME
>NEUTRAL

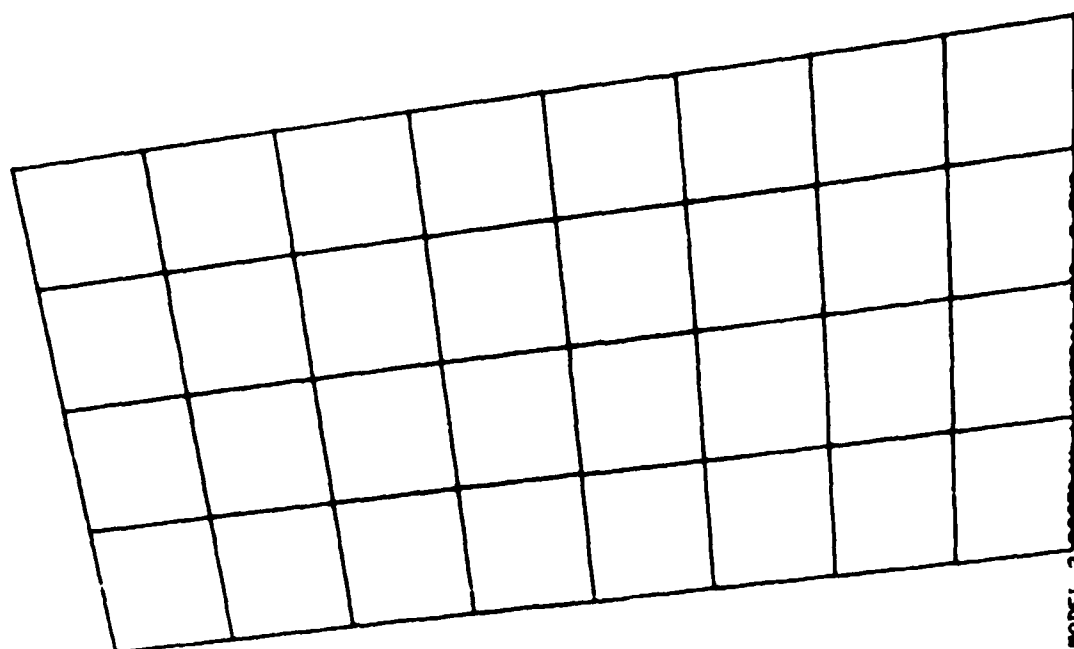
DO YOU WISH TO OFFSET ANY NEUTRAL INPUT IDS? (Y/N)
>N

LAYERED BEAM WITH EDGE STIFFENERS
SHALL WE PROCEED WITH THE READING OF THIS FILE? (Y/N)
>Y

READING NODE RECORDS:
100

READING ELEMENT RECORDS:
READING MATERIAL PROPERTY RECORDS:
READING PHYSICAL PROPERTY RECORDS:
READING PRESSURE RECORDS:
READING DISPLACEMENT RECORDS:
READING GRID RECORDS:
READING LINE RECORDS:
READING PATCH RECORDS:
READING HYPERPATCH RECORDS:
READING DATA RECORDS:
READING GFEG RECORDS:
READING CFEG RECORDS:

Listing D.9. Continued



NODE? 1.GEOMETRY MODEL 2.ANALYSIS MODEL 3.DISPCHY 4.NEUTRON 5.S-210

Listing D.9. Continued

NUMBER OF ITEMS READ FROM NEUTRAL FILE:

NUM NODE,	ELEM,	MATL,	PROP,	CORD,	PRES,	FORC,	DISP,	DEFO,	TEMPN,	TEMPE
45	32	1	1	0	0	0	0	0	0	0
NUM GRID,	LINE,	PATCH,	HPAT,	DLINE,	DPAT,	DHPAT,	LIST,	DATA		
6	0	2	0	0	0	0	0	0		
NUM GFEG,	CFEG									
2	2									

MODE? 1.GEOMETRY MODEL 2.ANALYSIS MODEL 3.DISPLAY 4.NEUTRAL SYS. 5.END
>4

NEUTRAL FILE? 1.CREATE OUTPUT 2.INPUT MODEL 3.POST-PROCESSING 4.END
>3

POSTPROCESS? 1.DEFORMATIONS 2.ELEMENT QUANTITIES 3.END
>2

INPUT THE KIND OF ATTRIBUTE YOU WISH TO SEE, EG: ID; MID;PID;
TEMP; PRES; DISP,N; STRAIN,N; STRESS,N; VON,N; COLUMN,N; LIGHT; NORMAL
>COL,14

INPUT THE NAME OF THE ELEMENT RESULTS FILE:
>ELERES

DATA WIDTH - 15
FILE TITLE - EXAMPLE PROBLEM
PROTEC ANALYSIS
EIGENVALUE RESULTS

DATA VALUES RANGE FROM .123E+05 TO .467E+06

ASSIGNMENT? 1.AUTO 2.MANUAL 3.SEMI-AUTO 4.USE CURRENT LEVELS 5.END
>5

POSTPROCESS? 1.DEFORMATIONS 2.ELEMENT QUANTITIES 3.END
>SET,SPECT,15,1,2,3,4,5,6,7,8,9,10,11,12,13,14,15

POSTPROCESS? 1.DEFORMATIONS 2.ELEMENT QUANTITIES 3.END
>RUN,CONT,COL,14

INPUT THE RESULTS FILE NAME:
>ELERES

AVERAGING COLUMN 5 OF ELEMENT RESULTS FILE AT NODES.
DATA WIDTH - 15
FILE TITLE - EXAMPLE PROBLEM
PROTEC ANALYSIS
EIGENVALUE RESULTS

DATA VALUES RANGE FROM .123E+05 TO .467E+06

Listing D.9. Continued

ASSIGNMENT? 1.AUTO 2.MANUAL 3.SEMI-AUTO 4.USE CURRENT LEVELS 5.END
>1

ASSIGNED CONTOUR VALUE CODES FOLLOW:

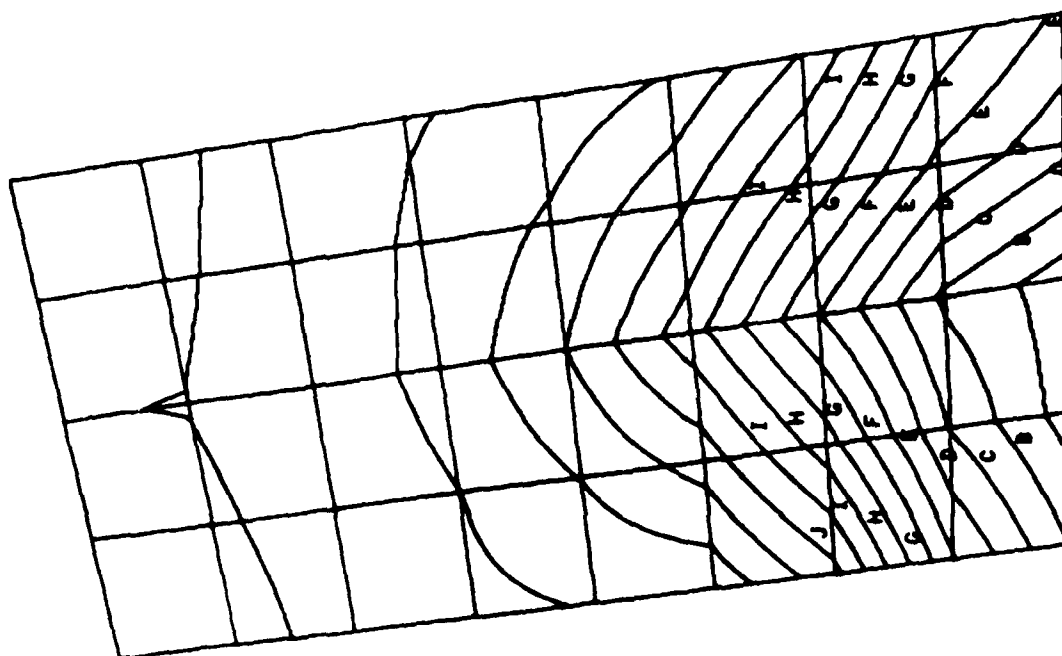
A	.4110E+06	B	.3815E+06	C	.3520E+06
D	.3224E+06	E	.2929E+06	F	.2634E+06
G	.2338E+06	H	.2043E+06	I	.1748E+06
J	.1452E+06	K	.1157E+06	L	.8617E+05
M	.5664E+05	N	.2711E+05		

A SINGLE COLUMN NODAL FILE CALLED "PATNOD " HAS BEEN PRODUCED.

POSTPROCESS? 1.DEFORMATIONS 2.ELEMENT QUANTITIES 3.END
>RUN,HIDE,CONT

BEGINNING PHASE-II HIDDEN LINE PLOT OF ACCURACY LEVEL .20

Listing D.9. Continued



EXAMPLE PROBLEM
PROTEC ANALYSIS
EIGENVALUE RESULTS

411013.00
381488.00
351850.00
322419.00
292888.00
263356.00
233825.00
204294.00
174762.00
145231.00
115700.00
86168.00
56637.00
27106.00

8

Listing D.9. Continued

POSTPROCESS? 1.DEFORMATIONS 2.ELEMENT QUANTITIES 3.END
>STOP

RESTART DATA BEING WRITTEN ON 87/09/29
PDA/PATRAN COMPLETED

Listing D.9. Concluded

APPENDIX E

DISSPLA INTERFACE (PRODIS)

PRODIS (PROTEC-to-DISSPLA) is an output processor for PROTEC which performs two primary functions:

- probabilistic (variance) computations
- presentation graphics using the DISSPLA¹¹ library

PRODIS uses the results file POSFIL (Appendix B) to generate x-y plots, surface plots, and histograms. Data used in PRODIS plots also can be written to separate files for use in other programs. PRODIS is written in ANSI FORTRAN-77, and is operational on the DEC VAX under VMS and CDC Cyber systems under NOS.

PRODIS generally allows plotting of any quantity versus another, although some combinations are best suited for specific types of analysis. Quantities which can be selected for plotting include:

- displacement components at a specified node
- displacement magnitude at a specified node
- maximum displacement for a collection of nodes
- principal moment for a specified element
- von Mises stress for a specified element
- maximum moment or stress for a collection of elements
- harmonic forcing frequency

In some cases, it is desirable to plot only one of the above quantities for a series of load cases (static analysis) or modes (natural frequency analysis). PRODIS will generate histograms for such cases, which permits an easy comparison of effects from different analysis cases. Results from steady-state harmonic analyses, with forcing frequency as an independent variable, are typically presented as x-y plots or 3-D surfaces.

Two modes of presentation are included in PRODIS for display of probabilistic data. In static or natural frequency analysis,

variance data for nodal or element results can be displayed in histogram form. The histogram shows variances in the requested quantity for each individual statistical parameter, and for all parameters combined. Recall that, for any result r which depends on the statistical parameters p_i , the total variance is (see Section 4.3):

$$\text{Var}[r] = \sum_{i=1}^n \left[\frac{\partial r}{\partial p_i} \right]^2 \text{Var}[p_i]$$

In effect, the histogram displays each term in this series as well as the total, for each of a series of loading conditions or vibration modes. This type of plot is useful for determining which statistical parameters contribute most to the uncertainty in the computed result, and for comparing this data for different modes or loading conditions.

The second mode of presentation for probabilistic results is most often used in steady-state harmonic analysis, where forcing frequency is nearly always an independent variable. This being the case, one can assemble frequency response (i.e., amplitude versus frequency) results for the deterministic response, or for a given percentile level (confidence level). Amplitudes versus both forcing frequency and confidence level may be presented as a family of curves, or as a three-dimensional surface. Some plots of this type can be found in Section 7.4.

One practical concern is the time and cost associated with processing of results. The results which are generated by the basic solution, sensitivity analyses, and probabilistic computations often represent a substantial amount of numerical data. We recommend using the "searching" options (those which search for a maximum value within a specified set of nodes or elements) with some care, since a great deal of calculation may be required.

In principal, PRODIS can produce output on any graphical device which is supported by DISSPLA. However, the program has been tested only for a relatively small subset of these devices. At present, PRODIS is equipped to generate graphical output on:

- Tektronix 4000 series graphics terminals
- Calcomp 1051 drum plotter
- Hewlett-Packard 7470-A pen plotter

The addition of other DISSPLA-supported devices is quite simple, involving only a call to the appropriate device nomination subroutine within the DISSPLA library.

PRODIS is fully interactive, and issues relatively simple prompts for all keyboard input. The listing which follows shows a short session with PRODIS, and the resulting histogram plots.

```

run pro-dis
=====
PROTEC - TO - DISPLA
SENSITIVITY PLOTTING PROGRAM

PRO-DIS is an interactive FORTRAN code
that can generate one or more different
graphical presentations of the sensitivity
analysis performed in PROTEC with the use
of the plotting routines in DISPLA.
=====

Please enter the name of the
PROTEC results file to be plotted .....: outpro

The title of the results file is ..
SIMPLIFIED BLADE/DISC SECTOR

Is this the correct file (Y/N) .....: y

Plotting Device Types:
Tektronix (1)
Calcomp (2)
Hewlett-Packard (3)

Please enter a selection ( 1-3 ) .....: 1

Please enter the Tektronix
Device Number .....: 4014

Please enter the transmission rate
in Characters per Second .....: 120

Post-Processing Options:
Linear Static (1)
Eigenvalues (2)
Steady-State Harmonic (3)

Please enter a selection ( 1-3 ) .....: 2

Enter the number of nodes ( 2 max ) .....: 3

Natural Frequency Result Types:
Displacement/Rotation (1)
Stress Resultants (2)
Natural Frequency Variances (3)

Please enter a selection ( 1-3 ) .....: 1

Displacement Components:
X - Displacement (1)
Y - Displacement (2)
Z - Displacement (3)
X - Rotation (4)
Y - Rotation (5)
Z - Rotation (6)
Magnitude of Displacement (7)

Please enter a selection ( 1-7 ) .....: 7

Specify the Nodes among which
the maximum value will be found
by designating a ...
Collection of Nodes (1)
Specific Node Number (2)

Please enter a selection ( 1-2 ) .....: 1

The Collection of Nodes can be defined by a
Range of Nodes (1)
List of Random Nodes (2)

Please enter a selection ( 1-2 ) .....: 1

Range Options:
All Nodes in the model (1)
Specific Range of Nodes (2)
Material Numbers (3)

Please enter a selection ( 1-3 ) .....: 1

Please enter the title of the plot
30 characters maximum .....: Displacement Result

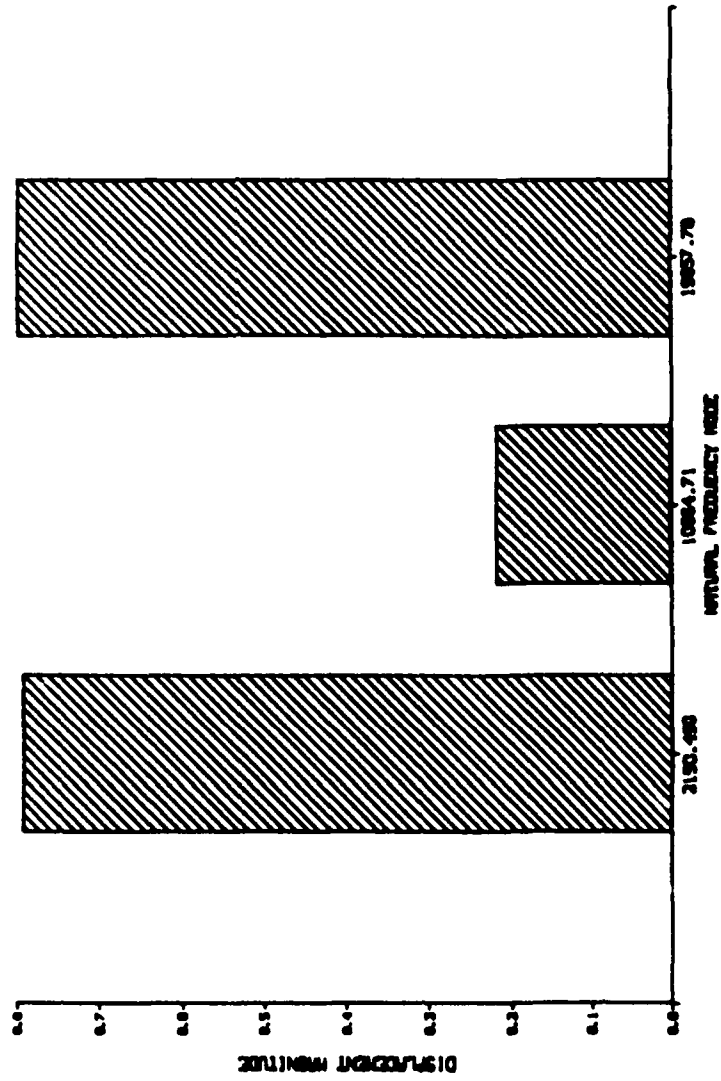
Do you wish to have a datafile
written which will contain the
plotted data (Y/N) .....: y

Please enter the file name .....: displot

```

Listing E.1. PRODIS Sample Execution.

DISPLACEMENT RESULTS



Listing E.1. PRODIS Sample Execution (continued).

```

END OF DISPLA 10.5 -- 1000 VECTORS IN 1 PLOTS.
RUN ON 10/16/87 USING SERIAL NUMBER 6165 AT UNIVERSITY OF
PROPRIETARY SOFTWARE PRODUCT OF ISSCO, SAN DIEGO, CALIF.
818 VIRTUAL STORAGE REFERENCES, 5 READS, 0 WRITES.

Continuation Options :
  Enter a new PROTEC results file (1)
  Enter a new Post-Processing Option (2)
  End

Please enter a selection ( 1-3 ) .....: 2

Post-Processing Options :
  Linear Static (1)
  Eigenvalue (2)
  Steady-State Harmonic (3)

Please enter a selection ( 1-3 ) .....: 2

Enter the number of modes ( 3 max ) ....: 3

Natural Frequency Result Types :
  Displacements/Rotations (1)
  Stress Resultants (2)
  Natural Frequency Variances (3)

Please enter a selection ( 1-3 ) .....: 2

Stress Resultant Components :
  Principal Stresses :
    Max.....(1) Min.....(2) Shear.....(3)
  Principal Moments :
    Max.....(4) Min.....(5) Shear.....(6)
  Principal Strains :
    Max.....(7) Min.....(8)
  Principal Curvatures :
    Max.....(9) Min.....(10)
  Von Mises Stress :
    Lower.....(11) Middle.....(12)
    Upper.....(13) Maximize.....(14)
  Strain Energy Density ....(15)

Please enter a selection ( 1-15 ) .....: 14

Specify the Elements among which
the maximum value will be found
by designating a...
  Collection of Elements (1)
  Specific Element Number (2)

Please enter a selection ( 1-2 ) .....: 1

The Collection of Elements can be defined by a
  Range of Random Elements (1)
  List of Random Elements (2)

Please enter a selection ( 1-2 ) .....: 1

Range Options :
  All Elements is the model (1)
  Specific Range of Elements (2)
  Material Numbers (3)

Please enter a selection ( 1-3 ) .....: 1

Search for the ...
  Algebraic Maximum (1)
  Magnitude Maximum (2)

Please enter a selection ( 1-2 ) .....: 2

Processing Please Wait ....

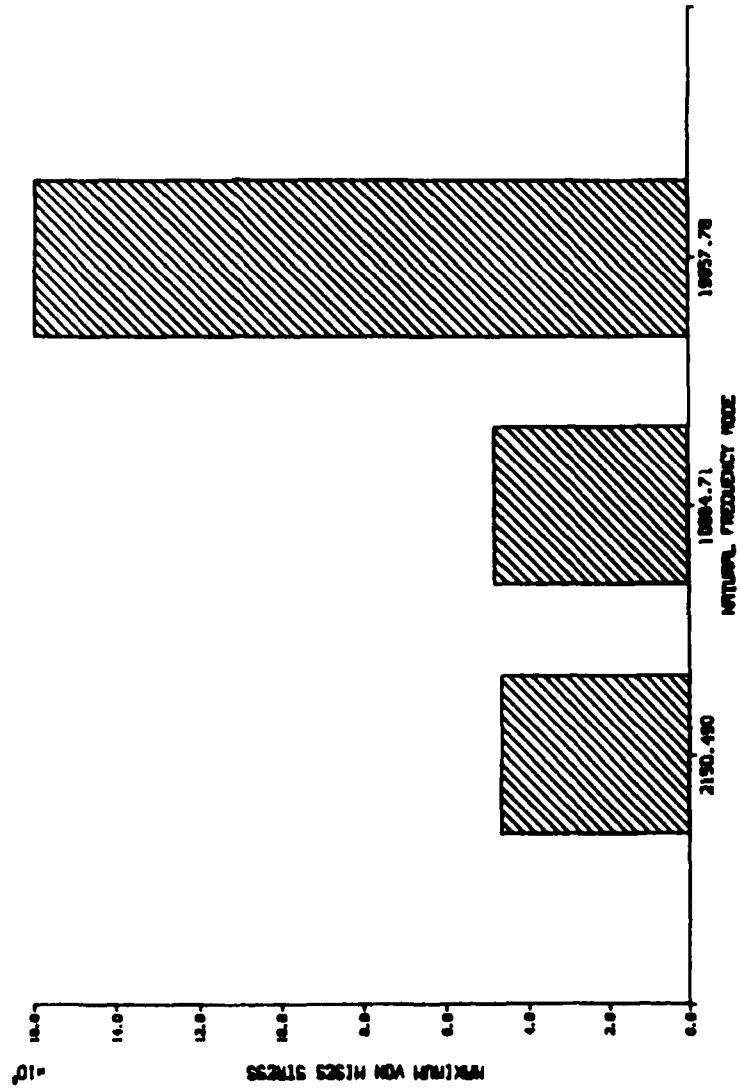
Please enter the title of the plot
30 characters maximum .....: Element Results

Do you wish to have a datafile
written which will contain the
plotted data ( Y/N ) .....: n

```

Listing E.1. PRODIS Sample Execution (continued).

ELEMENT RESULTS



Listing E.1. PRODIS Sample Execution (continued).

END OF DISPLA 10.5 -- 1100 VECTORS IN 1 PLOTS.
 RUN ON 10/16/87 USING SERIAL NUMBER 6105 AT UNIVERSITY OF DOWNTOWN
 PROPRIETARY SOFTWARE PRODUCT OF ISSCO, SAN DIEGO, CALIF.
 533 VIRTUAL STORAGE REFERENCES, 6 READS, 0 WRITES.

Continuation Options :
 Enter a new PROTEC results file (1)
 Enter a new Post-Processing Option (2)
 End (3)

Please enter a selection (1-3): 2

Post-Processing Options :

Linear Static (1)
 Eigenvalue (2)
 Steady-State Harmonic (3)

Please enter a selection (1-3): 2

Enter the number of modes (3 max): 3

Natural Frequency Result Types :

Displacements/Translations (1)
 Stresses Resultants (2)
 Natural Frequency Variances (3)

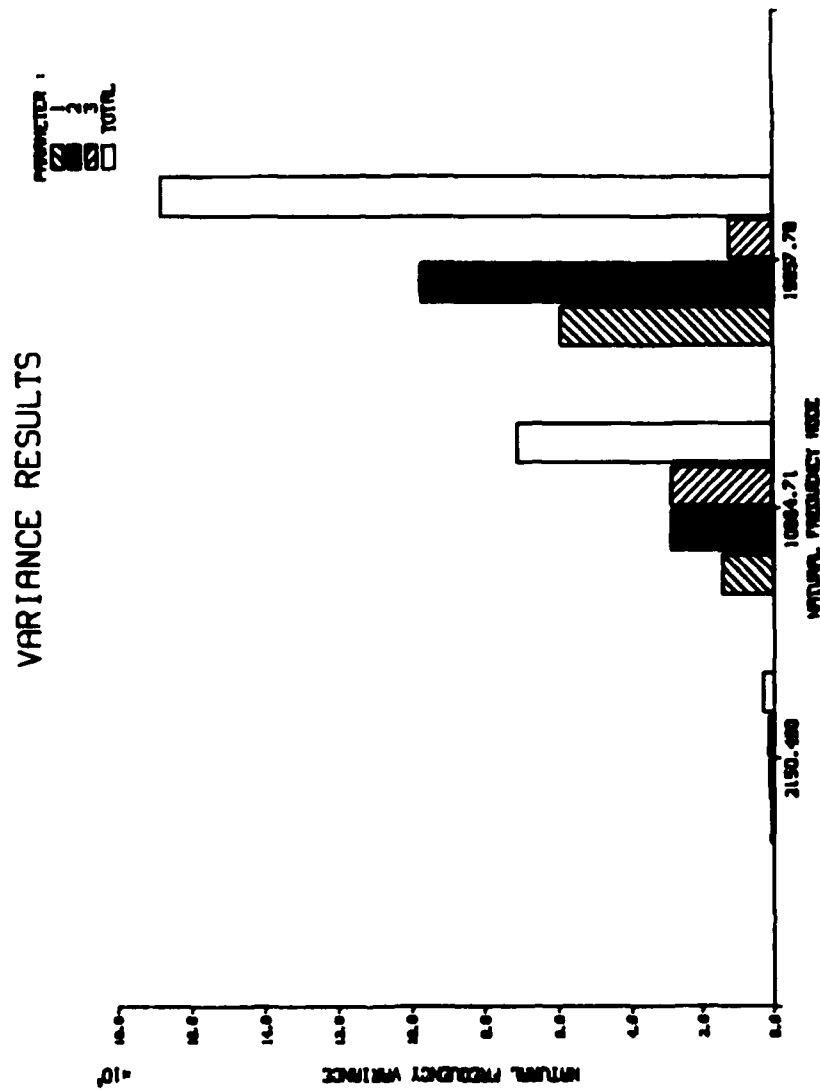
Please enter a selection (1-3): 3

Please enter the number of single
 parameter variances to add to the
 plot with the total variance
 (3 parameters max): 3

Please enter the title of the plot
 20 characters maximum: Variance Results

Do you wish to have a detail file
 written which will contain the
 plotted data (Y/N): n

Listing E.1. PRODIS Sample Execution (continued).



Listing E.1. PRODIS Sample Execution (continued).

END OF DISPLAY 10.5 -- 1198 VECTORS IN 1 PLOTS.
 RUN ON 10/16/87 USING SERIAL NUMBER 6108 AT UNIVERSITY OF SAN
 PROPRIETARY SOFTWARE PRODUCT OF IRECO, SAN DIEGO, CALIF.
 533 VIRTUAL STORAGE REFERENCES, 5 READS, 0 WRITES.

Continuation Options:

Enter a new PROTEC results file (1)
 Enter a new Post-Processing Option (2)
 End

Please enter a selection (1-3): 3
 FORTMAN STOP

Listing E.1. PRODIS Sample Execution (concluded).